www.coinweb.no

SINTEF Building and Infrastructure

Øyvind Bjøntegaard (Norwegian Public Roads Administration)
Knut O. Kjellsen (Norcem AS)

Property development and cracking tendency in hardening concrete: Effect of cement type and fly ash content

COIN Project report 40 – 2012

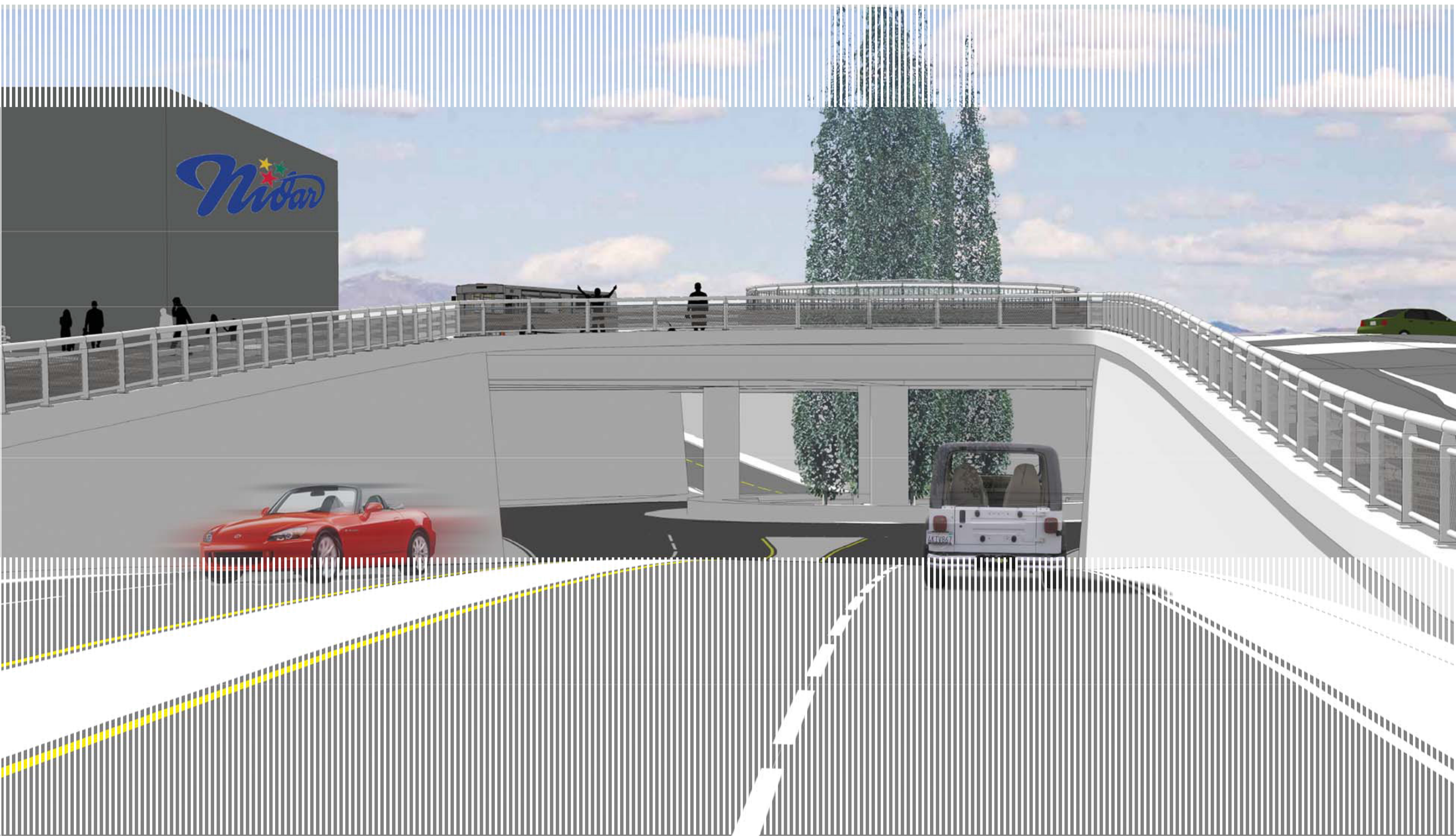

SINTEF Building and Infrastructure

Øyvind Bjøntegaard (Norwegian Public Roads Administration)
Knut O. Kjellsen (Norcem AS)

Property development and cracking tendency in hardening concrete: Effect of cement type and fly ash content

FA 3 Technical performance

SP 3.1 Crackfree concrete structures

COIN Project report 40 – 2012

COIN Project report no 40
Øyvind Bjøntegaard (Norwegian Public Roads Administration)
Knut O. Kjellsen (Norcem AS)

Property development and cracking tendency in hardening concrete: Effect of cement type and fly ash content

FA 3 Technical performance
SP 3.1 Crackfree concrete structures

Keywords:
Concrete, hardening phase, curing technology, property development, crack-risk, cement type, fly ash content

Project no.: 3D005930

Photo, cover: Norwegian Public Roads Administration, project E6 Trondheim Stjørdal

23 copies printed by AIT AS e-dit
Content: 100 g Scandia
Cover: 240 g Trucard

ISSN 1891–1978 (online)
ISBN 978-82-536-1279-9 (pdf)
ISBN 978-82-536-1281-2 (printed)

Address: Forskningsveien 3 B
POBox 124 Blindern
N-0314 OSLO
Tel: +47 22 96 55 55
Fax: +47 22 69 94 38 and 22 96 55 08

www.sintef.no/byggforsk
www.coinweb.no

Cooperation partners / Consortium Concrete Innovation Centre (COIN)

Aker Solutions
Contact: Jan-Diederik Advocaat
Email: jan-diederik.advocaat@akersolutions.com
Tel: +47 67595050

Saint Gobain Weber
Contact: Geir Norden
Email: geir.norden@saint-gobain.com
Tel: +47 22887700

Norcem AS
Contact: Terje Rønning
Email: terje.ronning@norcem.no
Tel: +47 35572000

NTNU
Contact: Terje Kanstad
Email: terje.kanstad@ntnu.no
Tel: +47 73594700

Mapei AS
Contact: Trond Hagerud
Email: trond.hagerud@mapei.no
Tel: +47 69972000

SINTEF Building and Infrastructure
Contact: Tor Arne Hammer
Email: tor.hammer@sintef.no
Tel: +47 73596856

Skanska Norge AS
Contact: Sverre Smeplass
Email: sverre.smeplass@skanska.no
Tel: +47 40013660

Norwegian Public Roads Administration
Contact: Kjersti K. Dunham
Email: kjersti.kvalheim.dunham@vegvesen.no
Tel: +47 22073940

Unicon AS
Contact: Stein Tosterud
Email: stto@unicon.no
Tel: +47 22309035

Veidekke Entreprenør ASA
Contact: Christine Hauck
Email: christine.hauck@veidekke.no
Tel: +47 21055000

Preface

This study has been carried out within COIN - Concrete Innovation Centre - one of presently 14 Centres for Research based Innovation (CRI), which is an initiative by the Research Council of Norway. The main objective for the CRIs is to enhance the capability of the business sector to innovate by focusing on long-term research based on forging close alliances between research-intensive enterprises and prominent research groups.

The vision of COIN is creation of more attractive concrete buildings and constructions. Attractiveness implies aesthetics, functionality, sustainability, energy efficiency, indoor climate, industrialized construction, improved work environment, and cost efficiency during the whole service life. The primary goal is to fulfil this vision by bringing the development a major leap forward by more fundamental understanding of the mechanisms in order to develop advanced materials, efficient construction techniques and new design concepts combined with more environmentally friendly material production.

The corporate partners are leading multinational companies in the cement and building industry and the aim of COIN is to increase their value creation and strengthen their research activities in Norway. Our over-all ambition is to establish COIN as the display window for concrete innovation in Europe.

About 25 researchers from SINTEF (host), the Norwegian University of Science and Technology - NTNU (research partner) and industry partners, 15 - 20 PhD-students, 5 - 10 MSc-students every year and a number of international guest researchers, work on presently 5 projects:

- Advanced cementing materials and admixtures
- Improved construction techniques
- Innovative construction concepts
- Operational service life design
- Energy efficiency and comfort of concrete structures

COIN has presently a budget of NOK 200 mill over 8 years (from 2007), and is financed by the Research Council of Norway (approx. 40 %), industrial partners (approx 45 %) and by SINTEF Building and Infrastructure and NTNU (in all approx 15 %).

For more information, see www.coinweb.no

Tor Arne Hammer
Centre Manager

Summary

The concrete mix design influence the risk of thermal cracking in the hardening phase. Here the effect of binder composition has been investigated, where the variables are cement type and fly ash dosage. The fly ash was added during concrete mixing. Seven concretes (f_{c28} = 60 - 80 MPa) with a water-to-binder ratio of 0.40 (silica fume not used) have been tested with regard to properties relevant for thermal cracking: Hydration heat, free deformation, mechanical properties and restraint stresses have been measured at 20 ^{o}C and semi-adiabatic conditions (relevant for a 1 m thick wall). Based on compressive strength tests the activation energy has been determined. 1-dimensional stress calculations were performed and a relative ranking of the concretes with regard to the tendency of through-cracking was made.

The results show that among the three cement types the crack index varies around 15%. There is a systematic reduction of the crack index with fly ash dosage; about 20% lower crack index for the concrete with 35% fly ash compared to the reference without fly ash.

Sammendrag

Betongens sammensetning influerer faren for termoriss i herdefasen. Effekten av bindemiddelsammen-setning er undersøkt her, hvor sementtype og flygeaskedosering har vært variablene. Flygeasken ble tilsatt ved betongblanding. Syv betonger (f_{c28} = 60 - 80 MPa) med vann-bindemiddelforhold 0.40 (silikastøv ikke brukt) er undersøkt mht. egenskaper relevant for vurdering av risstendens i herdefasen: Hydratasjonsvarme, fri deformasjon, mekaniske egenskaper og spenningsoppbygging ved fastholding er målt ved 20 ^{o}C isoterme forhold og ved semi-adiabatiske forhold (relevant for en 1 m tykk vegg). Aktiveringsenergi er bestemt fra trykkfasthetsforsøk. 1-dimensjonale spenningsberegninger er utført og en relativ rangering av betongenes risstendens et gjort.

Resultatene viser at blant tre sementtypene varierer rissindeksen ca. 15%. Økt flygeaskedosering gir en systematisk reduksjon i rissindeksen; ca. 20% lavere rissindeks for betongen med 35% flygeaske sammenliknet med referansen uten flygeaske.

Notations

c = cement
FA = fly ash
f_c = compressive strength
f_t = direct tensile strength
f_{ts} = splitting strength
E = E-modulus
CTE = coefficient of thermal expansion

TSTM = Temperature-Stress Testing Machine (stress measurement on a restraint beam subjected to a desired temperature history)
Dilation Rig = Free deformation measurement (free beam subjected to a desired temperature history)

Table of contents

1 Introduction

The present report is based on previously unpublished results from the Norwegian research project NOR-CRACK (2001 – 2005). The full name of that project was: "*Deformation properties and crack sensitivity in young concrete: IT-based system for planning and production*". The project was a joint collaboration between Elkem ASA Materials, Norcem ASA, Norwegian Public Roads Administration, Fesil ASA, Skanska Norge AS and the Norwegian University of Science and Technology (NTNU) who was project leader. The project was financially supported by the Research Council of Norway (NFR-project 143983). The COIN-project has made possible the given presentation and evaluation of the results.

Concrete has an inherent potential of developing so-called "thermal cracking" during the hardening phase due to its volume changes caused by thermal dilation and autogenous shrinkage. When quite massive concrete members are subjected to external restraint, which very often is the case, significant hydration heat accumulates and quite uniform tensile stresses may develop over the concrete cross-section, and "through-cracks" sadly quite frequently occur. It is desired to avoid these cracks since they may for instance lead to water leakage and ingress of chlorides, as well as causing an aesthetical deterioration in quality. Avoidance of thermal cracking can be achieved by proper choice of concrete part materials and execution technique on-site. The present report only considers the effect of concrete part materials.

Seven concretes have been investigated with regard to the properties that are relevant for evaluating the cracking tendency in the hardening phase. The tested concretes have a water-to-binder (w/b) ratio of 0.40 and a binder volume fraction of 28.3%. Four cement types have been investigated, three Portland cement cements (CEM I) of different composition and one Blastfurnace cement (CEM III/B). In addition, one of the Portland cements was combined with FA at 10, 20 and 35% replacement levels, respectively.

Hydration heat, free deformation, mechanical properties and stress development during restraint conditions have been measured (sealed curing) both at 20 ^{o}C isothermal conditions and at semi-adiabatic conditions, where the latter reflects the situation for each concrete when used in a 1 m thick wall structure. Materials model parameters have been identified and 1-dimensional stress calculations performed as a quality control of the materials models and to evaluate the relative cracking tendency among the concretes.

2 Materials, mix proportions and mixing

2.1 Materials

Cements
Composition of the cements and FA is given in *Table 2.1*. All cements were delivered by Norcem A.S., except the slag cement which was delivered by ENCI, The Netherlands.

Anleggsement (ANL): A low-alkali high strength cement of grade CEM I-52.5 LA according to EN-197 and NS 3086. The *ANL*-cement contains 4.1% limestone.

Modified sulphate resistant cement (SR_{mod}): Sulphate resistant low alkali cement (CEM I-42.5 R-SR-LA), according to EN-197 and NS 3086.

Modified Anleggsement (ANL_{mod}): Composed of sulphate resistant clinker and ordinary Portland cement clinker in proportion 4 to 1. The cement contains 4.1% limestone. ANL_{mod} is sulphate resistant and low alkali (CEM I-42.5 R-SR-LA), according to EN-197 and NS 3086.

Dutch slag cement (NL-slag): Consists of 26% Portland cement clinker, the rest is slag (CEM III/B 42.5 LH HS).

Table 2.1 Characteristics of the cements and the fly ash. Numbers in % if not otherwise specified.

	ANL	**ANL_{mod}**	**SR_{mod}**	**NL-slag**	**Fly ash**
SiO_2	21.0	20.4	21.4	-	54.4
Al_2O_3	4.4	3.8	3.5	-	22.0
Fe_2O_3	3.4	4.8	5.2	-	5.8
CaO	63.8	63.7	62.9	-	4.8
MgO	1.78	1.9	1.75	-	2.22
SO_3	3.0	3.0	2.7	-	0.52
LOI	2.52	2.60	1.15	-	4.08
K_2O	0.50	0.55	0.50	-	2.21
Na_2O	0.19	0.23	0.16	-	1.15
Na_2O_{ekv}	0.52	0.59	0.49	0.5	-
Free CaO	0.84	0.64	0.84	-	-
Fineness (Blaine, m^2/kg)	385	362	383	495	388
Specific weight (kg/m^3)	3.12	3.13	3.15	2.95	2.20
C_3S	57	63	55	26% OPC	-
C_2S	17	11	20		-
C_3A	5.8	1.9	0.5		-
C_4AF	10.4	14.6	15.7		-

The *aggregate* is non-alkali-silicate reactive natural sand (0 - 8 mm) and crushed stone (8 - 16 mm) from NorStone AS, Årdal, Norway (gneiss and granite mostly). It is used as standard laboratory aggregate in Norway.

Admixtures: Scancem P, a lignosulphonate based water-reducing agent (P), and Scancem Mighty 150, a naphthalen based super plasticizing agent (SP).

Deionized water

2.2 Concrete acronyms and mix proportions

Mix proportions are given in *Table 2.2*, including the air-, density- and slump measurements performed just after mixing. The concretes all have w/b = 0.40 and a binder volume fraction of 28.3%. No silica fume is used. The four cement products (*Table 2.1*) are investigated, in addition ANL_{mod} is replaced with 10, 20 and 35% FA corresponding to CEM II/A-V (10 and 20% FA) and CEM II/B-V (35% FA). Replacement level calculation according to NS-EN 197-1.

The *FA*-content is given as percentage of the weight of binder (c + FA). No air entraining admixture is used, hence all air is “natural” (entrapped air). The amount of SP was added to a target slump of 180 - 200 mm. The concretes do not contain silica fume.

The concretes are given the following names:

Concrete acronym	**Binder description**
NL-Slag	Concrete made with slag cement from The Netherlands.
ANL	Concrete made with Anleggsement
SR_{mod}	Concrete made with modified sulphate resistant cement
ANL_{mod}	Concrete made with modified anleggsement
ANL_{mod} ***10% FA***	Concrete made with ANL_{mod} and 10% FA
ANL_{mod} ***20% FA***	Concrete made with ANL_{mod} and 20% FA
ANL_{mod} ***35% FA***	Concrete made with ANL_{mod} and 35% FA

Table 2.2 Mix proportions for the tested concretes(kg/m^3), and fresh concrete measurements. All concretes have a w/b-ratio of 0.40.

	Constituent	SR_{mod} concrete	*NL-slag* concrete	*ANL* concrete	ANL_{mod} concrete	ANL_{mod} 10% FA concrete	ANL_{mod} 20% FA concrete	ANL_{mod} 35% FA concrete
Cement	SR_{mod}	391.1	0	0	0	0	0	0
Cement	NL-slag	0	391.3	0	0	0	0	0
Cement	ANL	0	0	391.0	0	0	0	0
Cement	ANL_{mod}	0	0	0	391.3	345.7	301.8	238.9
	FA-content	0	0	0	0	38.4	75.4	128.5
	Free water	156.5	156.5	156.4	156.5	153.6	150.9	147.0
	Sand 0 - 8mm Norstone, Årdal	960						
	Stone 8 - 16mm Norstone, Årdal	904						
	SCANCEM P [1)]	1.0	2.0	2.0	1.0	0.9	0.8	0.6
	SCANCEM M150 [2)]	3.4 / 3.5	3.8 / -	4.4 / 3.5	3.4 / 3.5	3.9 / 3.9	3.5 / 3.9	3.8 / 4.3
	Slump (mm)	215 / 80	245 / -	240 / 200	210 / 165	210 / 185	190 / 200	180 / 145
	Air content (%)	2.3 / 2.2	2.1 / -	1.4 / 1.7	1.7 / 0.6	2.1 / 2.3	1.5 / 1.7	2.0 / 2.0
	Density	2440 / 2470	2390 / -	2450 / 2450	2440 / 2450	2430 / 2420	2440 / 2430	2420 / 2420

1) The concrete made with *ANL* have a Scancem P (P) dosage of 0.5% of cement weight, while the concretes made with ANL_{mod}- and SR_{mod}-cements have half of that (0.25%) which is due to their low C_3A-content and to avoid significant retardation. The *NL-slag*-concrete has a P-dosage of 1.9% of cement weight which is due to the fact that the slag cement only consists of only 26% portland cement (the rest is slag) and, the content of Scancem P as % of cement weight is therefore 0.5%/0.26=1.9%. This was a mistake in the proportioning causing extra retardation, and setting did not occur before around 24 hour. This concrete should really have been re-run with less P or without P.

2) Two dosages of superplasticiser is given for each concrete, the first is for the 20 ^oC test, the second for the semi-adiabatic test. The same is due for slump, air content and density.

2.3 Mix procedure

The following mixing procedure was used:

(1) 1 min dry mixing (cement + FA + aggregate)
(2) Addition of mixing water + P + parts of the SP and then 2 min wet mixing
(3) 2 min rest
(4) 1 min final mixing (with adjustments of SP)

Fresh concrete measurements were:
- Slump
- Density
- Air
- Bleeding over the first 4 - 5 hours

3 Experimental program

3.1 Experimental program, NTNU

The concretes are tested (sealed curing) both at 20 ^{o}C isothermal condition and at semi-adiabatic conditions, see *Table 3.1*, where the latter reflects the situation for each concrete when used in a 1 m thick wall structure. One exception is for the *NL-slag* concrete which was only tested isothermally and also less comprehensively in terms of mechanical properties. NTNU test equipment and procedures are described in /1/. The experimental program for each concrete is given below. Fresh concrete temperature was 22 ± 0.5 ^{o}C for all concretes.

Note that any surface bleeding water collected on the Dilation Rig- and TSTM-specimens during the dormant period was removed before setting to avoid the disturbance of bleed water reabsorption after setting which to a certain extent influences both thermal dilation and autogenous deformation /2//3/. The bleeding measurements are discussed in Section 8.1.

Table 3.1 Test program overview - NTNU

Measurement	Temperature history	Testing times
Free deformation in the Dilation Rig. (100 x 100 x 500 mm prism)	20^{o} C isothermal + Semi-adiabatic	Measured continuously from ½ hour until 13 days for semi-adiabatic and around 3-4 weeks for isothermal conditions
Stress generation in the TSTM. (90 x 100 x 1000 mm prism)	20^{o} C isothermal + Semi-adiabatic	Measured continuously from setting until 13 days for semi-adiabatic and around 3-4 weeks for isothermal conditions
Compressive strength (100 x 100 mm cube)	20^{o} C isothermal + Semi-adiabatic	Tested at 28 days
E-modulus (100 x 200 mm cylinder) and Tensile splitting strength (100 x 100 mm cube)	20^{o} C isothermal + Semi-adiabatic	Tested at 28 days
Semi-adiabatic heat calorimetry (NTNU-box, 15 liters sample)	Semi-adiabatic (self-generated)	Measured continuously from ½ hour until 7 days

3.2 Experimental program, Norcem

The report also contains test results from similar concretes (except the NL-slag concrete) generated in the laboratory at Norcem A.S., Brevik, see also Appendix 2. The test results were submitted to NTNU and then evaluated and integrated as a part of the present work. Norcem performed hydration heat measurements, as well as compressive strength tests over time at 5 ^{o}C, 20 ^{o}C and 35 ^{o}C. These results are also included here, first of all, to determine the activation energy for each concrete. The activation energies have then been used in the further evaluation. Note that the concrete part materials used in the tests at NTNU and at Norcem come from the same batches, hence the common measurements are directly comparable.

4 Hydration heat results

4.1 NTNU-results

The results from the semi-adiabatic calorimeter tests are shown in the Fig. 4.1 and Fig. 4.2 as adiabatic temperature developments, see also Appendix 1. The results are discussed in the following section in connection with the corresponding results from Norcem. The concrete with *ANL* was tested twice from two successive batches (parallel with the TSTM and Dilation Rig tests), and both results are given in Fig. 4.1.

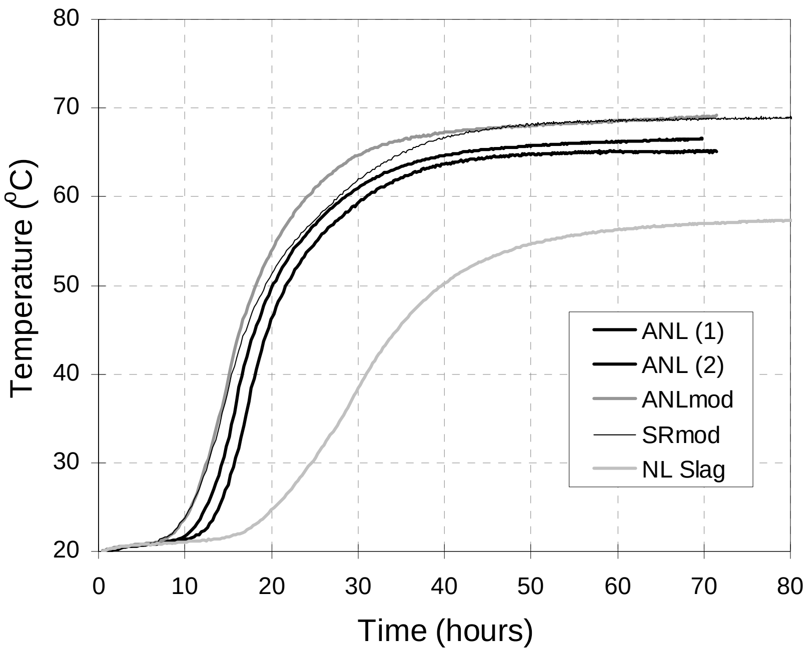

Fig. 4.1 Adiabatic temperature development, effect of cement type.

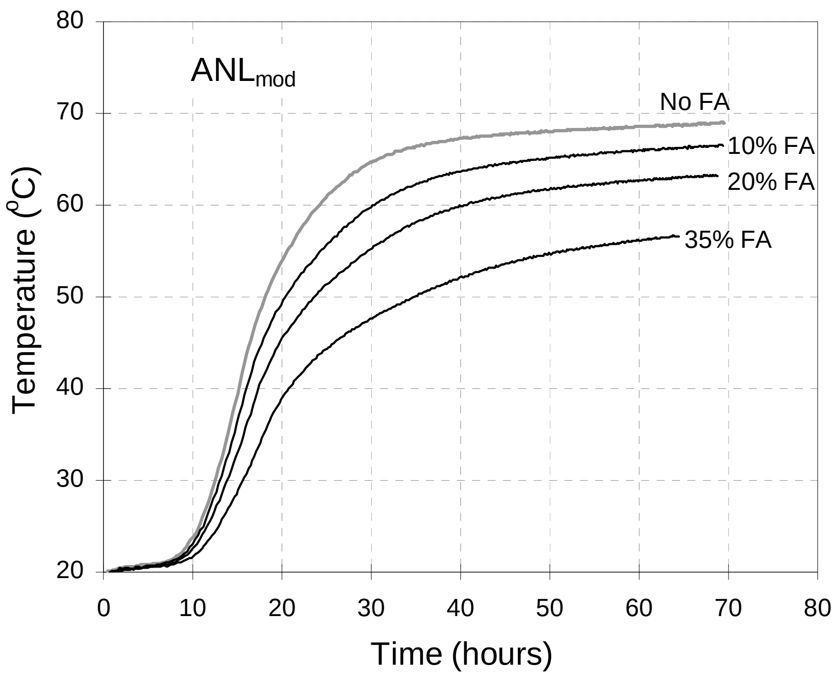

Fig. 4.2 Adiabatic temperature development, effect of FA-dosage.

4.2 NTNU vs. Norcem results

The Norcem heat results are given in Fig. 4.3 and Fig. 4.4. The results are treated similar to the NTNU-results shown in the previous section. Fig. 4.5 gives corresponding results from NTNU and Norcem; one sub-figure for each concrete composition. The table below, *Table 4.1*, gives adiabatic temperature rise values after 60 hours, and, as can be seen, the differences between the two laboratories vary between 0.8 ^{o}C and 5.7 ^{o}C for the 6 sets of concretes. The average adiabatic temperature rise for all concretes is quite similar from the two labs, while the coefficient of variation (COV) is 8%. The ANL_{mod} *35%FA* concrete has clearly the largest deviation (5.7 ^{o}C) and if this result is excluded the COV is reduced to 5%.

Results from other Round Robin investigations on hydration heat have been treated and collected below in order to study trends on the deviation in such tests on nominally identical concretes made in different laboratories. Note that in point 1, 3 and 5 in the list below there was very deviating heat behaviour in one result from one of the laboratories; these are not considered.

1) The present investigation: No systematic difference between the two laboratories: COV = 5%.
2) 2 laboratories testing the same concrete: COV = 5% /9/ (SVV-NTNU)
3) 4 laboratories testing the same concrete: COV = 4% /10/ (NOR-IPACS Maridalen)
4) 5 laboratories testing the same concrete: COV = 3% /11/ (IPACS, Basisbetong)
5) 9 laboratories testing the same concrete: COV = 6% /12/ (RILEM TC119)

When including the very deviating result in point 1 (present investigation) the COV increases from 5% to 8%, as already discussed, while the COV in point 5 increases similarly from 6% to 10%. Consequently, for the present Round Robin investigation (point 1) it can therefore be stated that the variation is quite in line with other similar comparisons. Furthermore, point 5 consisted of 14 measurements of heat of which 9 were adiabatic calorimeters and 5 were semi-adiabatic; all these measurements were treated together here. When looking at the two types of calorimeters separately, it is notable that the COV is quite similar. The same is also due for point 4 (3 adiabatic and 2 semi-adiabatic).

Table 4.1 Adiabatic temperature rise results after 60 hours, NTNU and Norcem (^{o}C)

		SR_{mod}	ANL	ANL_{mod}	ANL_{mod} 10% FA	ANL_{mod} 20% FA	ANL_{mod} 35% FA	NL-slag
NTNU	**ΔT_{ad} (60 h)**	**48.5**	**45.5**	**48.9**	**46.0**	**42.7**	**36.2**	**36.3**
	Relative to ANL_{mod}	*0.99*	*0.93*	*1.00*	*0.94*	*0.87*	*0.74*	*0.74*
Norcem	**ΔT_{ad} (60 h)**	**50.4**	**43.2**	**50.7**	**49.3**	**43.5**	**30.5**	-
	Relative to ANL_{mod}	*0.99*	*0.85*	*1.00*	*0.97*	*0.86*	*0.60*	-
Difference Norcem - NTNU		**1.90**	**-2.30**	**1.80**	**3.30**	**0.80**	**-5.70**	
Norcem relative to NTNU		*1.04*	*0.95*	*1.04*	*1.07*	*1.02*	*0.84*	

The heat data from Norcem and at NTNU show somewhat different setting times. *Table 4.2* shows setting according to criteria $t_{Q=12kJ}$, which is the time where 12 kJ pr. kg cement of heat is produced above the "baseline" heat production during the dormant period /14/. Setting in the NTNU-results is systematically later (average = 2 hours) than in the Norcem-results. The table also shows setting as found from the compressive strength tests at Norcem (extrapolated from the linear increasing part, see *Table 7.2*) and from the TSTM-rig tests at NTNU (defined as the time where the compressive stress is 1/10 of the maximum compressive stress during heating is reached during semi-adiabatic test conditions). Of course these "setting times" are not directly comparable, but supports the trend that setting was later at NTNU. The adiabatic temperature results obtained at Norcem and at NTNU are compiled in Fig. 4.5.

Table 4.2 Setting indicators, NTNU and Norcem (Mh = maturity hours)

	$t_{Q=12\ kJ}$ Norcem [Mh]	$t_{Q=12\ kJ}$ NTNU [Mh]	Difference NTNU-Norcem [Mh]	$t_{0,\ fc}$ Norcem [Mh]	$t_{0,\ TSTM}$ NTNU [Mh]	Difference NTNU-Norcem [Mh]
NL-slag	-	20.5	-	-	25.0	-
SR_{mod}	8.0	9.8	1.8	10.0	12.0	2.0
ANL	9.5	13.8	4.3	8.0	15.5	7.5
ANL_{mod}	8.6	10.0	1.4	9.5	13.0	3.5
ANL_{mod} 10% FA	8.8	10.6	1.8	9.5	13.0	3.5
ANL_{mod} 20% FA	8.6	10.8	2.2	10.0	13.5	3.5
ANL_{mod} 35% FA	11.0	11.7	0.7	12.0	15.0	3.0
Average	9.1	11.1	2.0	9.8	13.7	3.8

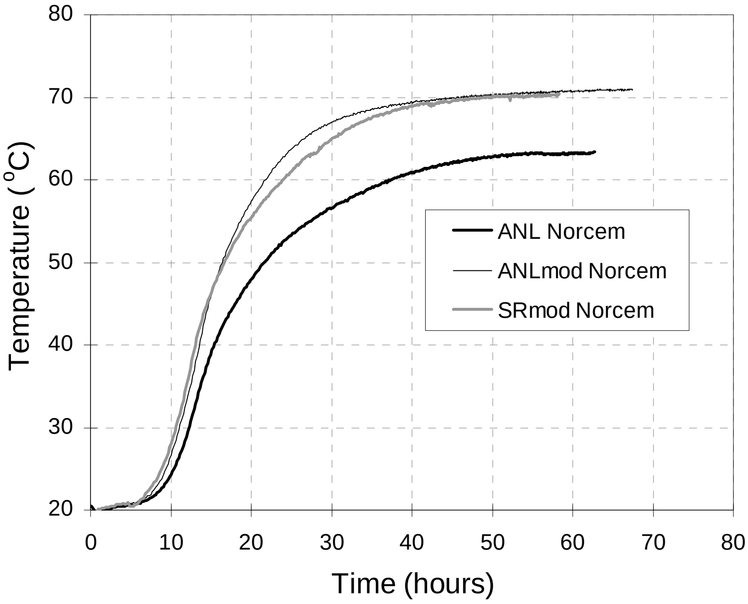

Fig. 4.3 Norcem results: Adiabatic temperature development, effect of cement type.

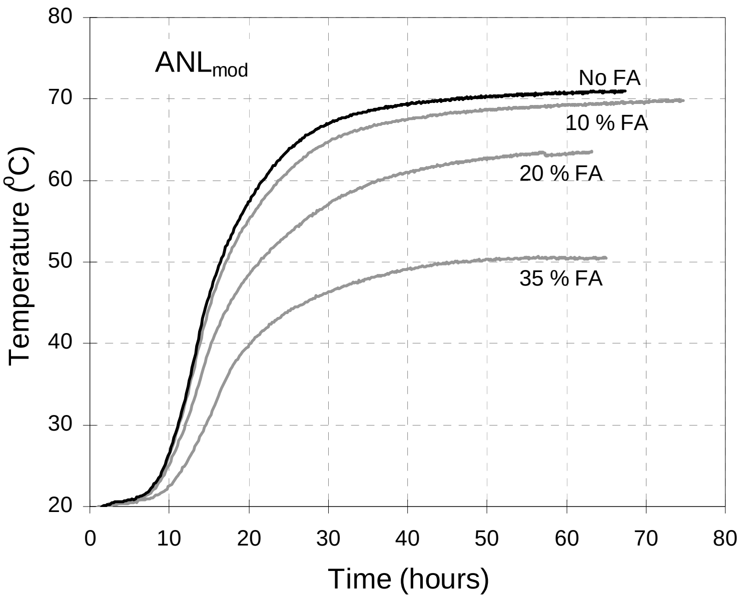

Fig. 4.4 Norcem results: Adiabatic temperature development, effect of FA-content.

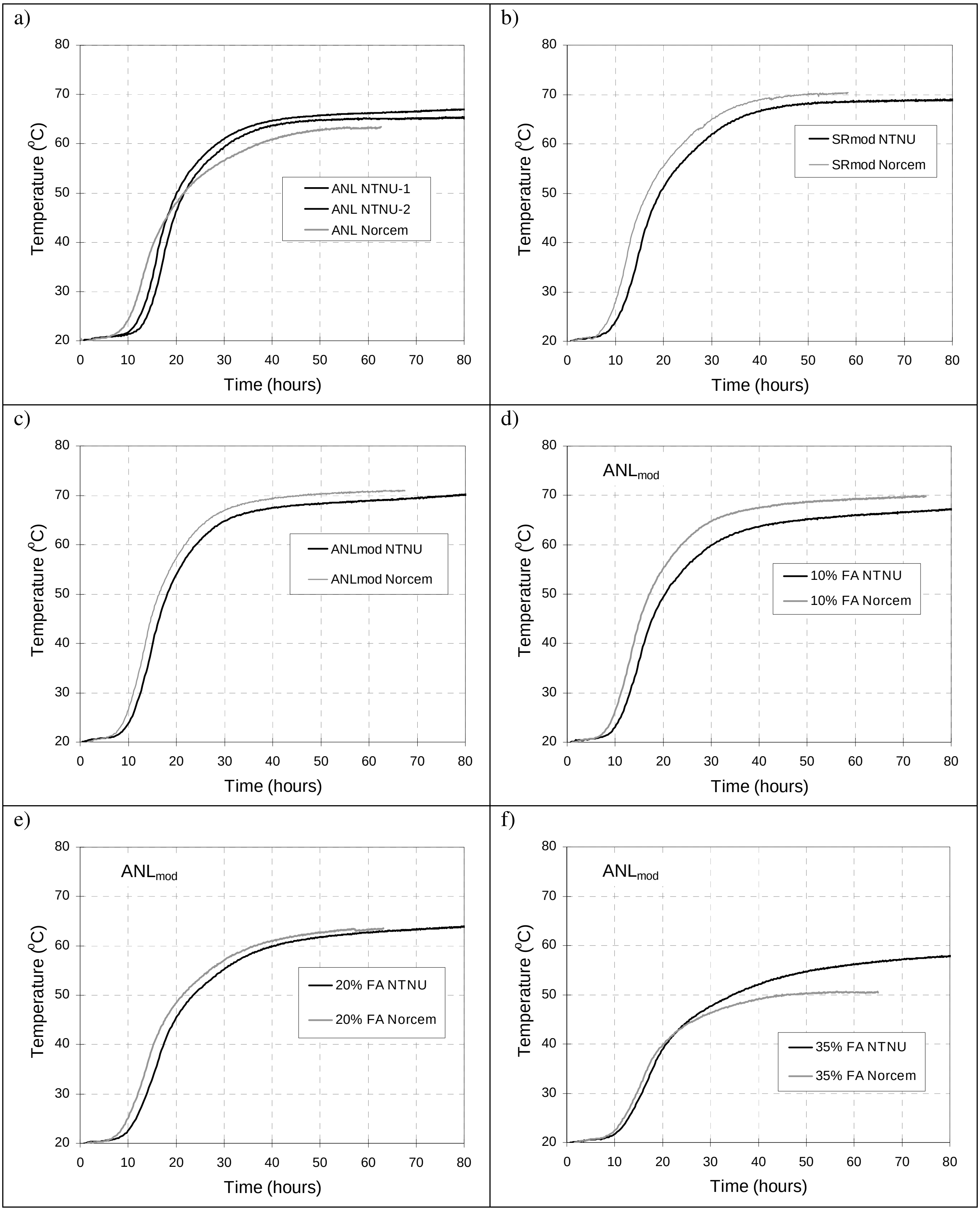

Fig. 4.5 Norcem- and NTNU-results: Adiabatic temperature development. One sub-figure for each concrete composition.

5 Semi-adiabatic test temperatures

5.1 Temperature calculations of a 1 m thick wall

The Dilation Rig, TSTM and mechanical property tests were performed both at 20 ^{o}C isothermal and under semi-adiabatic conditions, except for the NL-slag concrete which was only tested at 20 ^{o}C. The semi-adiabatic temperature developments used in the tests correspond to the average temperature in a 1.0 m thick and 6.0 m high wall structure for the given concrete (standing on a 1.2 m thick slab), as calculated by the Danish FEM program 4C-Temp&Stress, see Fig. 5.1. The NTNU-heat results from the previous chapter were used as background for the calculations. The following presumptions were set for the calculation:

- 18 mm plywood as formwork is used on both sides of the wall, and one layer of plastic on top. The foundation is uncovered.
- 20 ^{o}C fresh concrete temperature, the initial temperature of the foundation is the same.
- 20 ^{o}C air temperature
- no solar radiation
- no wind

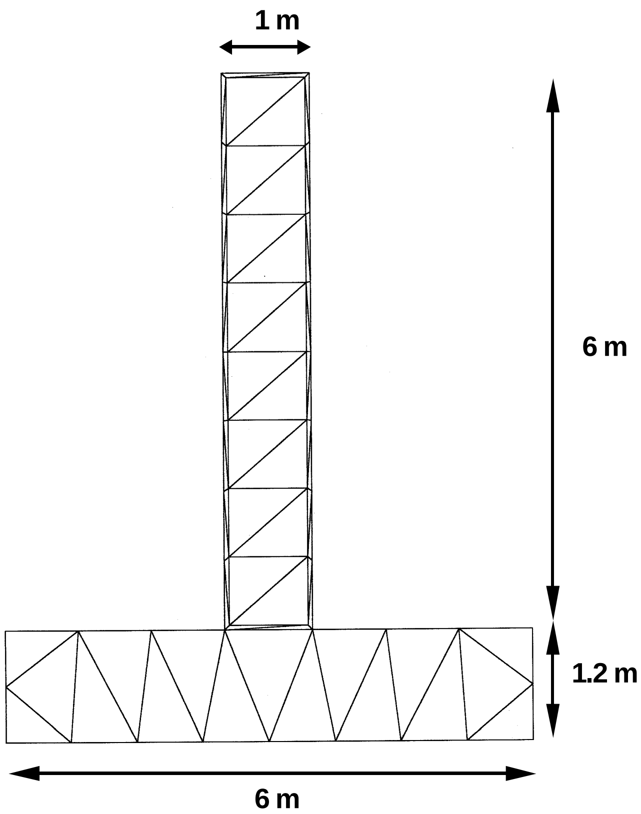

Fig. 5.1 Element net and dimensions

Calculated average temperatures for 4 of the 7 tested concretes are given in Fig. 5.2. In *Table 5.1* the maximum values are given, together with the adiabatic temperature rise values from the heat calorimeter tests. Temperature calculations were not performed for ANL_{mod} and ANL_{mod} *10% FA* (nor for *NL-slag*)

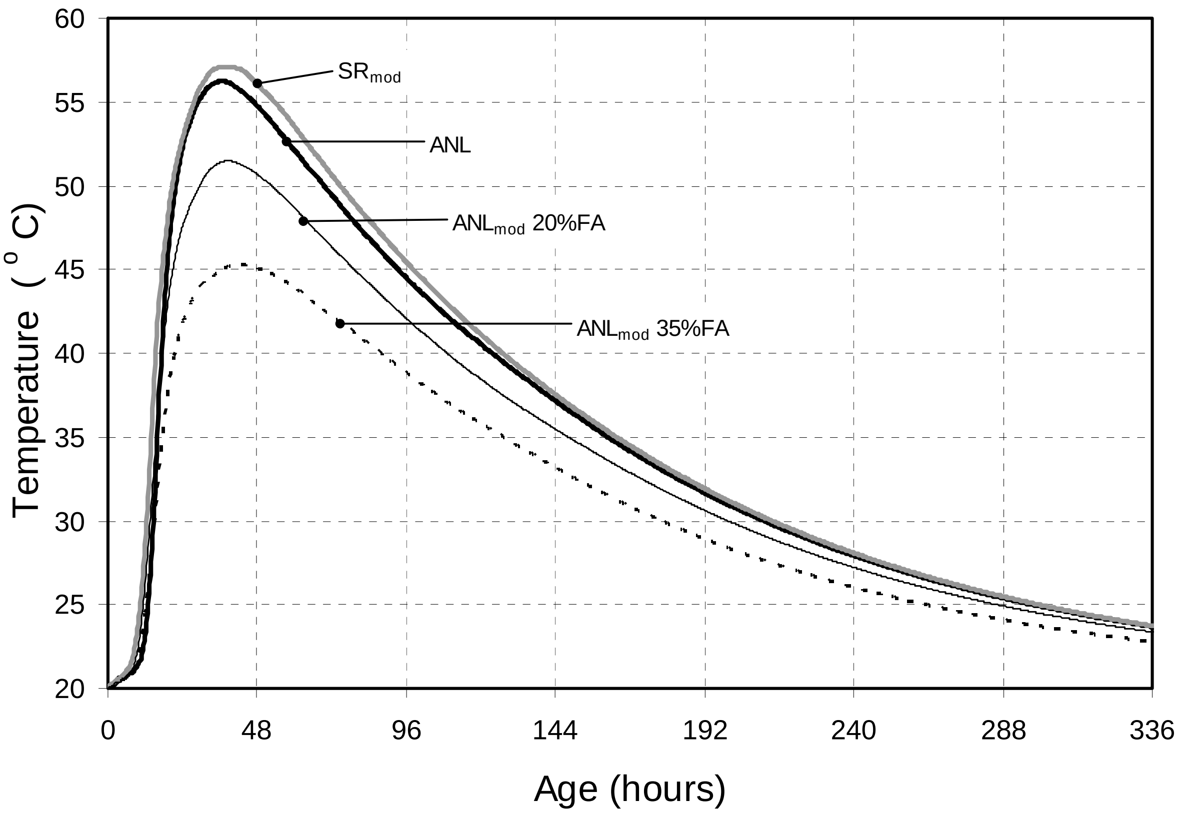

Fig. 5.2 Calculated average temperature development in the wall for 4 of the 7 tested concretes.

Table 5.1 Measured adiabatic temperature rise from the calorimeter tests after 60 h ($\Delta T_{ad}(60h)$) calculated average maximum wall temperature ($T_{max,avg\ wall}$) and corresponding temp. rise ($\Delta T_{max,avg\ wall}$).

	SR_{mod}	ANL	ANL_{mod}	ANL_{mod} 10% FA	ANL_{mod} 20% FA	ANL_{mod} 35% FA	NL-slag
$T_{max,avg}$ wall	57.1	56.2	-	-	51.5	45.3	-
$\Delta T_{max,avg}$ wall	37.1	36.2	-	-	31.5	25.3	-
ΔT_{ad} (60 h)	48.5	45.5	48.9	46.0	42.7	36.2	36.3

5.2 Temperatures used to control the tests

During the laboratory tests, the following semi-adiabatic temperature developments (relevant for the already discussed 1 m wall) were used:

- The calculated temperature curve for the *ANL* in Fig. 5.2 was used to control the test temperature for this concrete. The same temperature was also used to control the tests on the concretes with *SR_{mod}*, *ANL_{mod}* and *ANL_{mod} 10% FA*, but adjusted to match the setting times (as indicated by the NTNU calorimeter tests, see previous chapter). This is a slight simplification since *$\Delta T_{ad}(60h)$* really differed around 4 °C among these concretes.
- The calculated temperature curve for ANL_{mod}20% FA was used to control the test temperature for this concrete.
- The calculated temperature curve for ANL_{mod}35% FA was used to control the test temperature for this concrete.

Note that the temperature histories used in the TSTM-tests were imposed as normal “smooth” temperatures, while those in the Dilation Rig tests were imposed in a “stepwise” manner in order to separate thermal dilation and autogenous deformation, see example in Fig. 5.3. The CTE-values determined in each temperature step are used to deduce the continuous thermal dilation for the whole test period. The measured total deformation during the test minus the deduced thermal dilation then gives the development of autogenous shrinkage. Note that autogenous shrinkage is also measured directly during the test at each isothermal period.

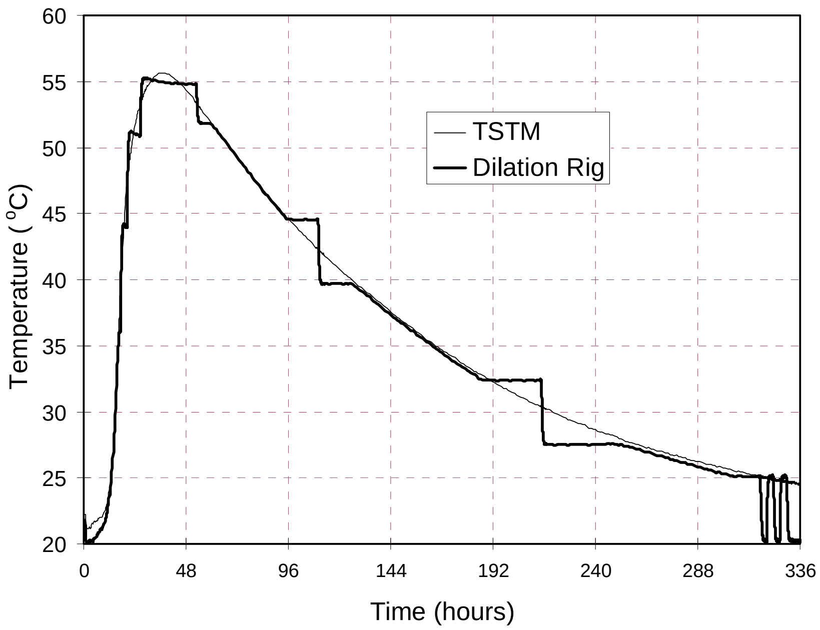

Fig. 5.3 Example of imposed temperature histories in the Dilation Rig (stepwise) and in the TSTM (smooth).

6 28-days strength and E-modulus results

The results are shown in Fig. 6.1 and Fig. 6.2. Compressive strength results from NTNU and Norcem are plotted together in Fig. 6.3. Curing at 20 ^oC and at semi-adiabatic conditions naturally result in very different maturity at the time of testing after 28 days. The concrete with *NL-slag* cement is not discussed. The following trends can be seen:

Effect of cement type
f_c and f_t: SR_{mod} has the highest strength, then *ANL* and ANL_{mod}.
f_{ts}: It is notable that the ranking is different from f_t; ANL_{mod} is highest, then SR_{mod} and *ANL*.
E: No significant effect of cement type

Effect of FA
f_c: Unsystematic effect, though there is tendency of a slight decrease with FA-content especially at 20 ^oC curing.
f_t: Little effect at 20 ^oC conditions, slight increase at semi-adiabatic conditions.
f_{ts}: The trend is a clear increase with FA-content.
E: Slight decrease at 20 ^oC conditions, while the trend is an increase at semi-adiabatic conditions.

Compressive strength, NTNU vs. Norcem (Fig. 6.3)
The Norcem strengths are 8.5% higher than NTNU as an average. (10% higher for the 20 ^oC tests, and 7% higher for the "semi-adiabatic" tests (Norcem: curing at 35 ^oC, NTNU: curing at semi-adiabatic). For ANL_{mod} and ANL_{mod} *10%FA* the difference is as high as around 20% at 20 ^oC. For the same two concretes it is notable that the 20 ^oC strength in the Norcem results is higher than the 35 ^oC strength. This is not the case in the NTNU results (20 ^oC vs semi-adiabatic curing).

Relation between direct tensile strength f_t and splitting strength f_{st}
The tensile strength is important in the calculation of the crack index, hence the relation between the two methods is interesting. It can be seen from Fig. 6.4 that there is no single relation. There is a trend that FA reduces the f_t/f_{st}-ratio.

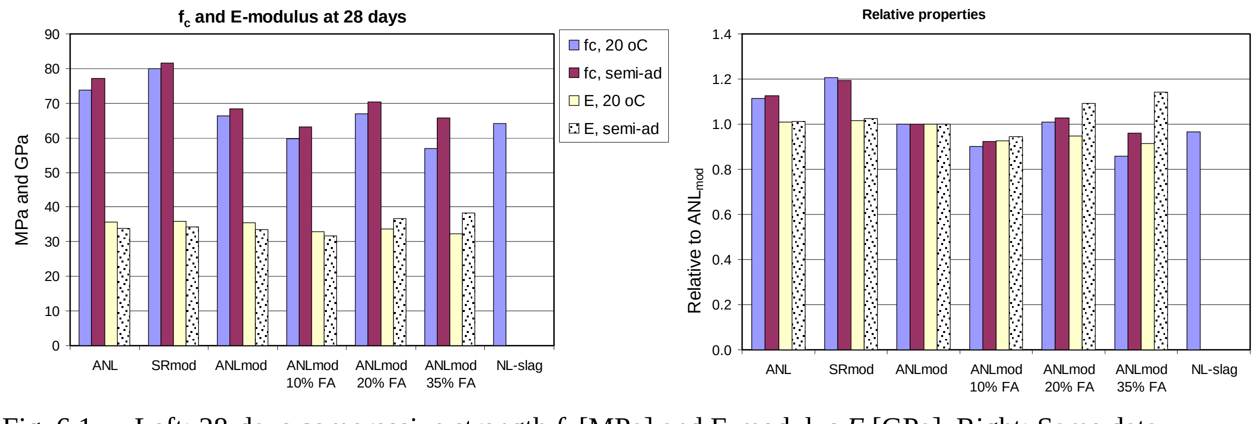

Fig. 6.1 Left: 28-days compressive strength f_c [MPa] and E-modulus *E* [GPa]. Right: Same data relative to ANL_{mod}. Note that ANL_{mod} *20%FA* was tested after 33 days.

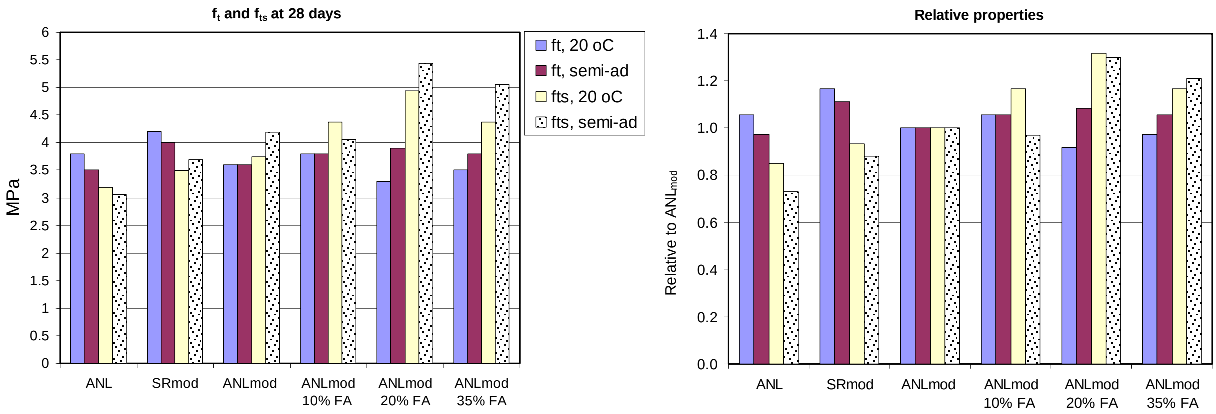

Fig. 6.2 Left: 28-days direct tensile strength f_t and splitting tensile strength f_{ts}. Right: Same data relative to ANL_{mod}. Note that ANL_{mod} *20%FA* was tested after 33 days.

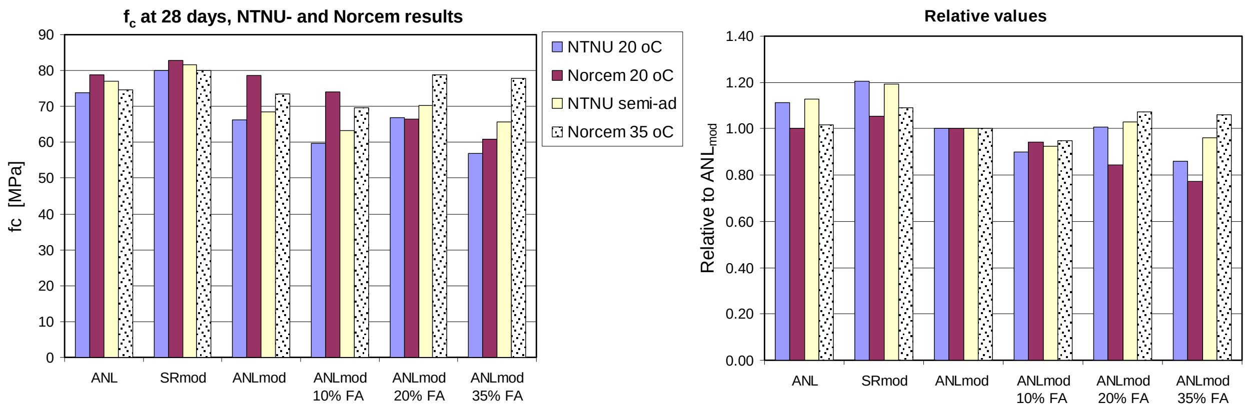

Fig. 6.3 Left: 28-days compressive strength f_c measured at NTNU and Norcem. Right: Same data relative to ANL_{mod}. Note that ANL_{mod} *20%FA* was tested after 33 days.

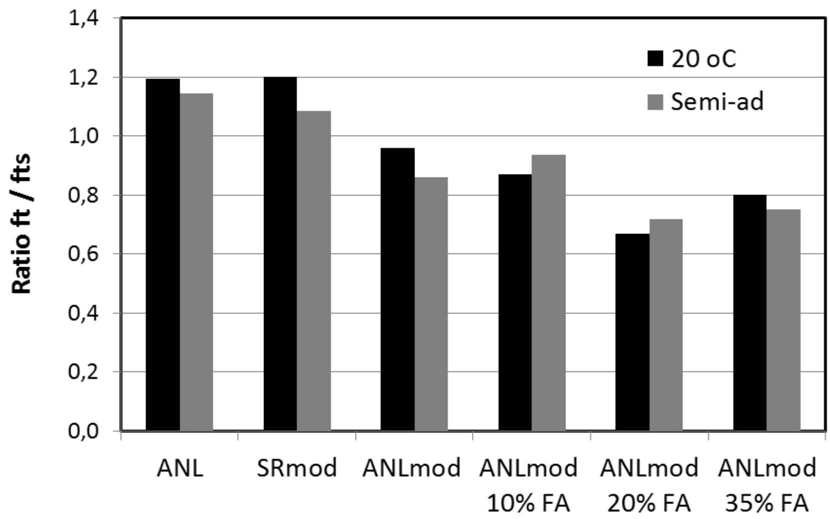

Fig. 6.4 Relation between direct tensile strength (f_t) and splitting strength (f_{st}) after 28 days at 20 °C isothermal curing and curing at semi-adiabatic conditions. Note that ANL_{mod} *20%FA* was tested after 33 days.

7 Compressive strength and activation energy, Norcem results

7.1 Model parameters

The formula used to express the properties, *Equation [1]* (modified Model code equation), contains an X_{28}-parameter which is the 28-days compressive strength (f_{c28}), E-modulus (E_{28}) or tensile strength (f_{t28}). A basic idea behind this formula /5/ is that the parameters *s* and t_0 are set to be the same for all the properties and, thus, they can be identified from the compressive strength tests. The parameter *n* is set to be 1.0 for the compressive strength. The time parameter t_0 is the starting (maturity) time for the properties (around time of final set), whereas t_{eq} is the concrete maturity in days (also denoted equivalent time).

- At NORCEM, Brevik, cubes have been cured at 5°C, 20°C and 35°C and compressive strength has been tested over time (giving the f_{c28} and *s*-parameters).
- At NTNU 28-days E-modulus and tensile strength have been tested (giving the E_{28} and f_{t28} parameters). In the stress calculations discussed in Chapter 9 the default parameter n_E=0.37 is used for the E-modulus and n_t=0.59 is used for tensile strength /**7**/.

Equation [1]

$$X(t_e) = X_{28} \cdot \left\{ \exp\left[s \cdot \left(1 - \sqrt{\frac{28}{t_{eq} - t_0}} \right) \right] \right\}^n$$

7.2 Activation energy, analyzing procedure

The maturity *M* (or equivalent time, t_{eq}) is defined as:

Equation [2]

$$t_{eq} = M = \sum_t \exp(E_r(\frac{1}{293} - \frac{1}{273 + T_i})) \times \Delta t_i$$

Where E_r [°K] (the activation energy divided by the gas constant R=8.314 [kJ/(mole K)]) is the temperature sensitivity parameter. $E_r = A$ for T > 20 and $E_r = A + B \cdot (20 - T)$ for T < 20

Two procedures are used:

1. Norwegian Standard method (NS 3656): The compressive strength results are plotted on a maturity scale and fitted at 40% of f_{c28} from the 20 °C test. The 35 °C test results are fitted first by choosing an appropriate *A*-parameter, then the 5 °C results, similarly, by choosing the "appropriate" *B*-parameter.
2. Curve-fitting /6/: The continuous function expressed by *Equation [2]* is fitted to the 20°C results. *A*- and *B-parameters* are then found (simultaneously) through minimizing (least square root deviation iteration) the deviation between the 35 °C- and 5 °C-results and the function. When *A* and *B* are found, the function (*Equation [2]*) is fit to all test results in a second iteration procedure. This gives the final f_{t28}, *s* and t_0 parameters ("best fit" parameters).

For both procedures actual temperatures measured during the tests were used as basis for calculating the maturity development. The results from both procedures are dealt with in this chapter, but for the next chapters only the **procedure 2** parameters are used.

7.3 Norcem-results: Strength and activation energy

The following sections give the compressive strength results from Norcem for each concrete and also activation energies found by the two procedures described above. The results are compiled in Section 7.4. The raw data is given in Appendix 3.

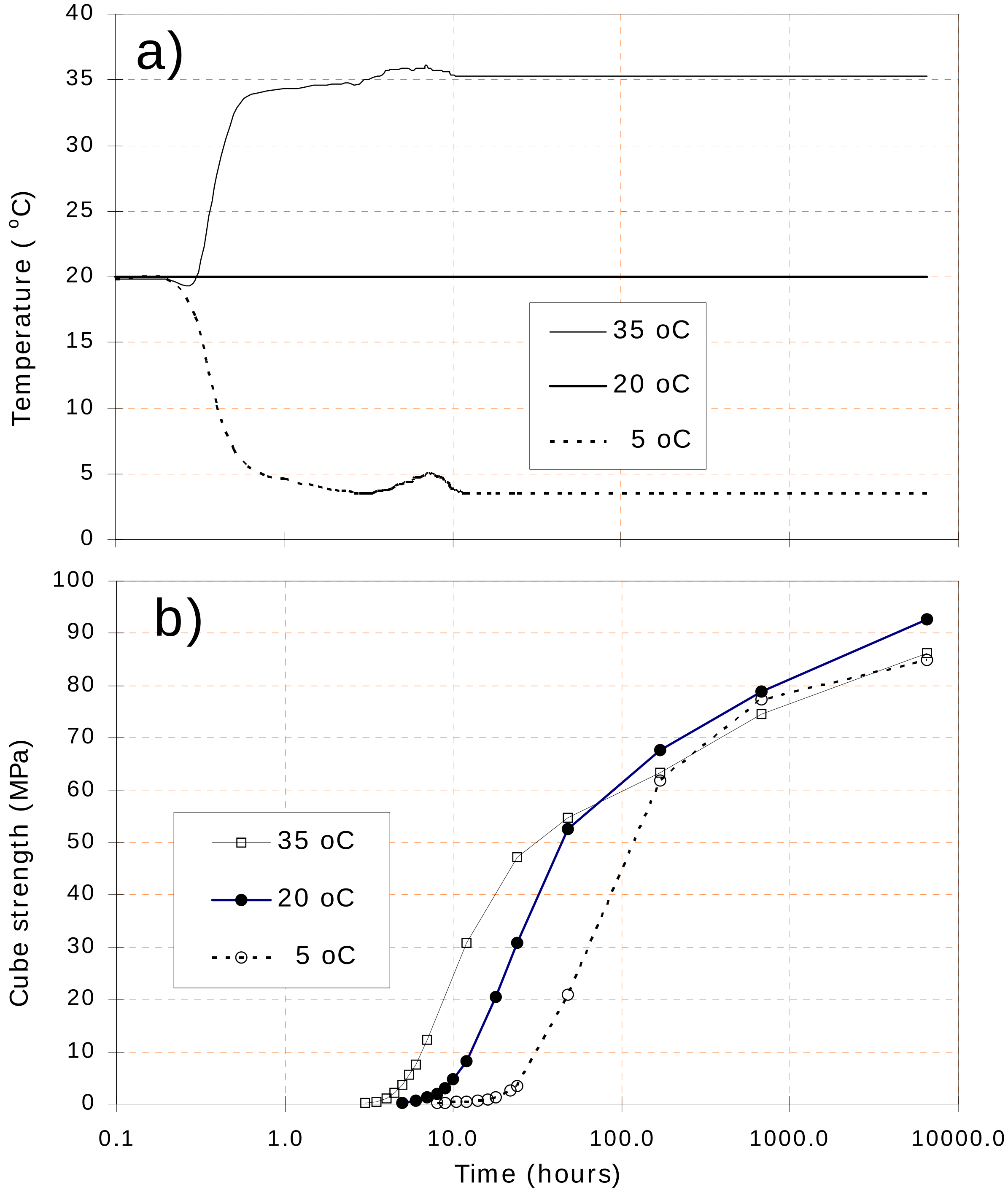

Fig. 7.1 ***ANL*****: Measured temperature and strength**

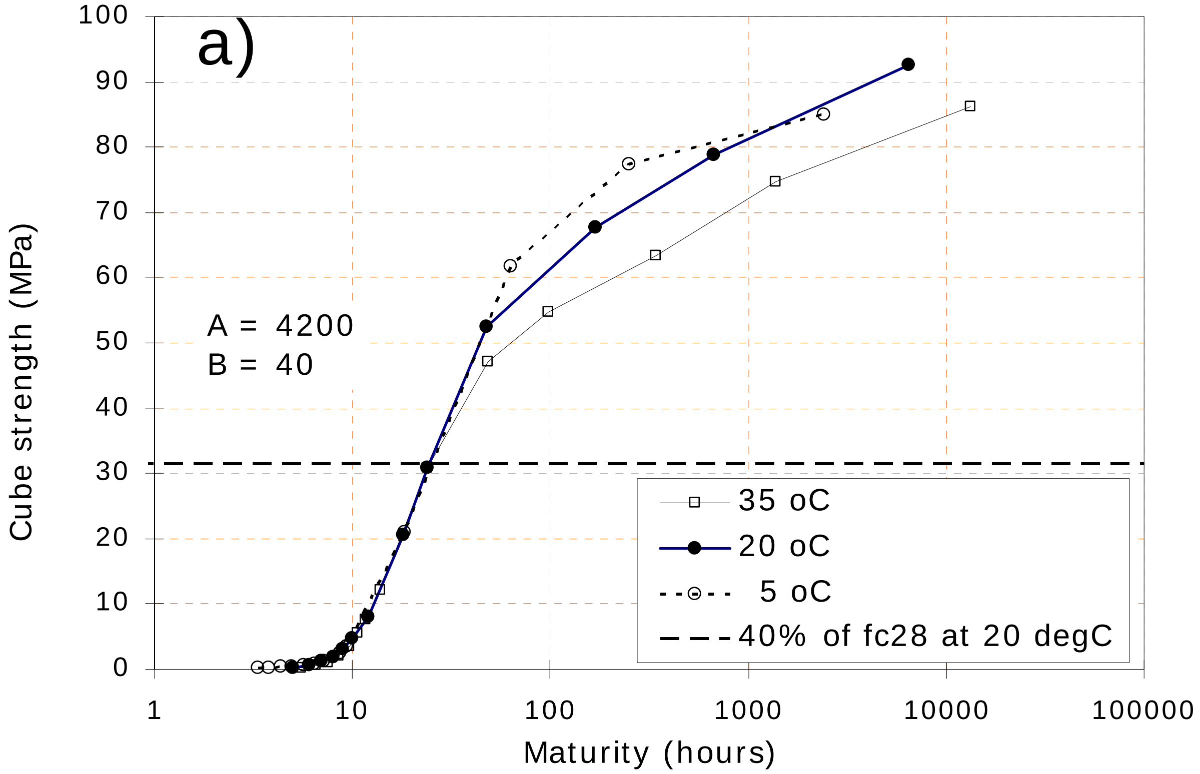

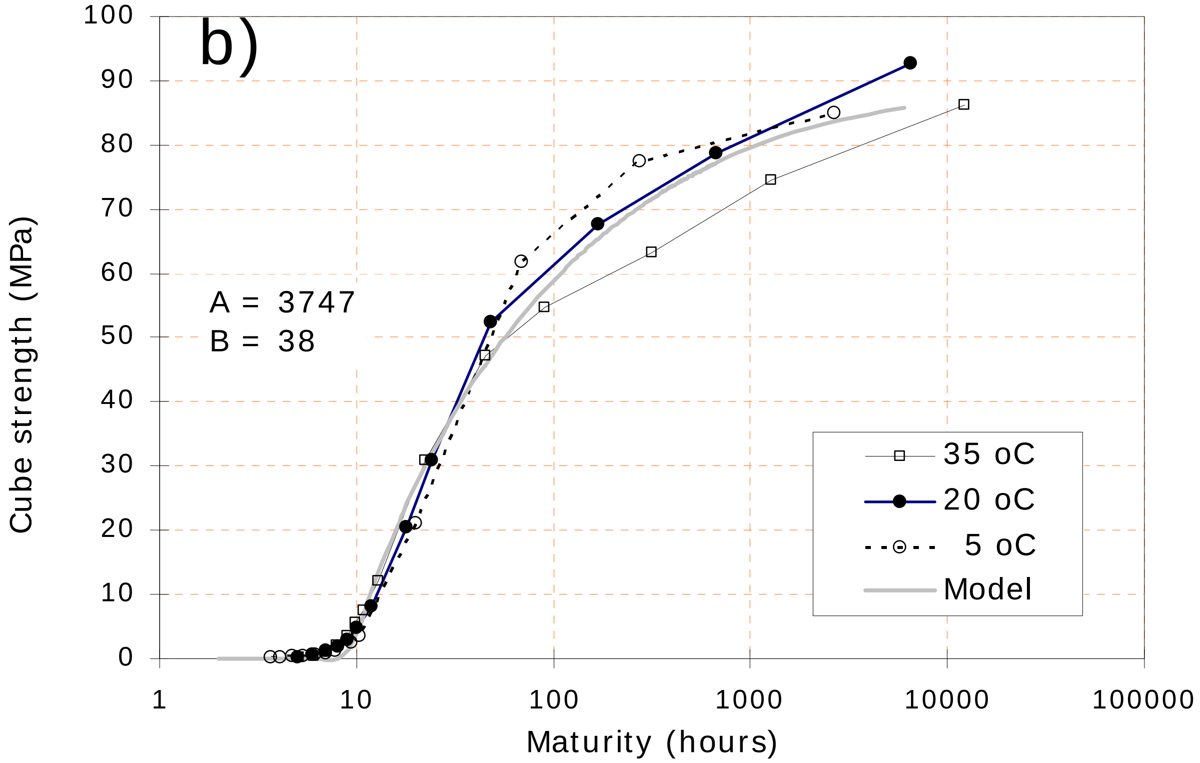

Fig. 7.2 *ANL*: **Strength vs. maturity time based on NS 3656 (a) and on best fit between model (20 °C) and results over time up to 28 days (b).**

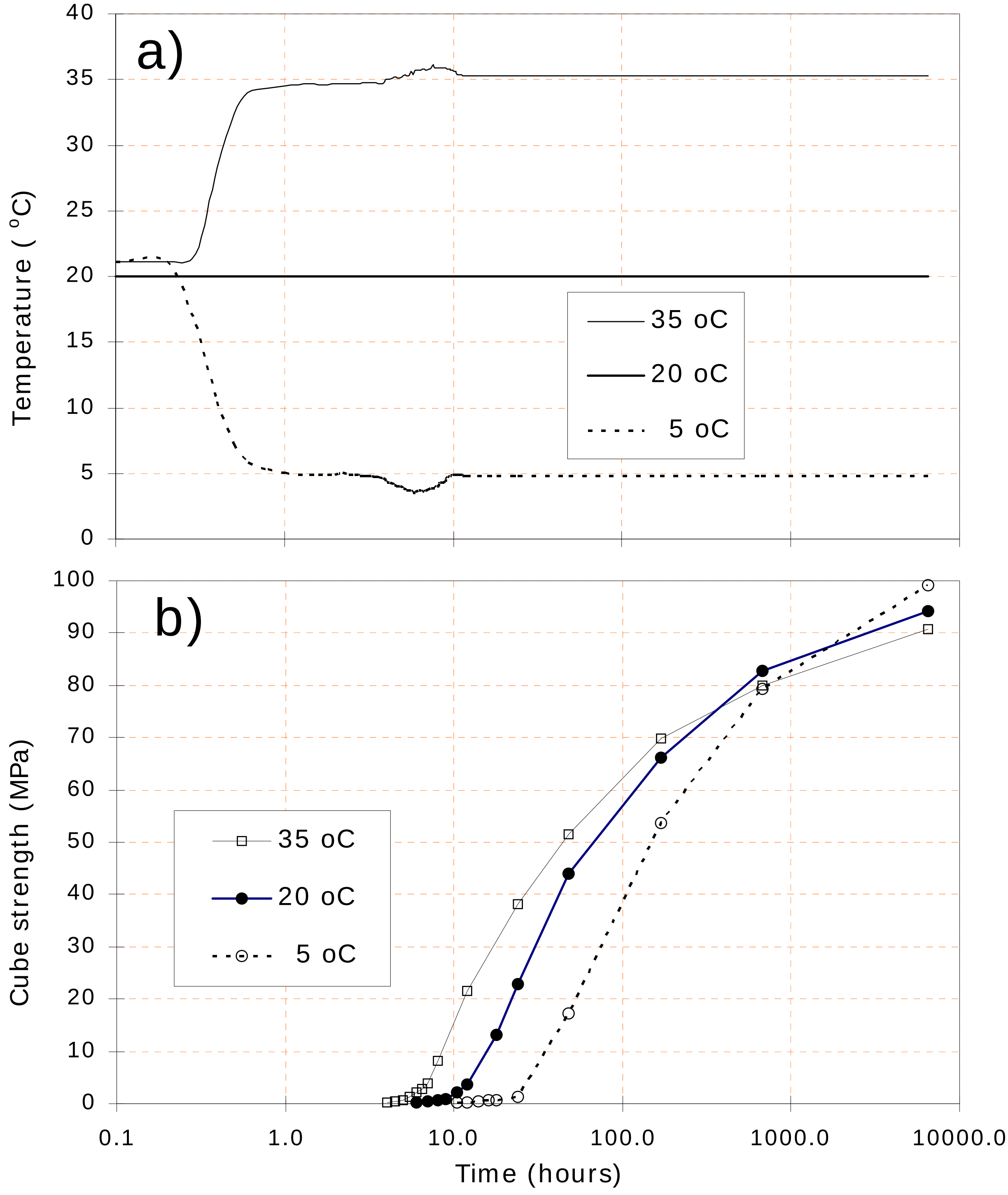

Fig. 7.3 *SR*$_{mod}$: Measured temperature and strength

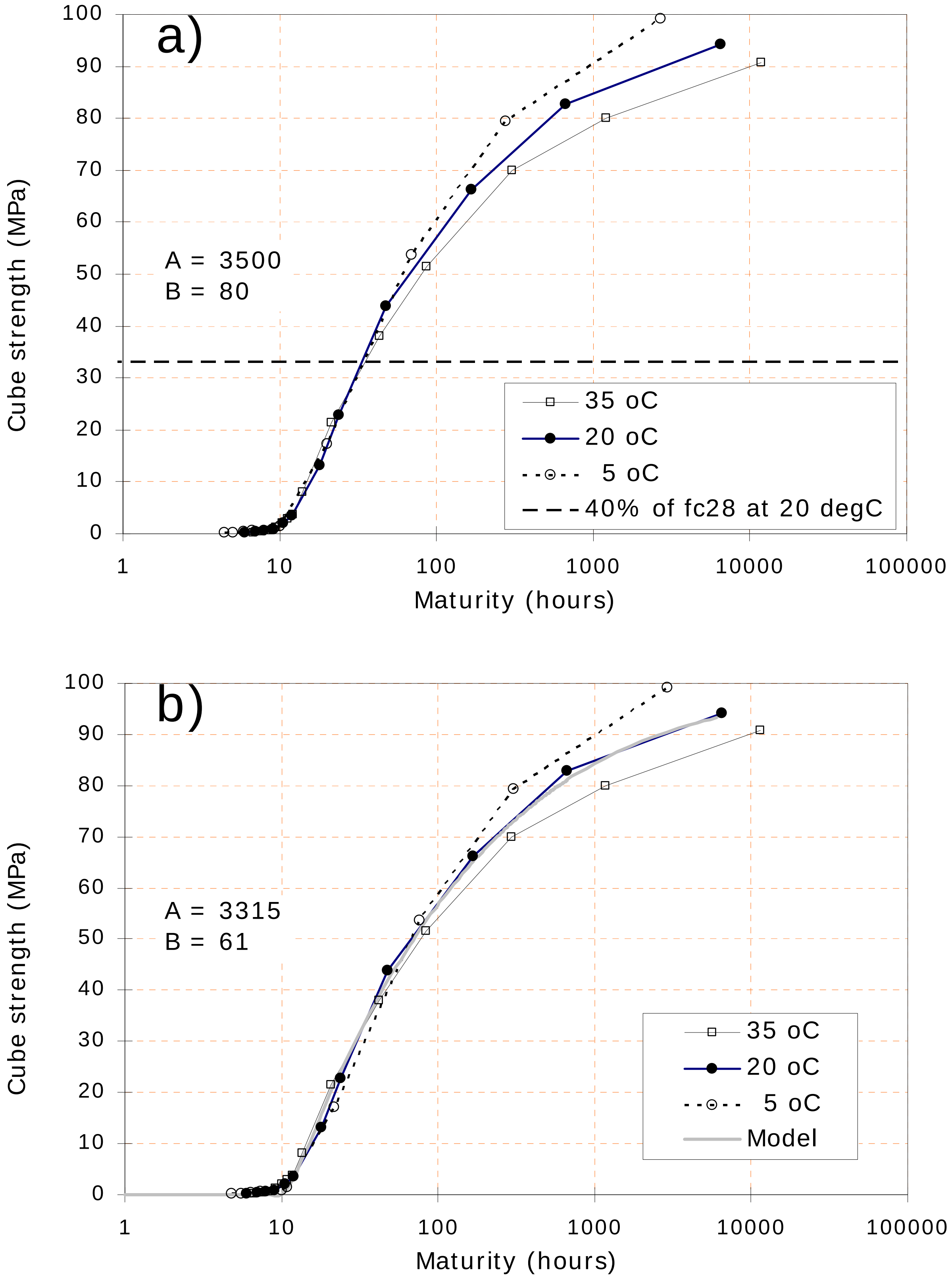

Fig. 7.4 ***SR$_{mod}$*: Strength vs. maturity time based on NS 3656 (a) and on best fit between model (20 °C) and results over time up to 28 days (b).**

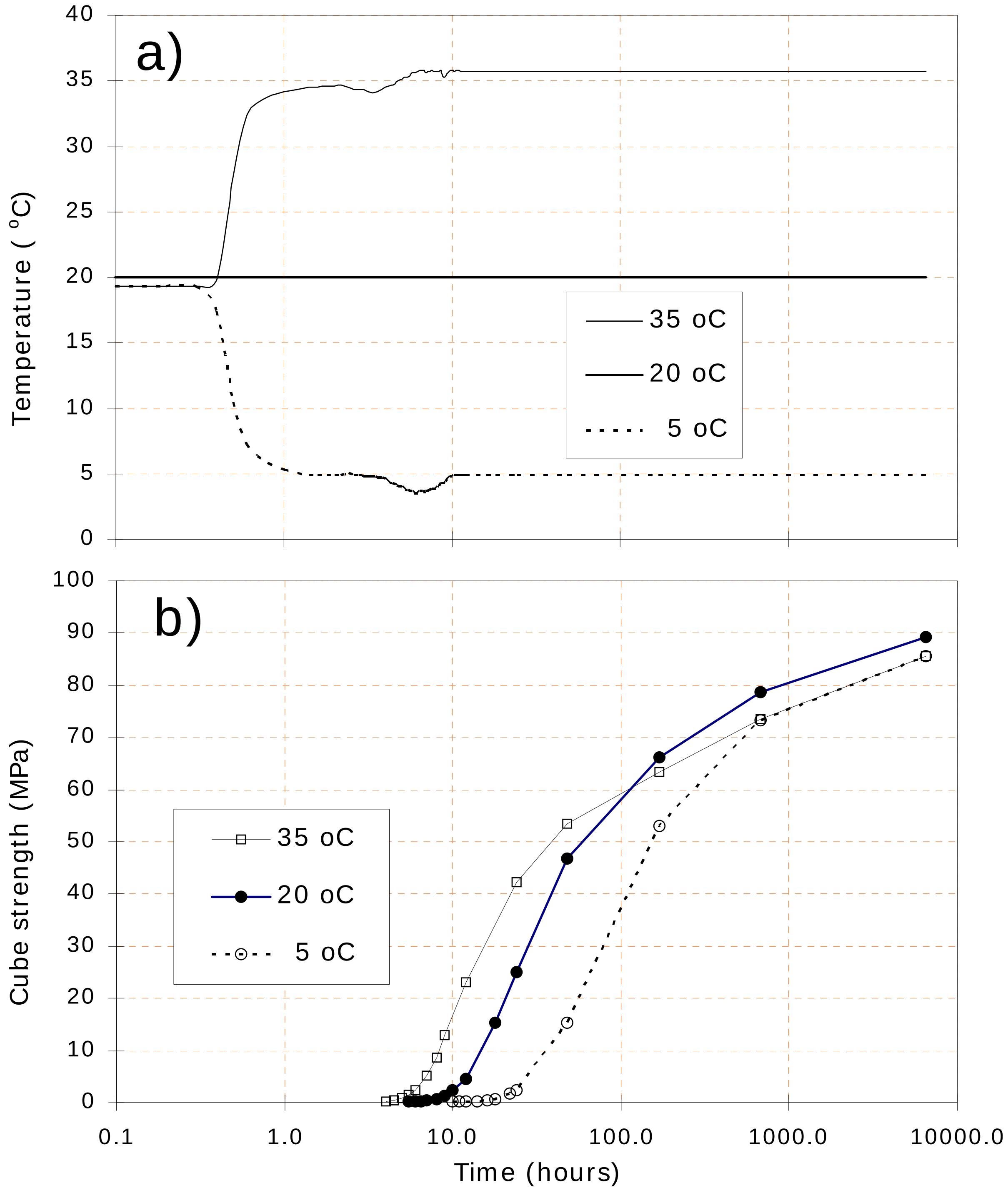

Fig. 7.5 *ANL_{mod}*: Measured temperature and strength

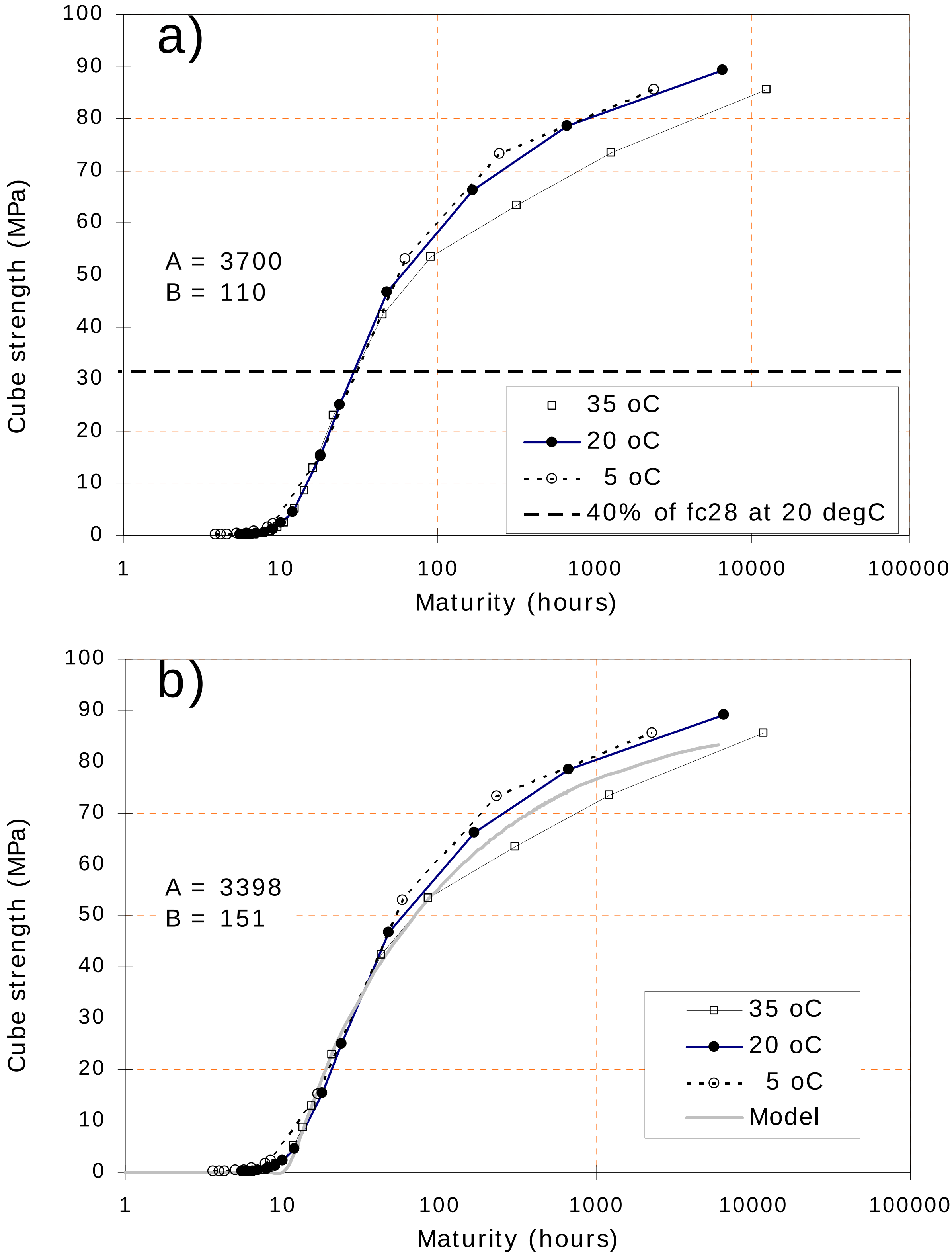

Fig. 7.6 ***ANL_{mod}*: Strength vs. maturity time based on NS 3656 (a) and on best fit between model (20 °C) and results over time up to 28 days (b).**

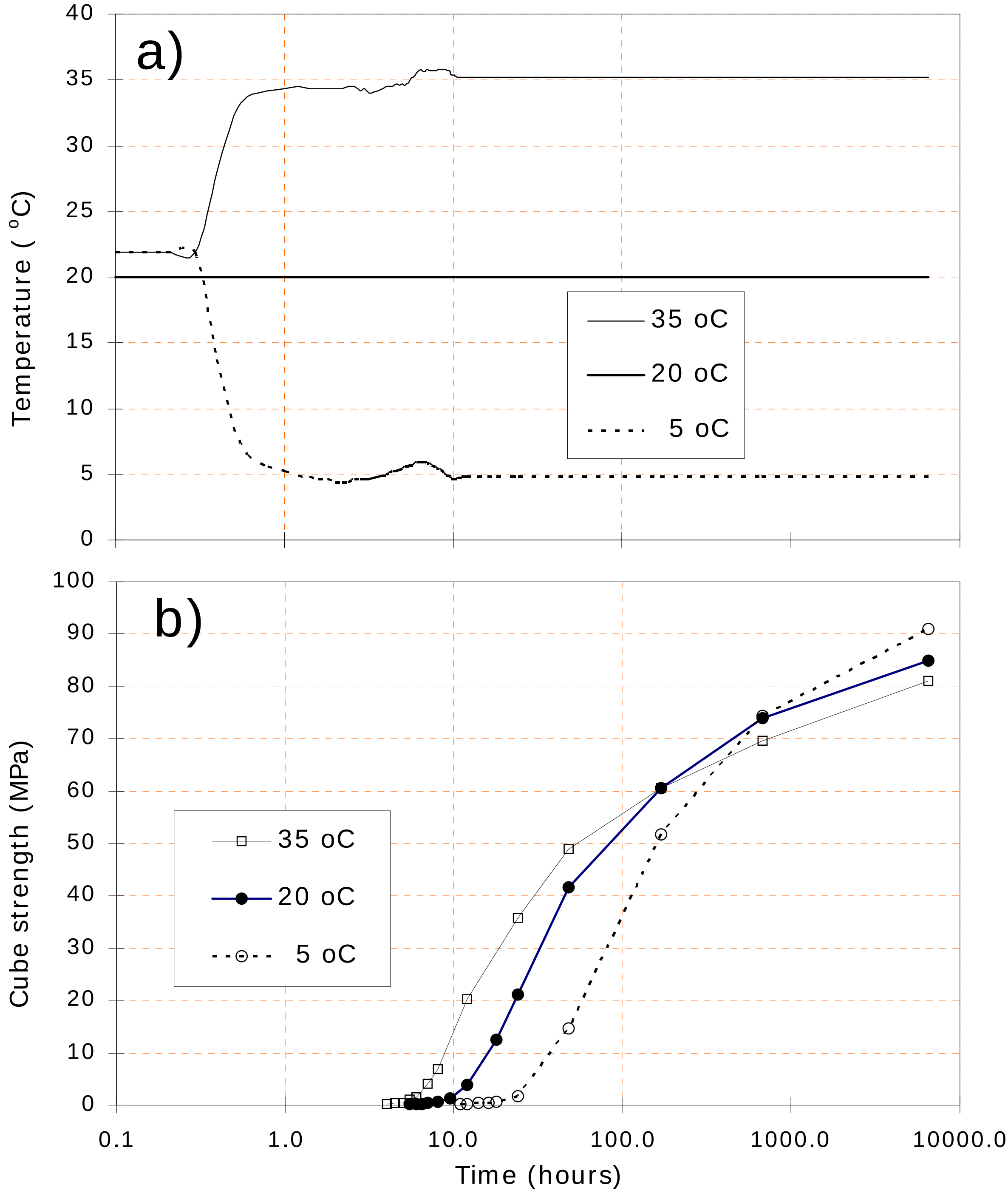

Fig. 7.7 ***ANL$_{mod}$ 10%FA*****: Measured temperature and strength**

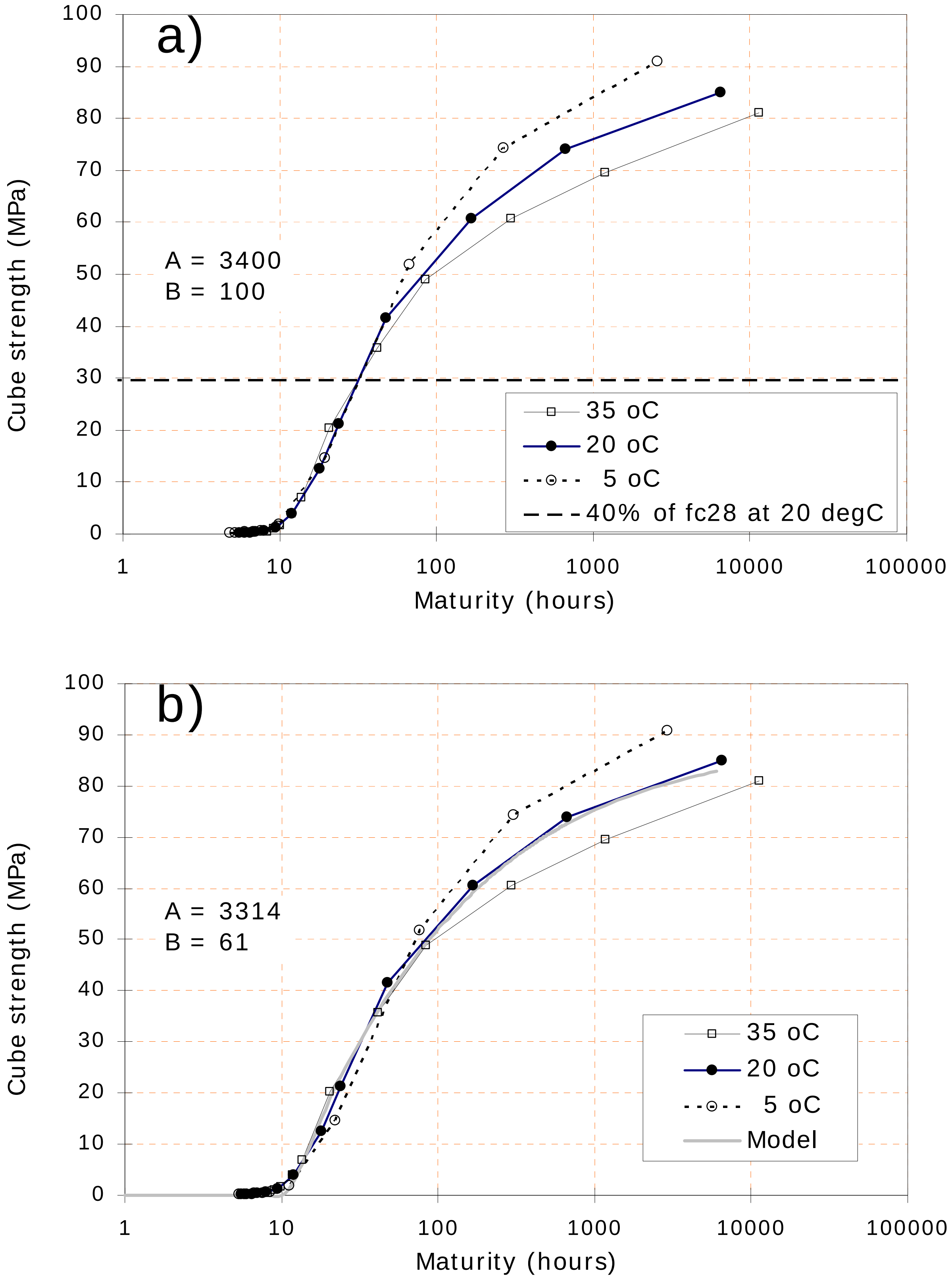

Fig. 7.8 ***ANL$_{mod}$* *10%FA*: Strength vs. maturity time based on NS 3656 (a) and on best fit between model (20 °C) and results over time up to 28 days (b).**

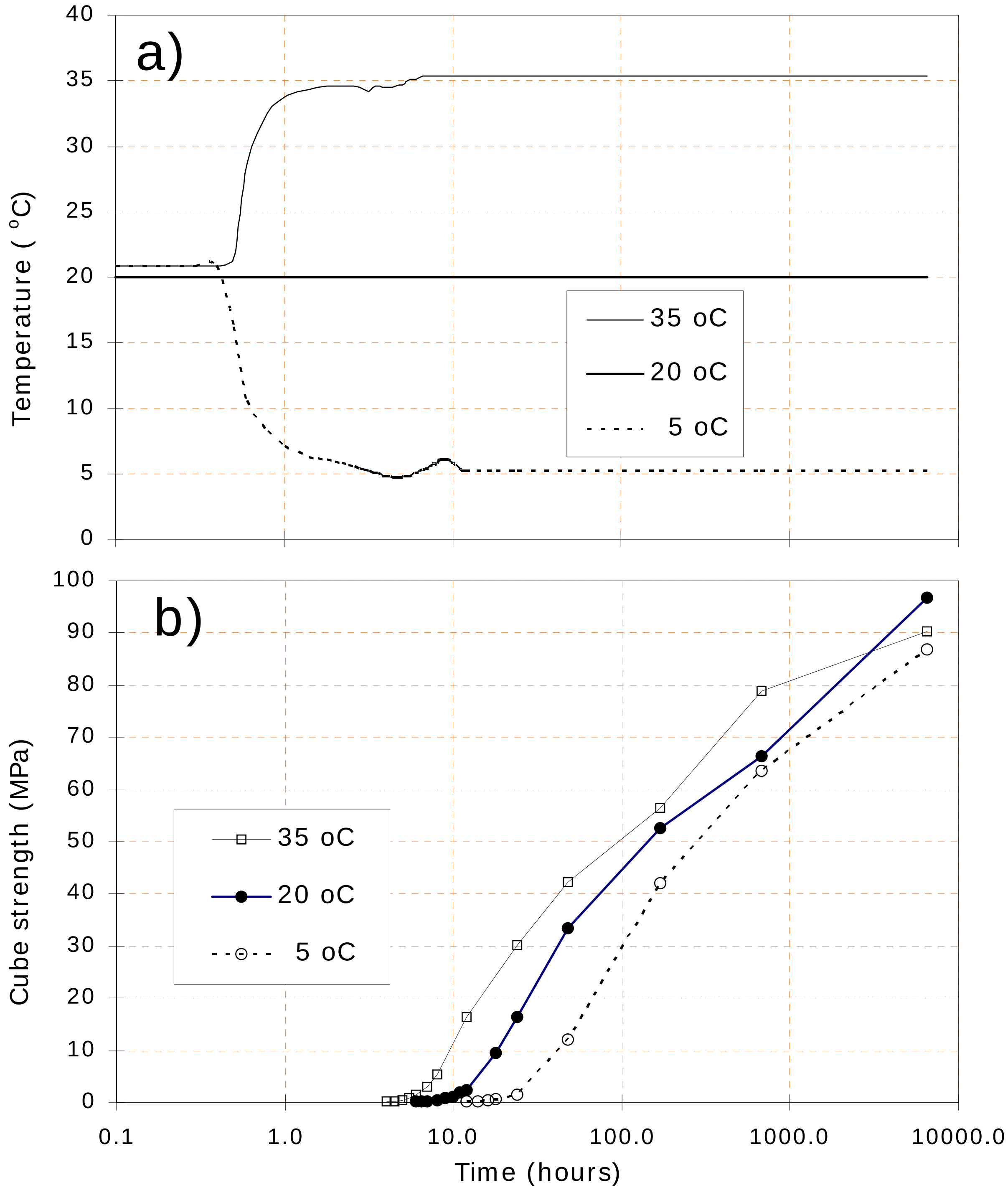

Fig. 7.9 ***ANL_{mod} 20%FA*****: Measured temperature and strength**

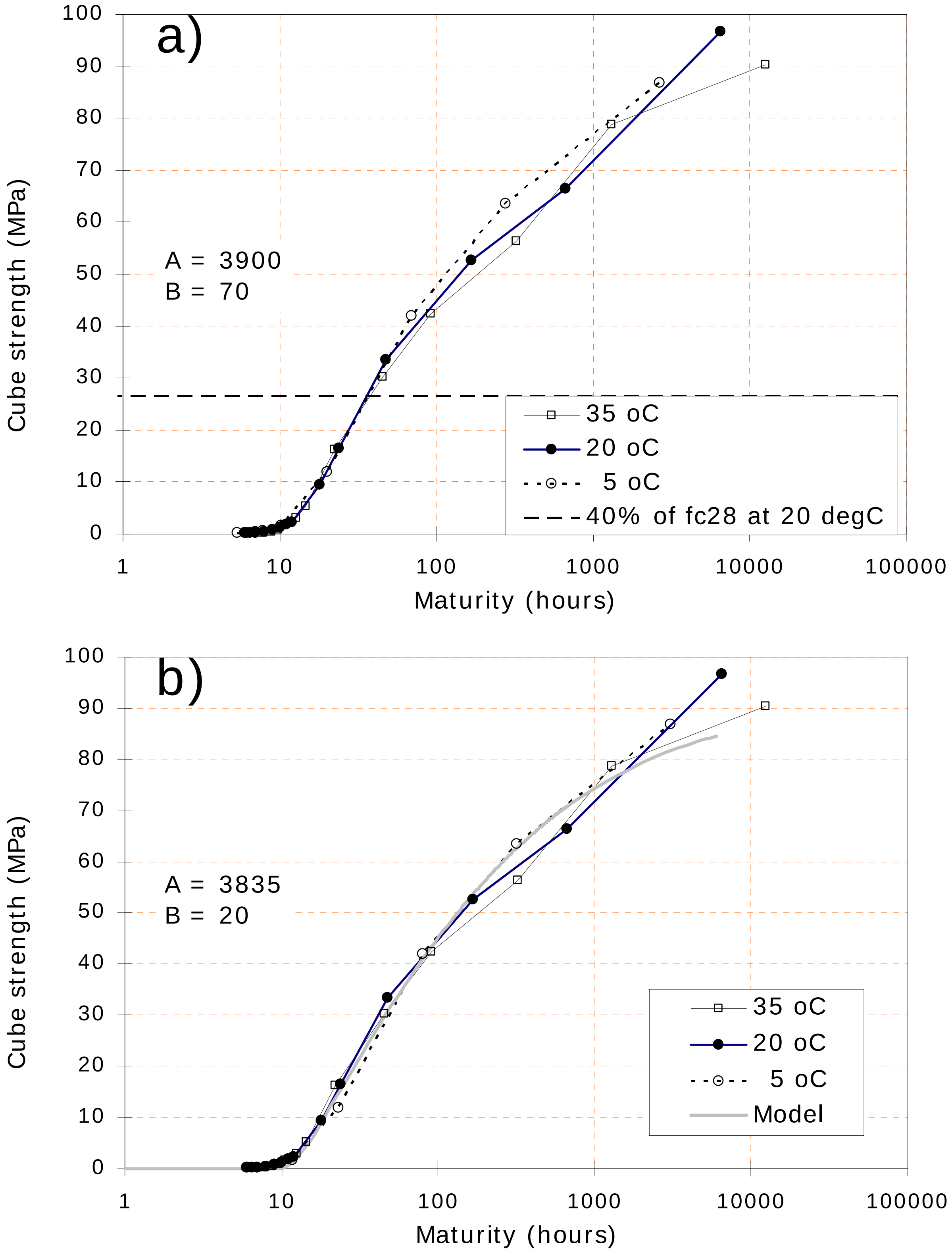

Fig. 7.10 ***ANL$_{mod}$ 20%FA*: Strength vs. maturity time based on NS 3656 (a) and on best fit between model (20 ^{o}C) and results over time up to 28 days (b).**

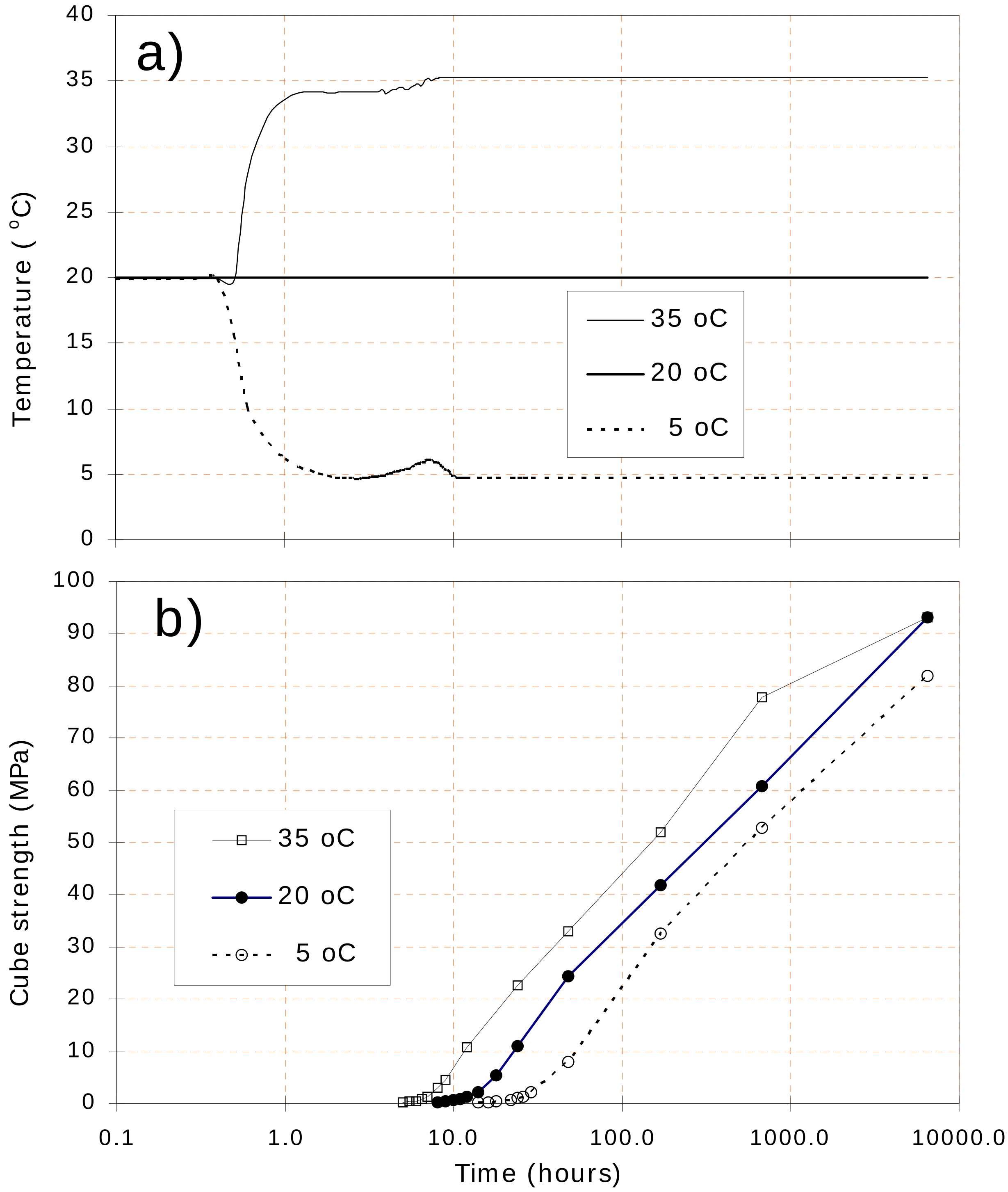

Fig. 7.11 ***ANL_{mod} 35%FA*****: Measured temperature and strength**

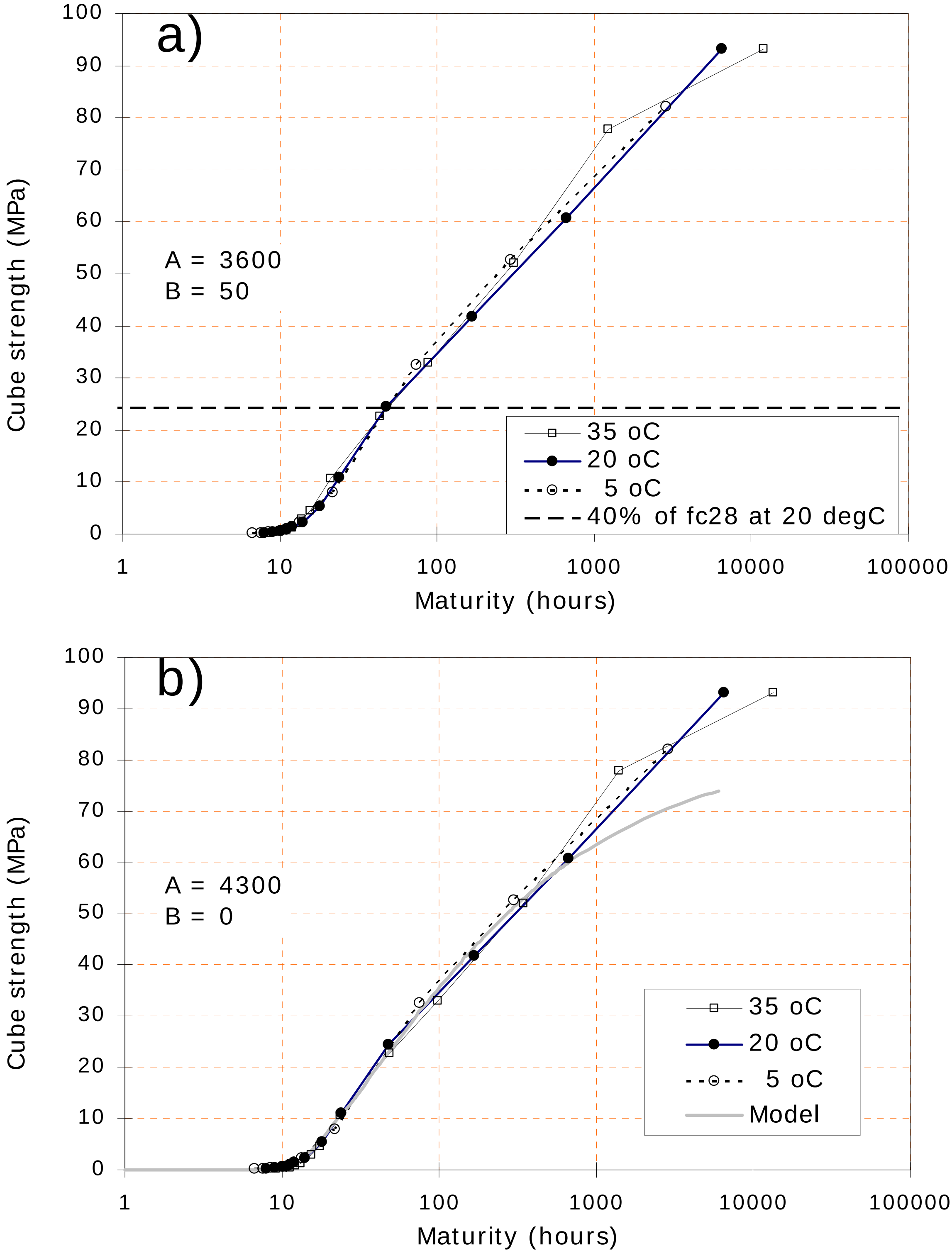

Fig. 7.12 *ANL$_{mod}$ 35%FA*: **Strength vs. maturity time based on NS 3656 (a) and on best fit between model (20 ^{o}C) and results over time up to 28 days (b).**

7.4 All concretes, activation energy and model parameters

The activation energy parameters, *A* and *B*, found from the compressive strength tests are collected in *Table 7.1* and plotted graphically in Fig. 7.13. The parameters A and B from procedure 1 are denoted "*A1*" and "*B1*" in the figure, and "*A2*" and "*B2*" from procedure 2. Only the latter values are discussed further.

It can be seen that *A2* varies from around 3400 to 3750 ^oK among the 3 cement types and from 3400 to 4300 ^oK among the plain ANL_{mod} mixture and the 10%, 20% and 35% FA-dosages. The effect of FA is not systematic, but there is a clear tendency of increased *A*-value for the two highest FA-dosages. The *B2*-values behaves rather "opposite" to the *A2*-value, since high *A2*-value tends to correlate with low *B2*-value, and the result of this is in fact that the activation energy at 5 ^oC calculated as $E = A + (20 - B)$ is practically the same for all the concretes ($E(5^oC) \cong$ 4100 - 4300 ^oK) except for ANL_{mod} where $E(5\ ^oC)$ becomes 5660 ^oK due to its high *B2*-value.

Table 7.2 gives the model parameters in *Equation [1]*. The table gives "best fit" values, which is based on a least square root sum iteration where all three parameters are free, and another where the parameter t_0 is not free - it is taken from extrapolation to zero strength from the "linear part" of the compressive strength development, see Fig. 7.14. The latter is the most related to real behavior. Note, however, that the t_0-values used in the calculations in Chapter 9 are taken from the TSTM-tests directly and, thus, differ somewhat from the values given here. The reason is that the results from Norcem and NTNU showed somewhat different setting times, see Section 8.2. *Equation [1]* is plotted for all concretes in Fig. 7.15 (t_0 taken from f_c extrapolation).

Table 7.1 Activation energy as found by procedure 1 (40% of f_{c28}) and procedure 2 (t_0 - 28 days). The bold values are used in the following chapters.

Concrete	Procedure	*A* [^oK]	*B* [-]
ANL	1	4200	40
	2	**3747**	**38**
SR_{mod}	1	3500	80
	2	**3315**	**61**
ANL_{mod}	1	3700	110
	2	**3398**	**151**
$ANL_{mod}10\%FA$	1	3400	100
	2	**3314**	**61**
$ANL_{mod}20\%FA$	1	3900	70
	2	**3835**	**20**
$ANL_{mod}35\%FA$	1	3600	50
	2	**4300**	**0**

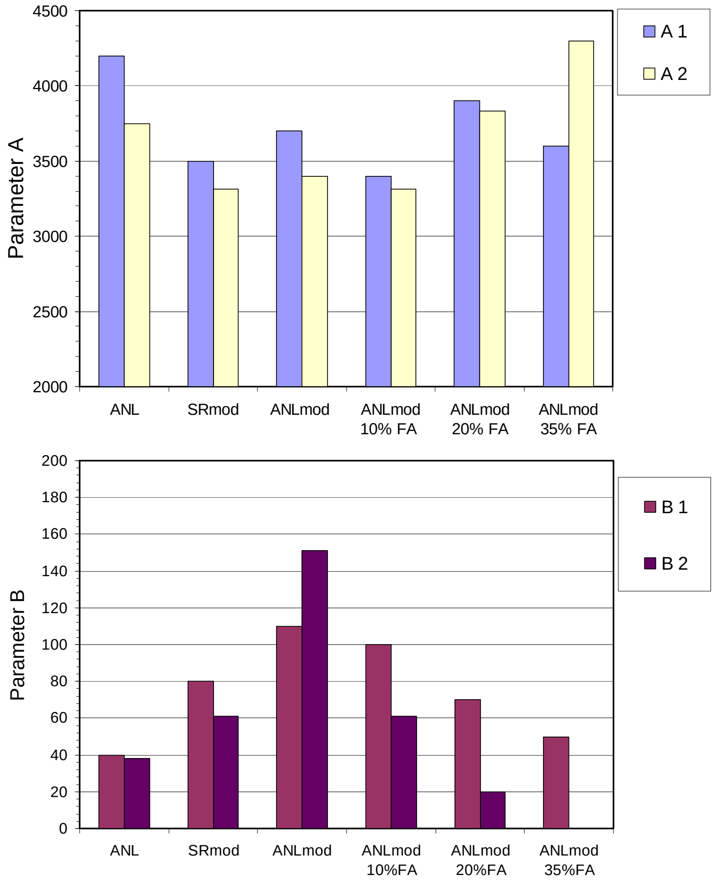

Fig. 7.13 The activation energy parameters from *Table 7.1*.

Table 7.2 Model parameters for f_c.

Concrete	Iteration	t_0 [h]	f_{c28} [MPa]	*s*
ANL	Best fit	8.3	77.2	0.159
	t_0 taken from f_c extrapolation	**8.0**	**77.5**	**0.163**
SR_{mod}	Best fit	9.5	81.2	0.208
	t_0 taken from f_c extrapolation	**10.0**	**81.0**	**0.205**
ANL_{mod}	Best fit	10.1	74.4	0.169
	t_0 taken from f_c extrapolation	**9.5**	**74.7**	**0.176**
ANL_{mod}10%FA	Best fit	9.9	72.8	0.194
	t_0 taken from f_c extrapolation	**9.5**	**73.0**	**0.199**
ANL_{mod}20%FA	Best fit	9.4	71.0	0.263
	t_0 taken from f_c extrapolation	**10.0**	**70.9**	**0.258**
ANL_{mod}35%FA	Best fit	6.7	64.3	0.362
	t_0 taken from f_c extrapolation	**12.0**	**63.4**	**0.310**

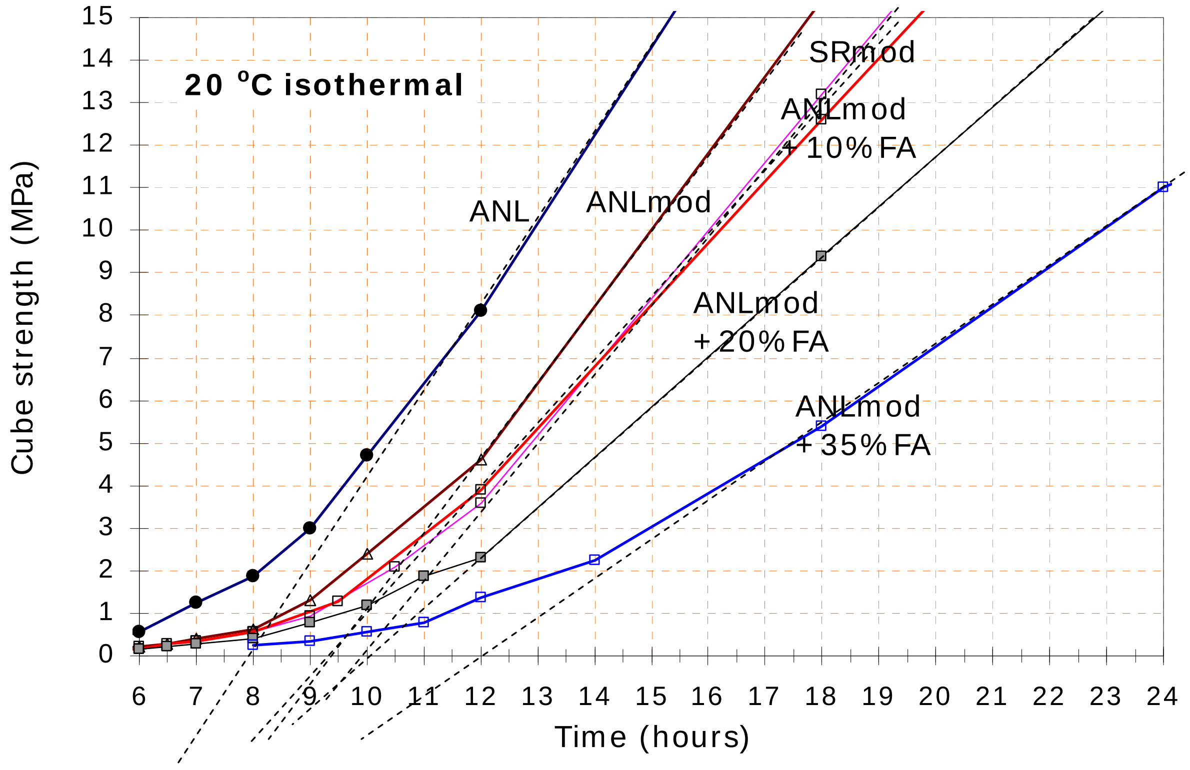

Fig. 7.14 20 °C isothermal conditions: Extrapolation to zero strength from the linear part.

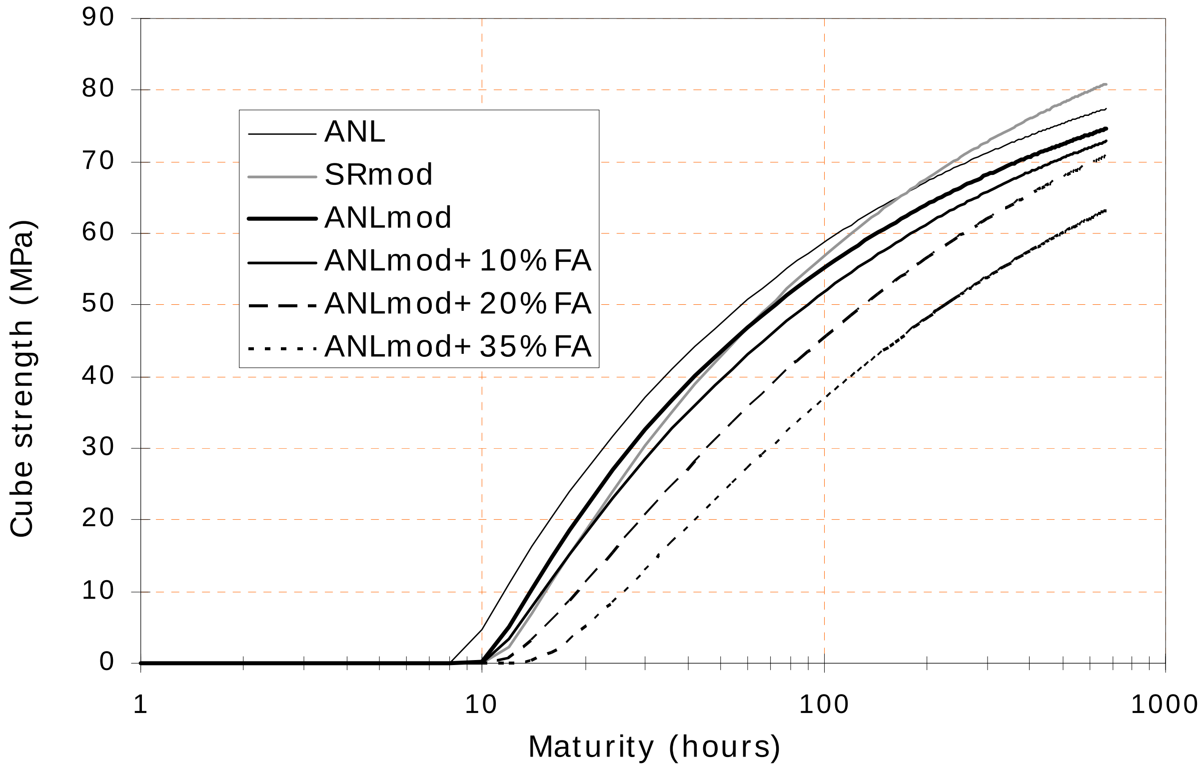

Fig. 7.15 Strength vs. maturity for all concretes as expressed by the model (see *Table 7.2*, bold values)

8 Dilation Rig and TSTM test results

8.1 Bleeding

The measurements of autogenous deformation can be influenced by bleed water collecting on the concrete surface during the fresh phase (i.e. before setting). After setting, this bleed water will be reabsorbed by the concrete as self-desiccation occurs, resulting in reduced autogenous shrinkage or even expansion /3/.

The bleed water was therefore removed in the present tests. The bleeding process was observed in a separate set-up, see Fig. 8.1. The measurements were not done systematically over time, but all bleed water was removed after the last measurement in Fig. 8.2. The top cover and foil of the rigs are then put aside for a moment and the bleed water is removed by covering the surface with dry clothes for about 1 min. Sealing and top cover is then put back in place.

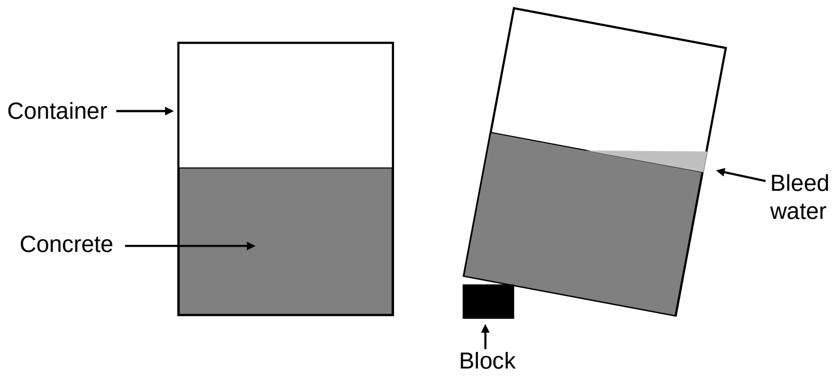

Fig. 8.1 Set-up for bleeding measurement (bucket with 5 ltr concrete volume)

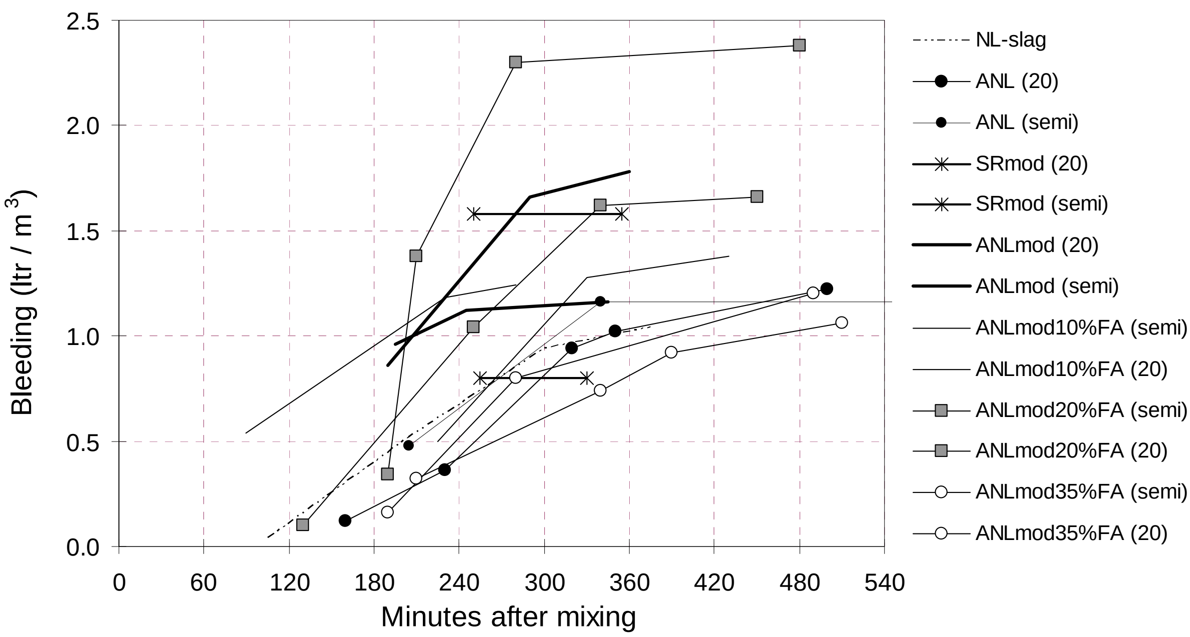

Fig. 8.2 Measurements of bleed water over time

8.2 Time zero from TSTM and heat measurements

The parameter time zero, t_0, is related to time of final set, but t_0 is ambiguous in a way as it depends on what purpose it shall serve and what model it is used in. As a part of models to be used in stress calculations the most important purpose of t_0 (expressed in maturity time) is to secure a correct start of the E-modulus development and also serve as the proper starting point for thermal dilation and autogenous shrinkage curves. As we may assume that the onset of all mechanical properties occur simultaneously t_0 can be found directly from compressive strength tests or from a semi-adiabatic TSTM-test, or, alternatively, indirectly from heat liberation tests (i.e. the maturity time where 12 kJ has been produced above the baseline heat release during the dormant period, denoted here $t_{Q=12kJ}$); all of these much easier to perform during the early age than, for instance, E-modulus measurements.

Table 8.1 shows such for t_0 from heat liberation and from TSTM-tests. An appropriate t_0 for stress calculations (with the use of the model showed in *Equation [1]*) has shown to be the point in time where the given semi-adiabatic TSTM-test has developed 1/10 of the maximum restraint compressive stress during the heating period; such procedure was used here. It can be seen that the t_0 from heat liberation is on average 2.6 hours earlier than setting according to the semi-adiabatic tests in the TSTM. It can be seen that the two types of "setting" times vary between 1.7 - 3.3 hours. Using *Equation [3]* to calculate t_0 gives a standard deviation (STD) of 0.6 hours compared to the measured $t_{0, TSTM}$ from the TSTM. *Equation [3]* is not used here, but it is included simply as a relation for possible later use.

Equation [3] $$t_{0,TSTM} = t_{Q=12kJ} + 2.6 \text{ hours} \qquad (\text{STD} = \pm 0.6 \text{ h})$$

Note that it is the $t_{0, TSTM}$-values in *Table 8.1* that have been used in the calculations in the next chapter.

Table 8.1 Setting (t_0) according to 12 kJ heat production ($t_{Q=12\ kJ}$) and from the TSTM ($t_{0,\ TSTM}$)

	$t_{Q=12\ kJ}$ NTNU [Mh]	$t_{0,\ TSTM}$ NTNU [Mh]	Difference $t_{0,\ TSTM} - t_{Q=12\ kJ}$ [Mh]
SR_{mod}	9.8	12.0	2.2
ANL	13.8	15.5	1.7
ANL_{mod}	10.0	13.0	3.0
ANL_{mod} 10% FA	10.6	13.0	2.4
ANL_{mod} 20% FA	10.8	13.5	2.7
ANL_{mod} 35% FA	11.7	15.0	3.3
Average	11.1	13.7	2.6

8.3 Isothermal tests

The 20 ^{o}C isothermal test results are given in the figures below; effect of cement type is shown in Fig. 8.3 and effect of FA-dosage in Fig. 8.4. Autogenous shrinkage is the only driving force behind these curves. The symbols "*" on the stress-curves indicate failure due to manual loading in tension at the end of the TSTM-test. One exception is for *NL-slag* which developed high stresses due to high autogenous shrinkage, leading to failure in tension in the TSTM-specimen after 336 hours (2 weeks). The origin of (small) early autogenous expansion for the *NL-slag* concrete is unclear, but has been seen in other tests /8//9/. As earlier discussed, the *NL-slag* concrete was noticeably retarded due to an over-dosage of P-type plasticizer.

SR_{mod} shows a peculiar behavior in the way that it has no autogenous shrinkage in the period between 24 and 168 hours (1 - 7 days). In the same period relaxation then works (alone) in the parallel TSTM-specimen with a slightly reduced tensile stress as result.

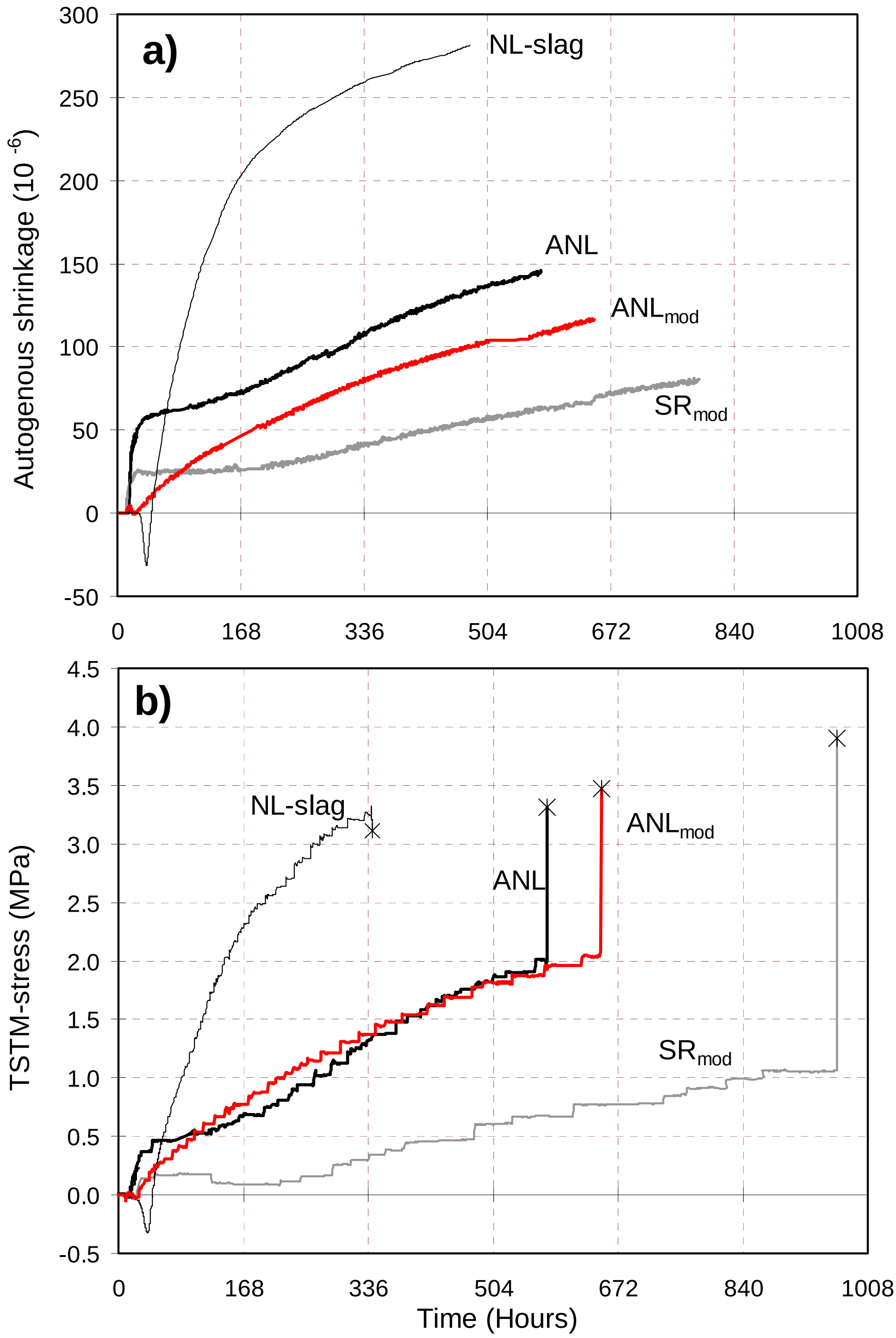

Fig. 8.3 Effect of cement type, 20 °C isothermal tests. Autogenous shrinkage (a) and stress development during 100% restraint (b), where positive stress is tension.

Autogenous shrinkage at 20 °C, see Fig. 8.4-a, is systematically reduced with FA-content beyond around 3 days (72 hours). Before that the shrinkage is about the same. The stress build-up in the parallel TSTM-test, see Fig. 8.4-b, reflects the autogenous shrinkage curves.

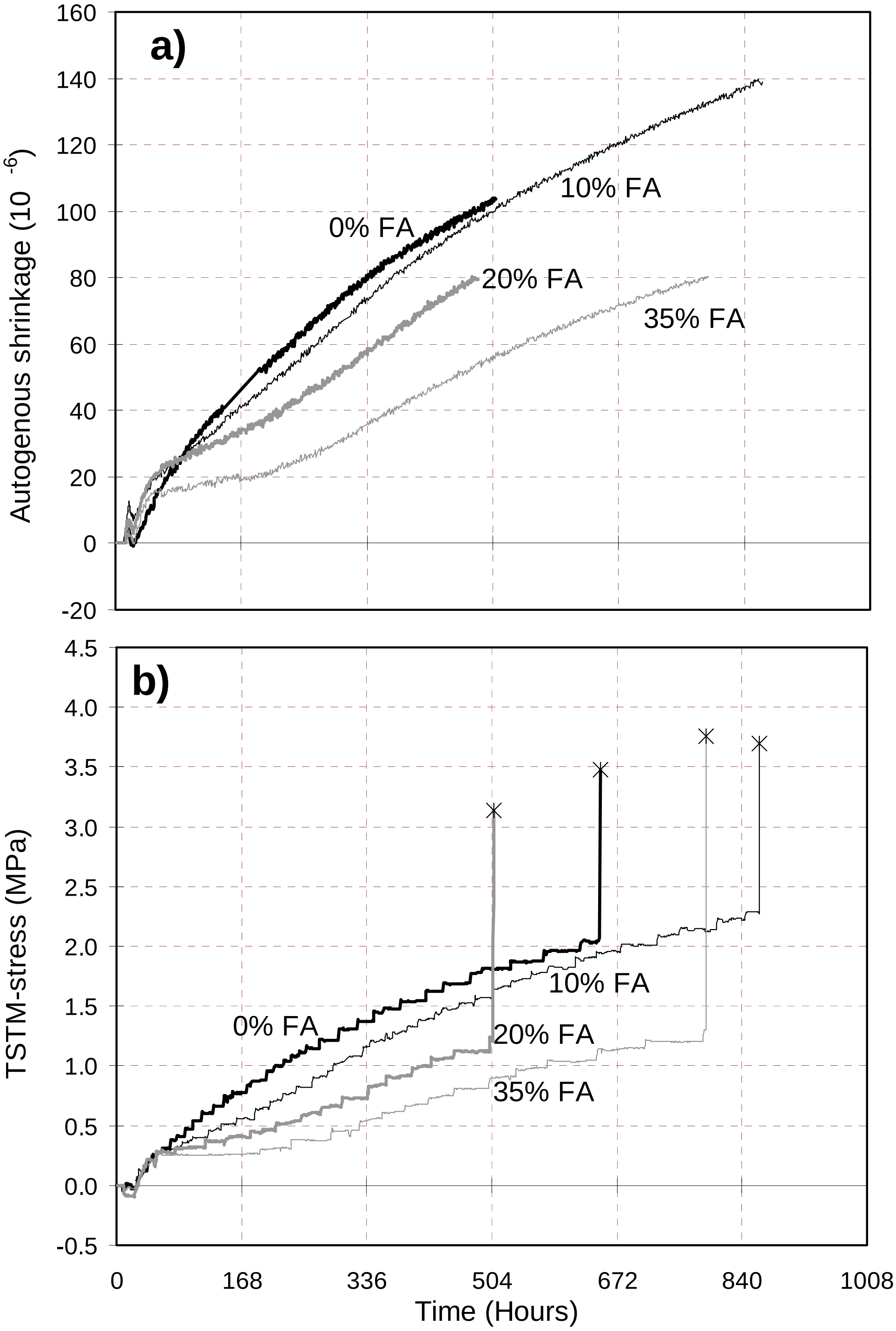

Fig. 8.4 Effect of FA-dosage (in combination with the ANL_{mod} cement), 20 °C isothermal tests. Autogenous shrinkage (a) and stress development during 100% restraint (b), where positive stress is tension.

8.4 Semi-adiabatic tests

8.4.1 Measured (and imposed) temperature histories

Measured temperature histories during the Dilation- and TSTM-tests are shown in Fig. 8.5 and **Fig. 8.6**, respectively. The temperatures from the TSTM-tests, **Fig. 8.6**, show that the two concretes *ANL_{mod} 10%FA* and *ANL_{mod} 20%FA* have peculiar temperature curves after around 5 **-** 7 days. For the former the reason was some computer/software problem causing rapid reading from the computer temperature file and subsequent increased cooling rate, while the latter was due to a power failure.

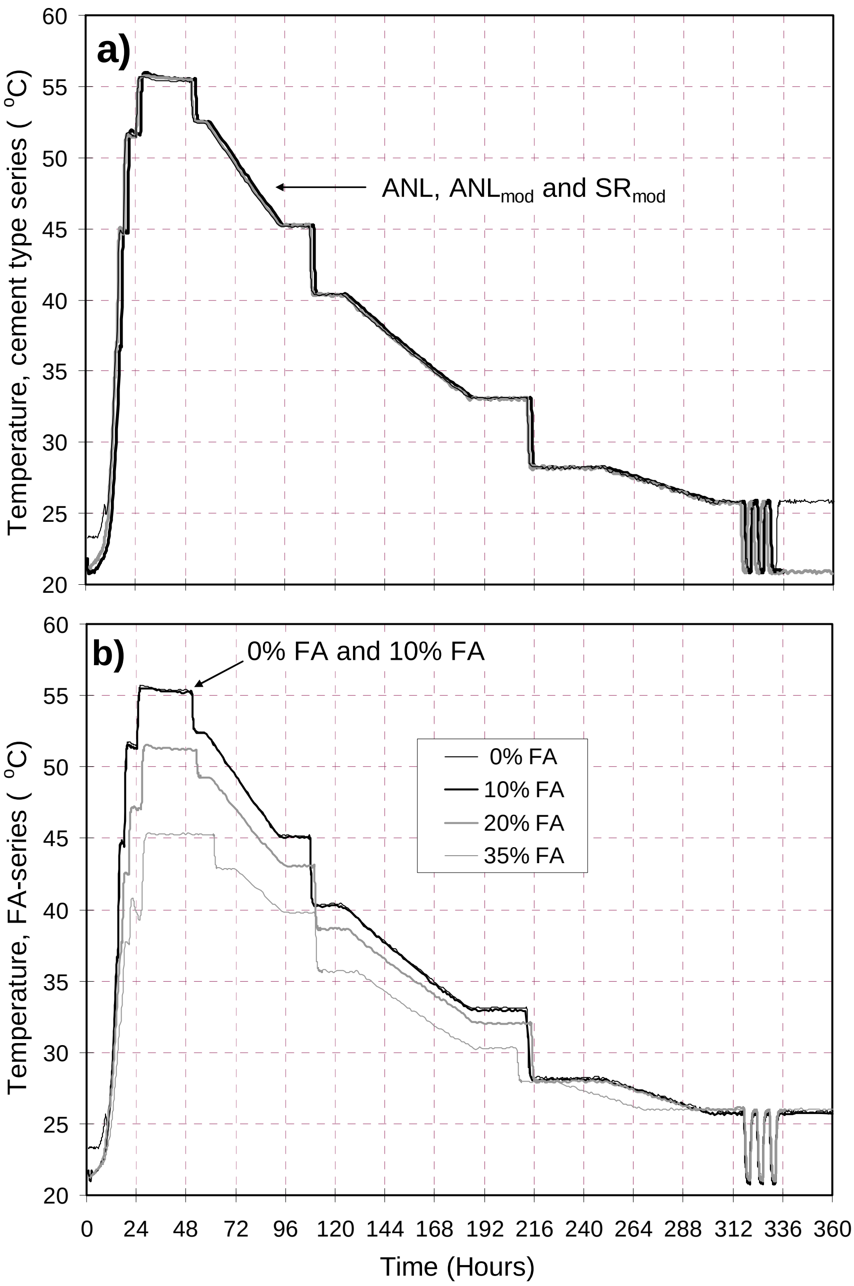

Fig. 8.5 Measured (and imposed) temperatures during the semi-adiabatic Dilation Rig tests. Cement type series (a) and FA-series in combination with *ANL_{mod}* (b)

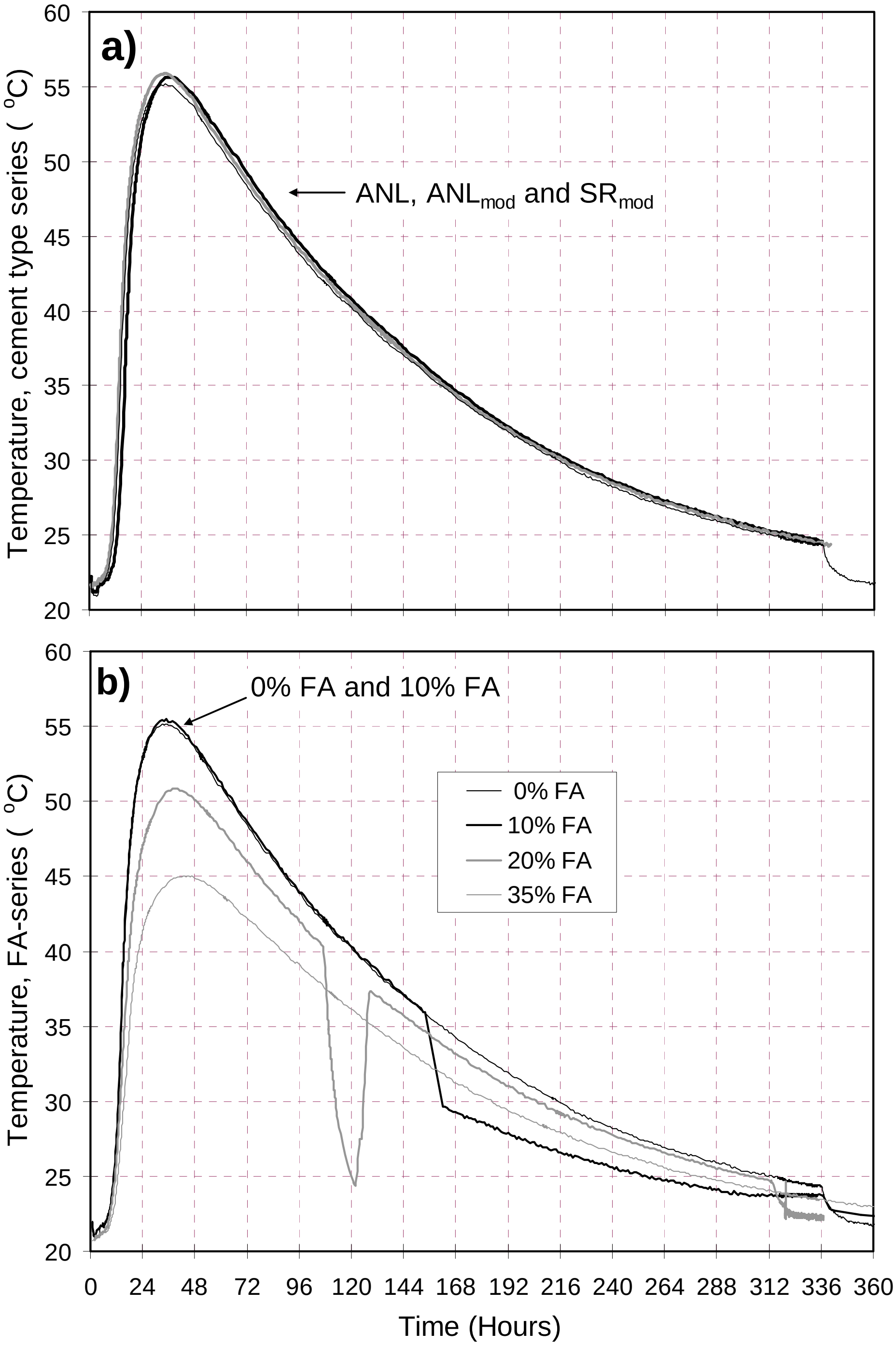

Fig. 8.6 Measured (and imposed) temperatures during the semi-adiabatic TSTM tests. Cement type series (a) and FA-series in combination with ANL_{mod} (b).

8.4.2 Results, semi-adiabatic tests

Measured total free strain and restraint stress are given in Fig. 8.7-a and -b, respectively. All tests were run at full restraint until the self-generated tensile stress reached 1.2 MPa. After that, the active deformation control in the TSTM was turned off and further restraint is provided by the stiffness of the frame (i.e. the rig works as a so-called “cracking frame”). The strain in the TSTM is always registered, and, as shown in Fig. 8.7-c, the specimen is partly allowed to move from the point where the feedback system is turned off. Comparing the deformations in the TSTM and the free strains from the Dilation Rig reveals that the degree of restraint drops from 100% to around 30-40% when turning off the feedback system.

It can be seen in Fig. 8.7 that the ANL_{mod} stress-curve is somewhat unstable between 2 and 5 days. This was due to partly failure in a wire connected to the load cell. The wire was repaired after 5 days. Hence, the test has run as normal but the registration of the load was “on and off” for a period. The most likely stress history in the specimen is indicated with a dashed line.

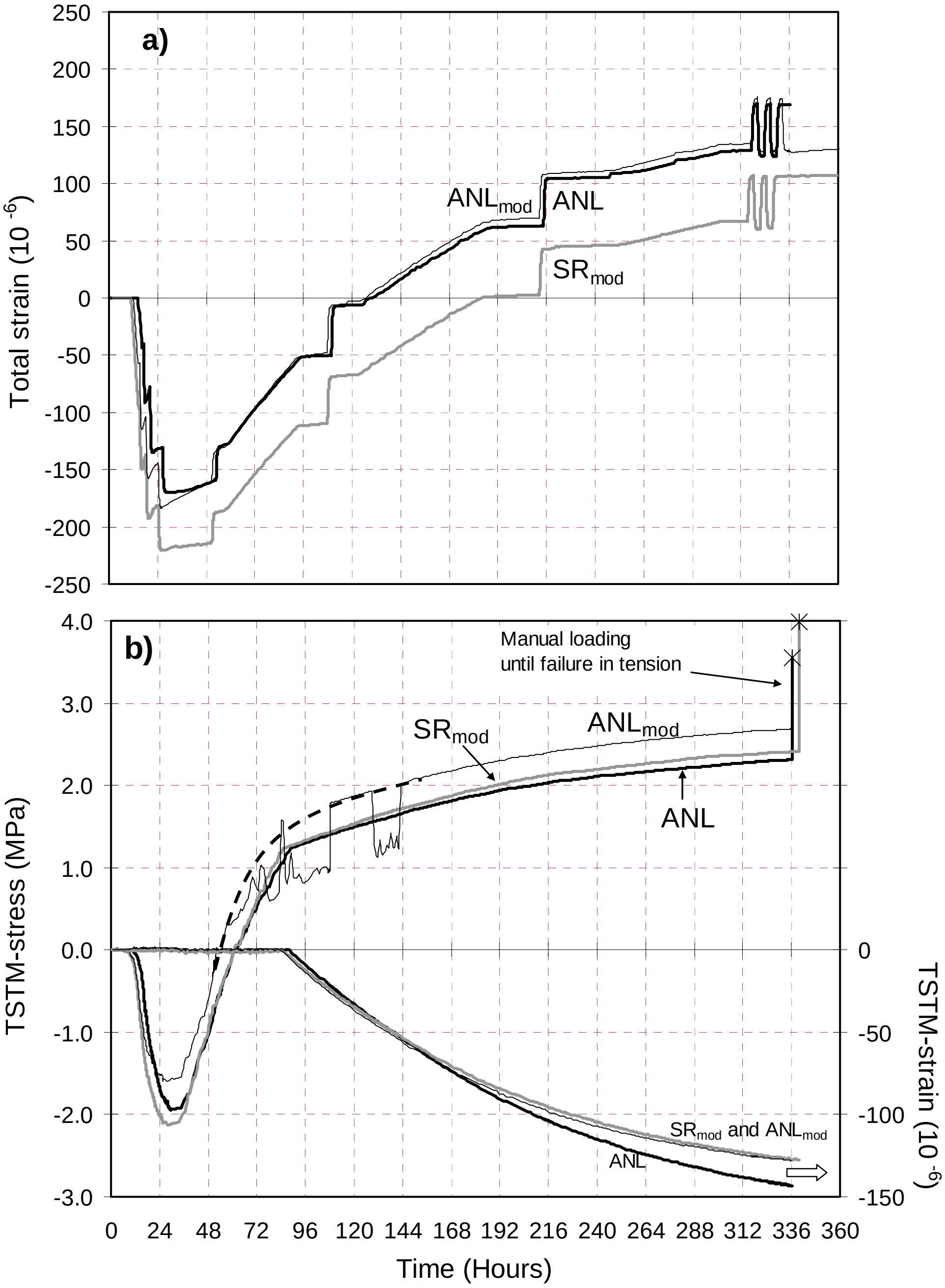

Fig. 8.7 Effect of cement type: Measured total strain in the Dilation Rig (a) and stress development in the TSTM (b), including the strain that occurs from the point (1.2 MPa in tension) where the feedback system is turned off and the specimen is partly restraint.

The same curve (*ANL$_{mod}$*) as above is also given in Fig. 8.8-b together with the concretes with 10, 20 and 35% FA. The deviating temperatures for the 10% and 20% FA concretes in the TSTM-test, as earlier discussed, are reflected in the respective curves in Fig. 8.8-b.

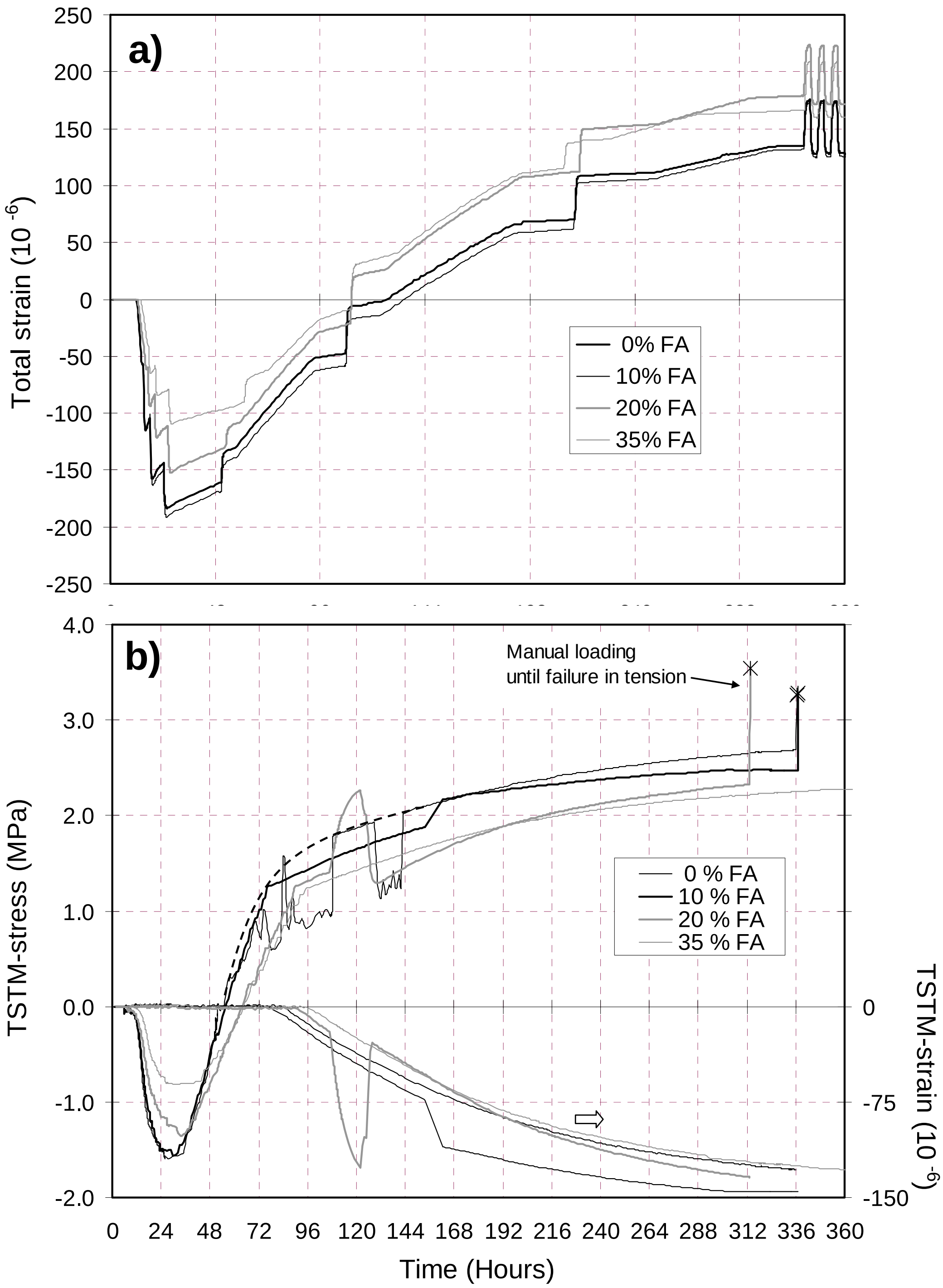

Fig. 8.8 Effect of FA-dosage: Measured total strain (a) and stress development (b), including the strain that occurs from the point (1.2 MPa in tension) where the feedback system is turned off and the specimen is partly restraint.

8.4.3 Coefficient of thermal expansion (CTE)

CTE-values determined at each temperature step in the Dilation Rig is shown in Fig. 8.9 and Fig. 8.10. All CTE-values are found during semi-adiabatic conditions, except *NL-slag* which was tested at 20 ^{o}C (based on periods with steps between 17 ^{o}C and 23 ^{o}C). The average CTE-value for each concrete is given in *Table 8.2*, where one column is based on all the CTE-data and the other only those after 24 hours (i.e. during the cooling period). It can be seen that the average CTE varies quite little, hence there is no clear effect of cement type and FA-content (except *NL-slag* which has a significantly higher CTE). There is however a tendency of FA to increase CTE at later ages.

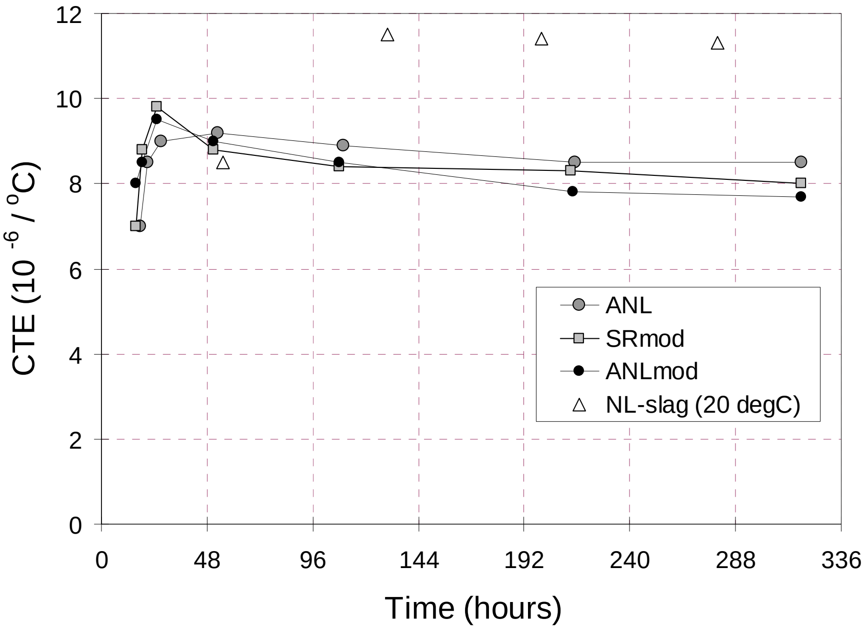

Fig. 8.9 Coefficient of thermal expansion (CTE), effect of cement type. Semi-adiabatic conditions for all concretes except *NL-slag* which was tested at 20 ^{o}C.

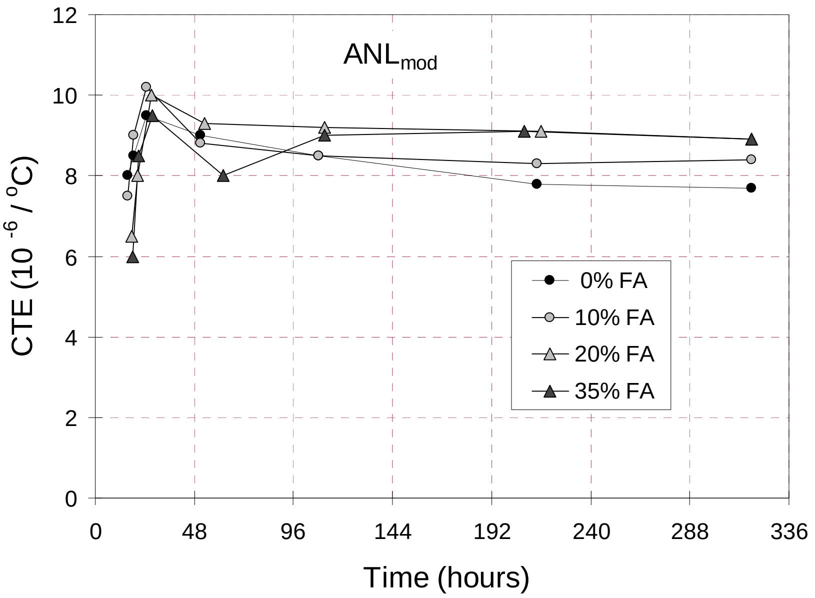

Fig. 8.10 Coefficient of thermal expansion (CTE), effect of FA-content in combination with ANL_{mod}. Semi-adiabatic conditions.

Table 8.2 Coefficient of thermal expansion (CTE) from the semi-adiabatic tests, average values.

	CTE [10^{-6} / °C]	
Concrete	All data	Data after 24 h
ANL	8.5	8.8
SR_{mod}	8.4	8.7
ANL_{mod}	8.4	8.5
ANL_{mod} *10%FA*	8.7	8.8
ANL_{mod} *20%FA*	8.7	9.3
ANL_{mod} *35%FA*	8.4	8.9

8.4.4 Autogenous deformation during semi-adiabatic conditions

The effect of cement type on autogenous shrinkage is shown in Fig. 8.11, and the effect of FA in Fig. 8.12. Autogenous shrinkage is found by eliminating the thermal dilation that occurs during each temperature step. See measured total strain curves in Section 8.4.2. Both Fig. 8.11 and Fig. 8.12 contain also the isothermal data (the (a) figures), as well as the development during semi-adiabatic conditions (the (b) figures). The curves start from t_0 (i.e. t_0 from the TSTM-tests = $t_{0, TSTM}$).

For the cement type series it can be seen that much of the differences in autogenous shrinkage at semi-adiabatic conditions occur in the early heating period, and thus influences the compressive phase in the TSTM, and it can be seen from the stress results in Fig. 8.7-b that ANL_{mod} has somewhat less compression due to its high early autogenous shrinkage which counteracts the thermal expansion. During the cooling period between 36 h and 336 h ANL_{mod} develops about 20 x 10^{-6} more autogenous shrinkage than the two other cements.

The FA-series (semi-adiabatic conditions) reveals that total autogenous shrinkage from t_0 is not significantly influenced by the FA-content, but there is a tendency of increased shrinkage with FA-dosage from 24 h to 336 h (during the cooling period) where 35% FA has 35 x 10^{-6} more than 0% FA. The higher temperature maximum for 0% FA concrete will promote more of the phenomenon “autogenous swelling” during the cooling phase /3/4/. This thermally induced autogenous swelling superimposes the gradual shrinkage caused by self-desiccation. This is probably the reason why the autogenous shrinkage curve for the 0% FA concrete in Fig. 8.12 bends off in the cooling period beyond 48 hours.

It is therefore notable that the autogenous shrinkage results from the 20 °C isothermal- and from the semi-adiabatic conditions do not display the same pattern, where for instance the effect of FA is opposite for the two curing conditions at longer times. This result is fully in line with earlier results also showing that autogenous shrinkage at semi-adiabatic temperatures can be fundamentally different from that of isothermal conditions. The thermally induced autogenous swelling mechanism at semi-adiabatic conditions is the reason for this /3/4/.

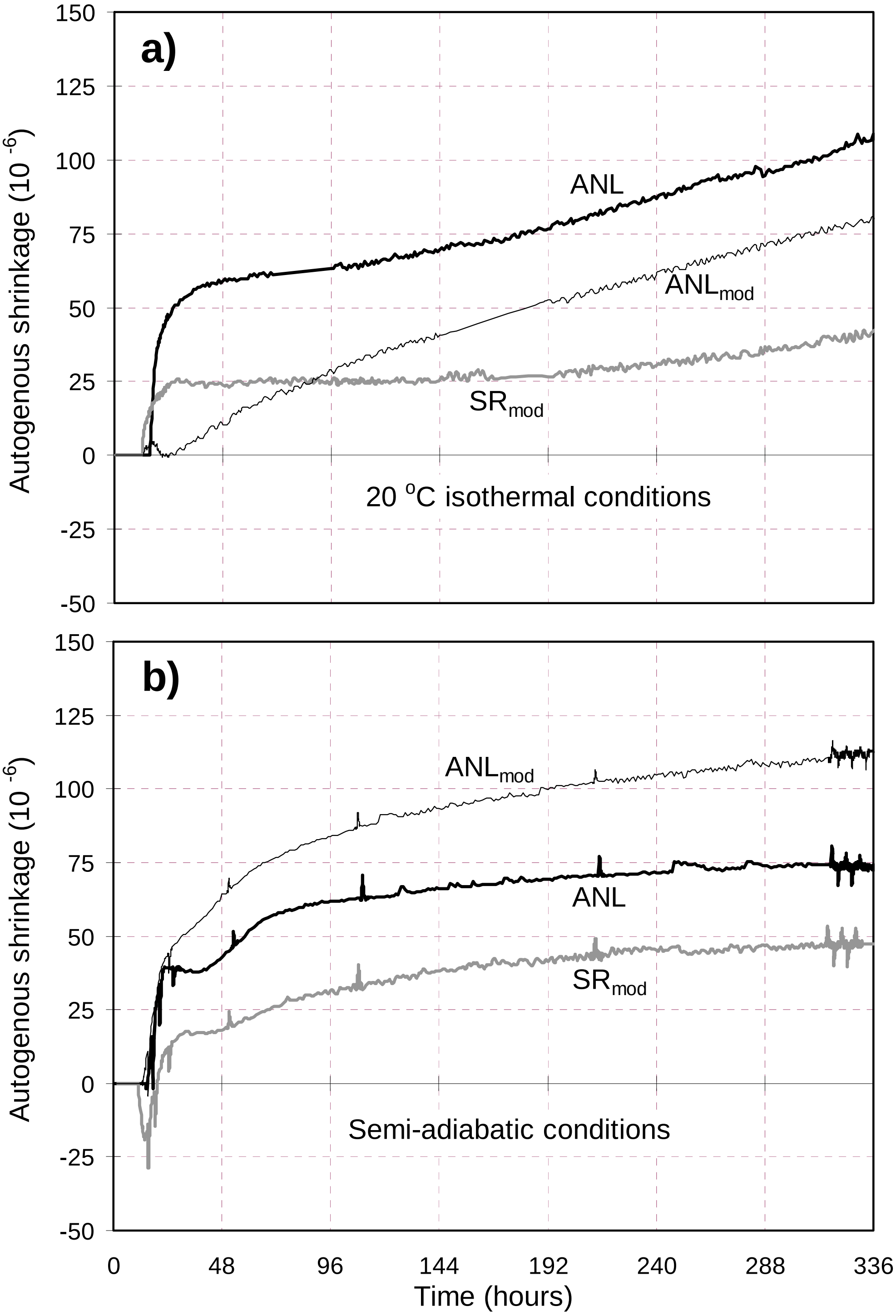

Fig. 8.11 Autogenous shrinkage at 20 °C (a) and during semi-adiabatic conditions (b), effect of cement type.

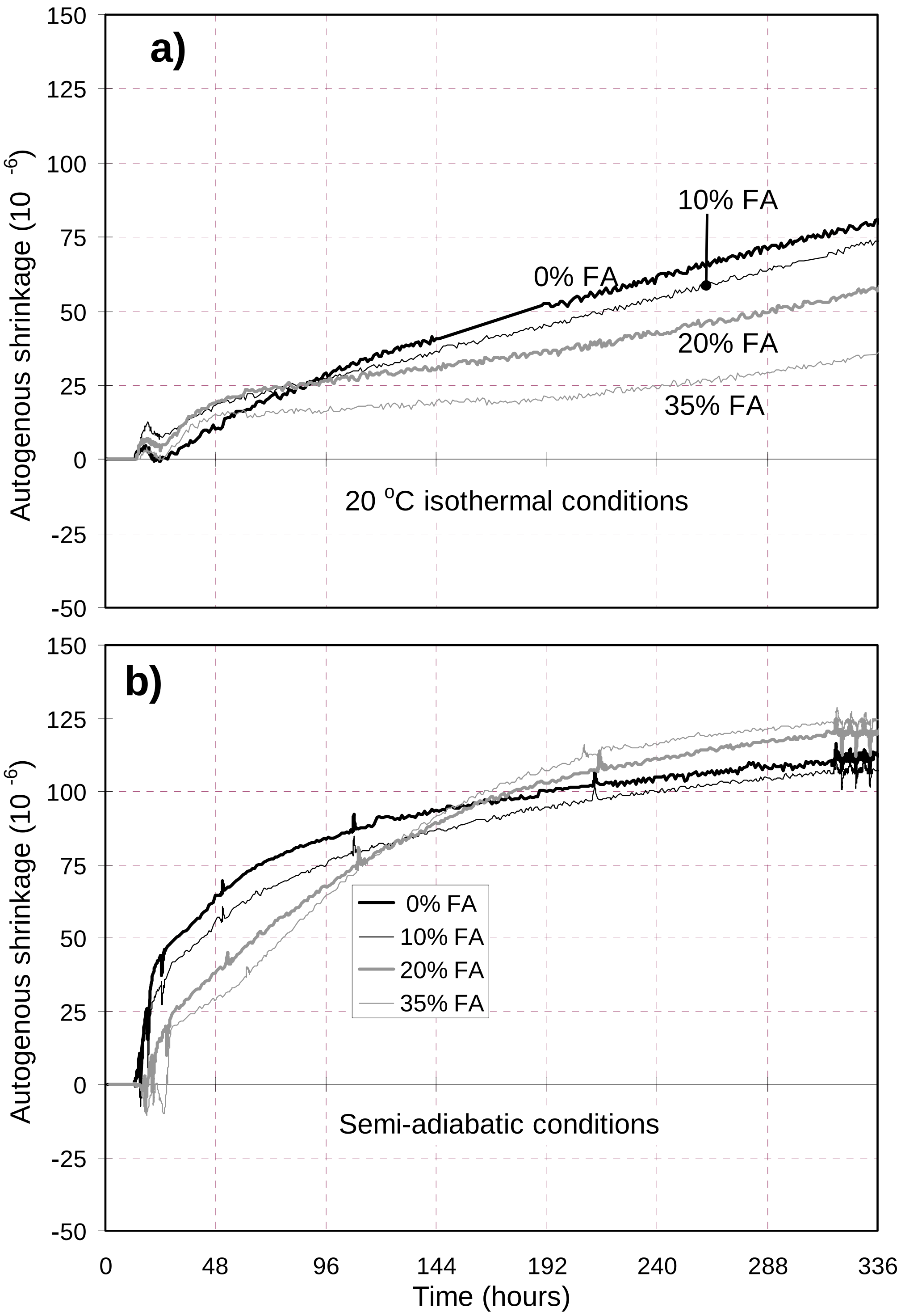

Fig. 8.12 Autogenous shrinkage at 20 °C (a) and during semi-adiabatic conditions (b), effect of FA-dosage.

9 Stress calculations

9.1 Calculation principle and input parameters

The stress calculations are based on linear visco-elasticity for aging materials. For a general stress history in the TSTM, the strains are in principle determined as:

Equation [4]

$$\varepsilon(t) = \int_0^t J(t_e',t,t')\cdot d\sigma(t') + \varepsilon_{Tot}(t) - \varepsilon_{TSTM}(t)$$

ε_{Tot} is the total free deformation (strain) measured during the Dilation Rig test and ε_{TSTM} is the deformation (strain) in the parallel TSTM-test that occurs during the partial restraint period when the feedback system is turned off. The compliance function *J(t,t')* and the creep ratio $\varphi(t,t')$ can be defined as:

Equation [5]

$$J(t,t') = \frac{1}{E(t_e')}(1+\varphi(t,t')) \quad \textbf{and} \quad \varphi = \varphi_0 t_e'^{-d}\cdot(t-t')^p$$

In these equations t is the actual time (concrete age), t' the time when a stress increment ($d\sigma$) is applied (concrete age), and t_e' is the maturity at t'. The creep model parameters φ_o, d and p are taken from Atrushi /13/; their values are <u>0.75, 0.20 and 0.21</u>, respectively (time units are in days). These parameters are denoted <u>default creep parameters</u> and they are based on a number of tests on a w/b = 0.40 concrete (SV40 concrete) with 5% silica fume. The parameters have shown earlier to work well for other concretes in the same quality class. For the present study, it will be shown that creep appears to be higher for the two concretes with highest FA-content and a higher φ_o-parameter (=1.37) was used to improve the match between measured and calculated stress. The parameters used in the calculations are given in the table below. Note that no calculations have been performed for the *NL-slag* concrete.

Table 9.1 Model parameters for activation energy and mechanical properties

Concrete	***A*** [K]	***B*** [K/°C]	t_0 [h]	f_{c28} [MPa]	***s*** [-]	f_{t28} * [MPa]	n_t [-]	E_{28} [MPa]	n_E [-]
NL-slag	-	-	25.0	64.1	-	-	-		
ANL	3747	38	15.5	77.5	0.163	3.70	0.59 (default value)	34.8	0.37 (default value)
SR_{mod}	3315	61	12.0	81.0	0.205	4.10		35.1	
ANL_{mod}	3398	151	13.0	74.7	0.176	3.60		34.5	
ANL_{mod}*10%FA*	3314	61	13.0	73.0	0.199	3.80		32.2	
ANL_{mod}*20%FA*	3835	20	13.5	70.9	0.258	3.60		35.1	
ANL_{mod}*35%FA*	4300	0	15.0	63.4	0.310	3.65		35.3	

*) The f_{t28}-value is based on semi-adiabatic temperature curing conditions.

For isothermal conditions the calculations are done according to the above description, but for the semi-adiabatic conditions the calculation is done in the following sequence:

1) All relevant strains are included in the first calculation, as indicated by *Equation [4]*. This calculation represents the situation in the TSTM, and calculated stress should be as close to the measured stress as possible. The results given in the next section show good correspondence.
2) In the second calculation the strain in the TSTM, ε_{TSTM}, is not included. This situation represents a (fictitious) 100% restraint situation. Hence, the calculated stress will be similar to the calculation in 1) from the start until the feedback system is turned off, but higher after that. Generally this case gives final stresses far above the tensile stress capacity of the concretes, but still it is the more relevant case for crack risk comparisons since it represents the same degree of restraint for all concretes.

For ANL_{mod} *20%FA* and ANL_{mod} *35%FA* an extra calculation was performed with a higher creep parameter (φ_o =1.37).

9.2 Calculations vs. measured stress in the TSTM

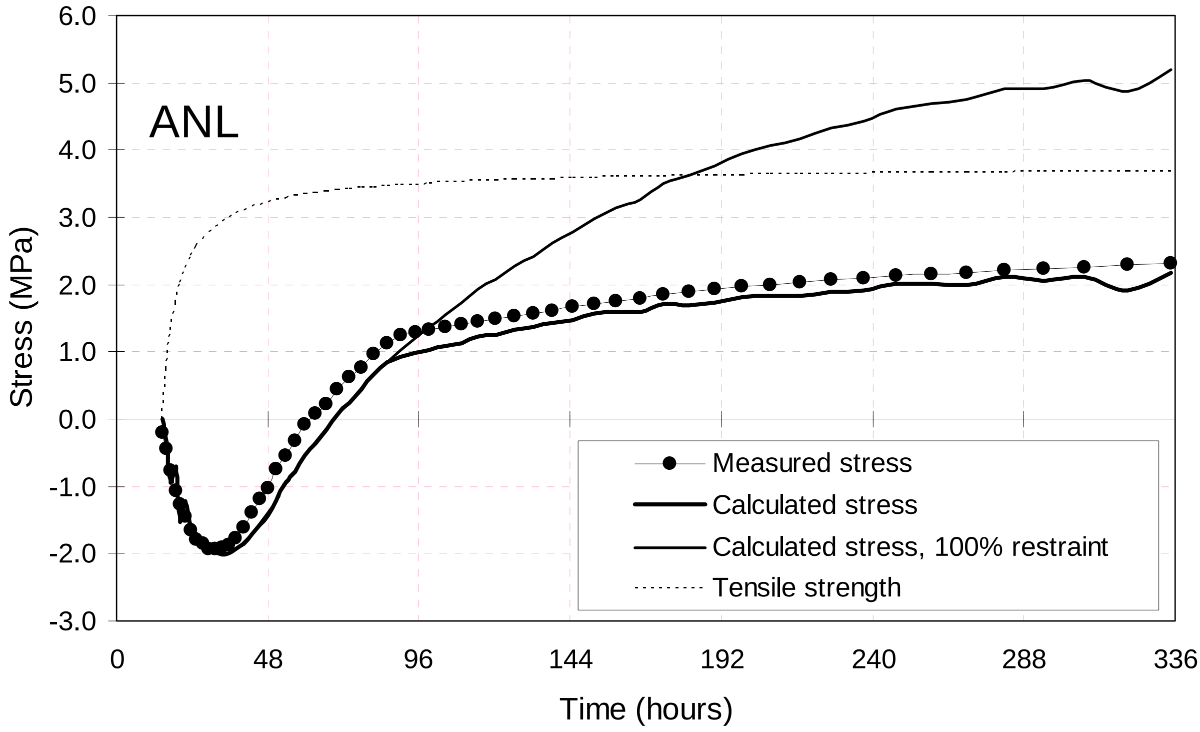

Fig. 9.1 *ANL:* Measured and calculated stress, semi-adiabatic conditions.

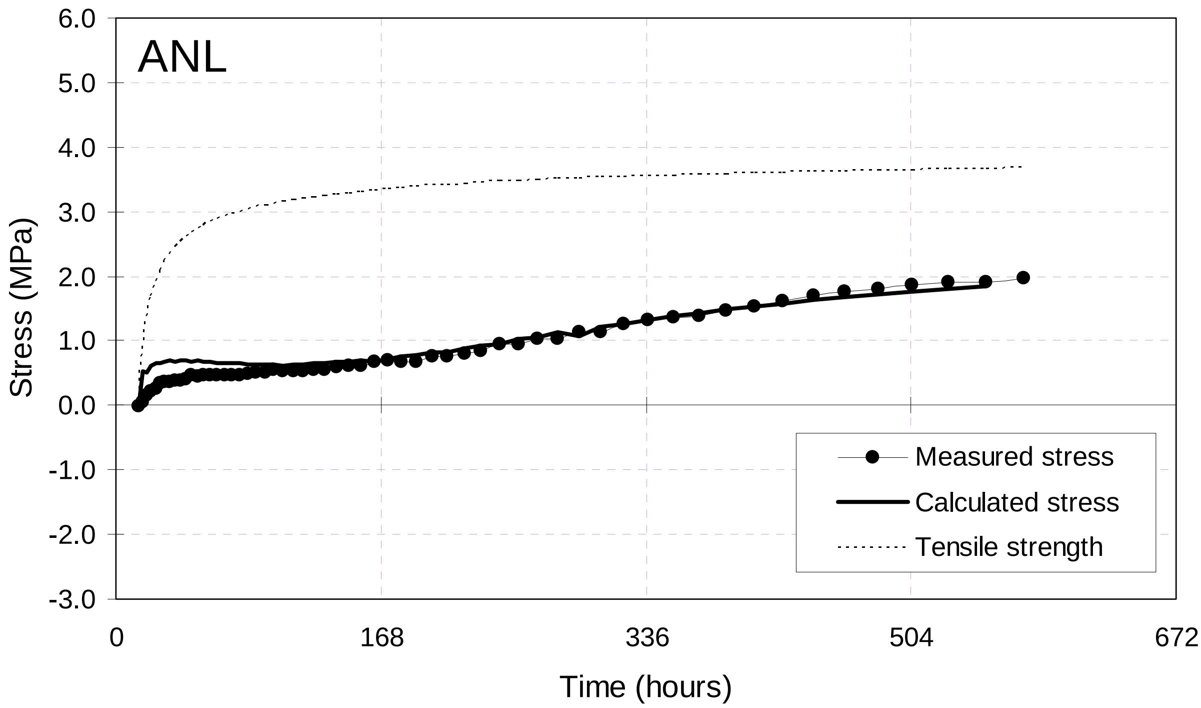

Fig. 9.2 *ANL:* Measured and calculated stress, 20 ^{o}C isothermal conditions.

.

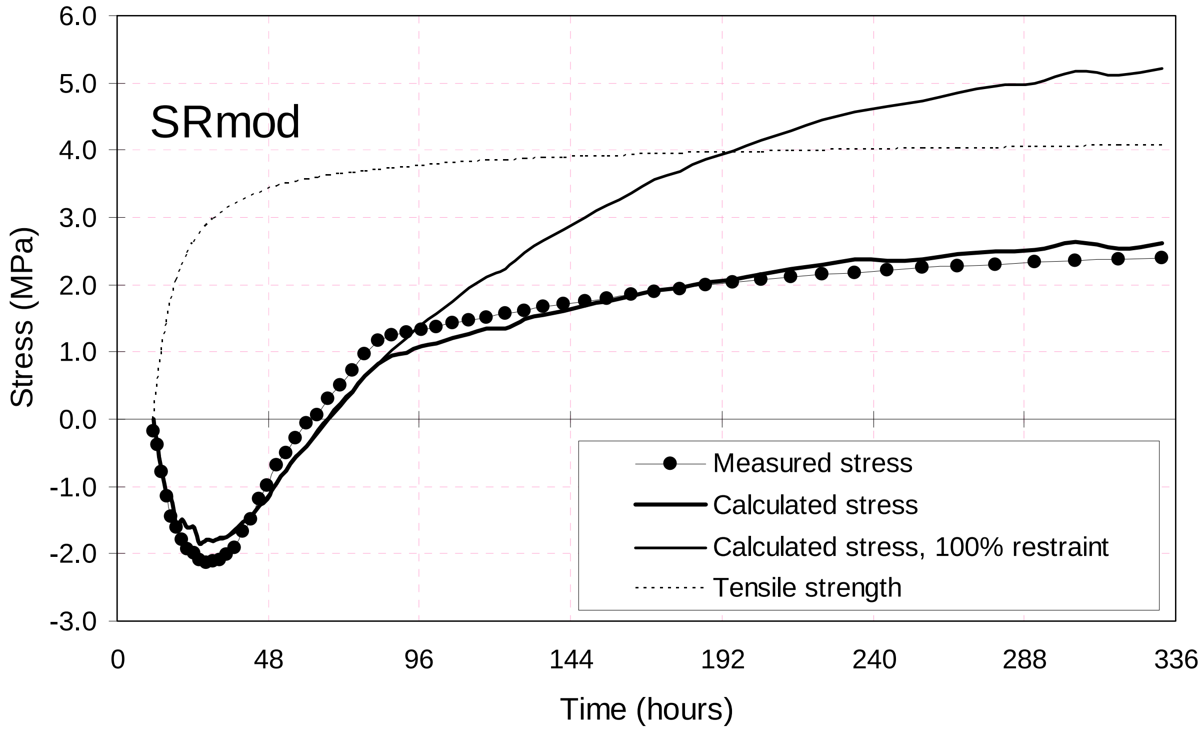

Fig. 9.3 SR_{mod}: Measured and calculated stress, semi-adiabatic conditions.

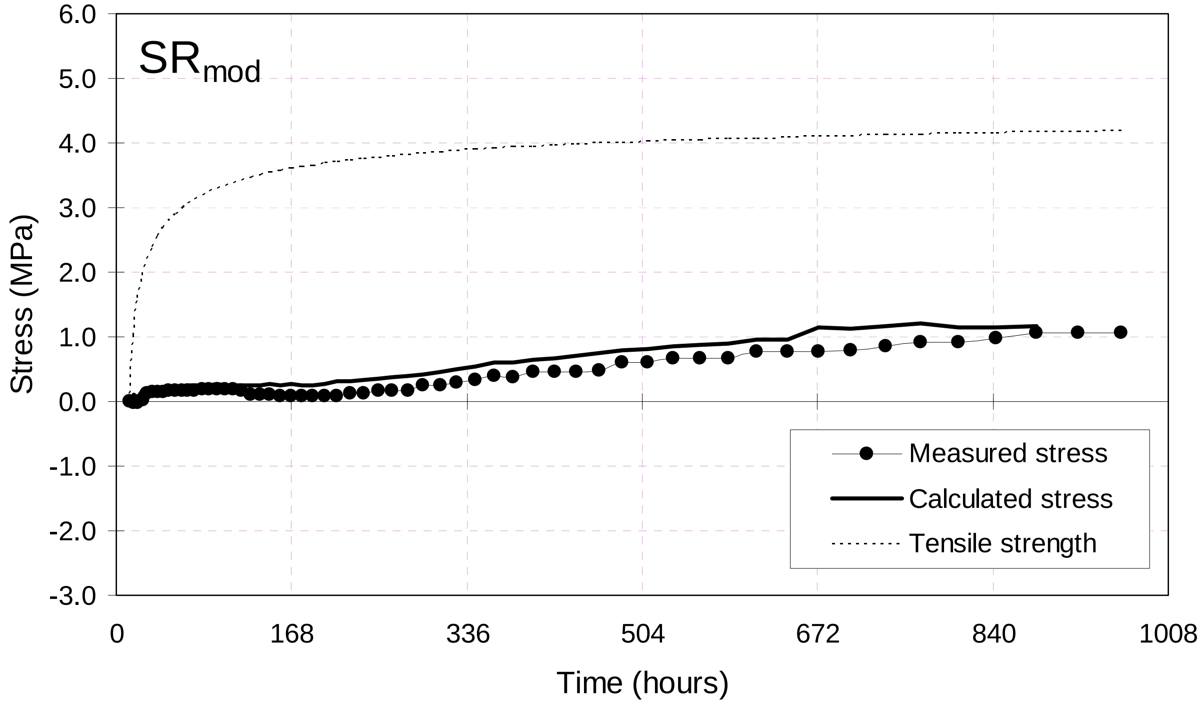

Fig. 9.4 SR_{mod}: Measured and calculated stress, 20 °C isothermal conditions.

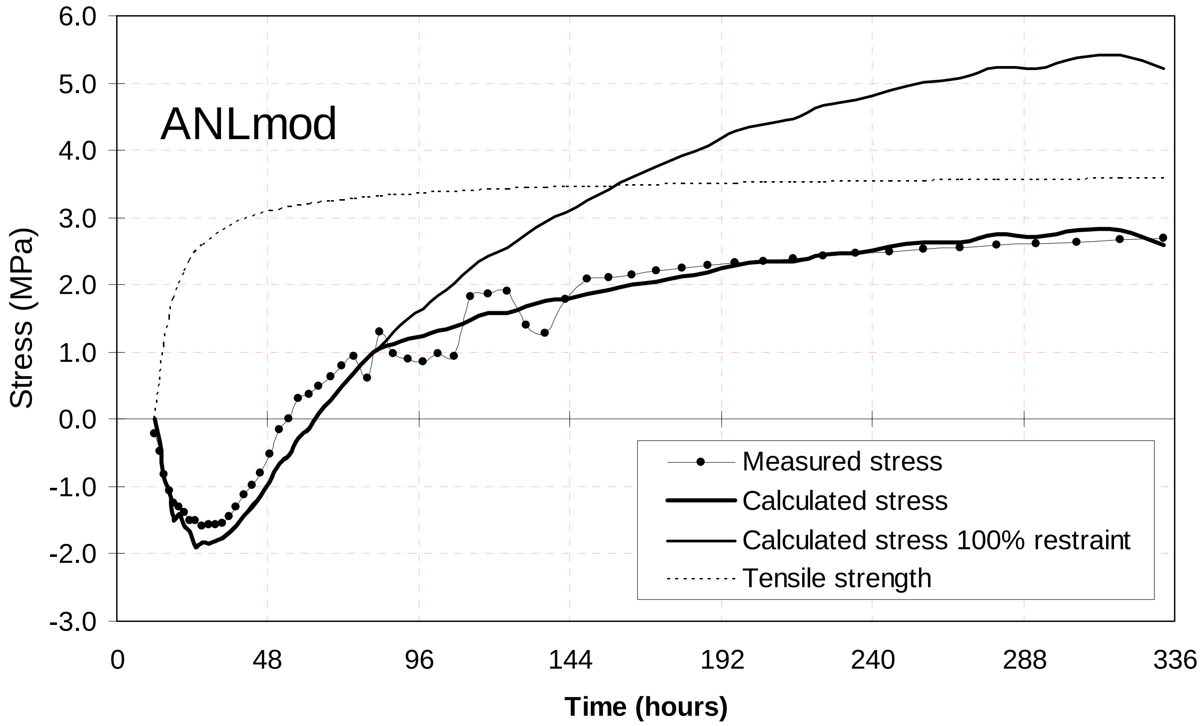

Fig. 9.5 *ANL*$_{mod}$: Measured and calculated stress, semi-adiabatic conditions

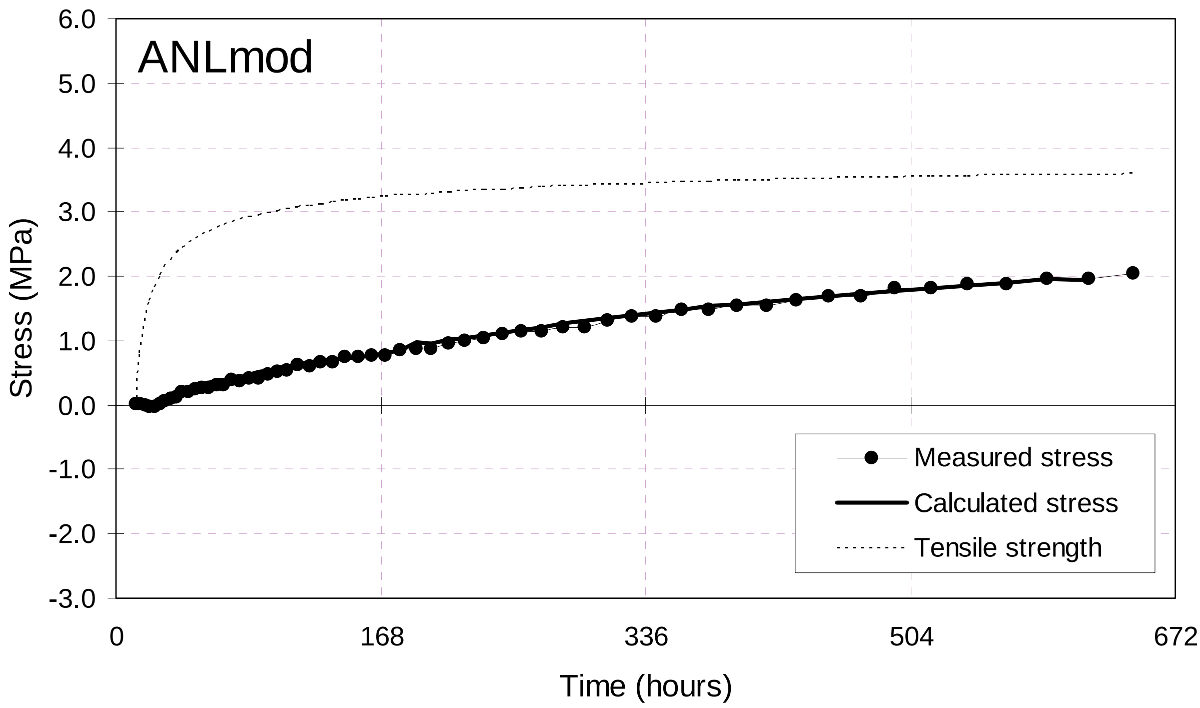

Fig. 9.6 *ANL*$_{mod.}$ Measured and calculated stress, 20 ^{o}C isothermal conditions.

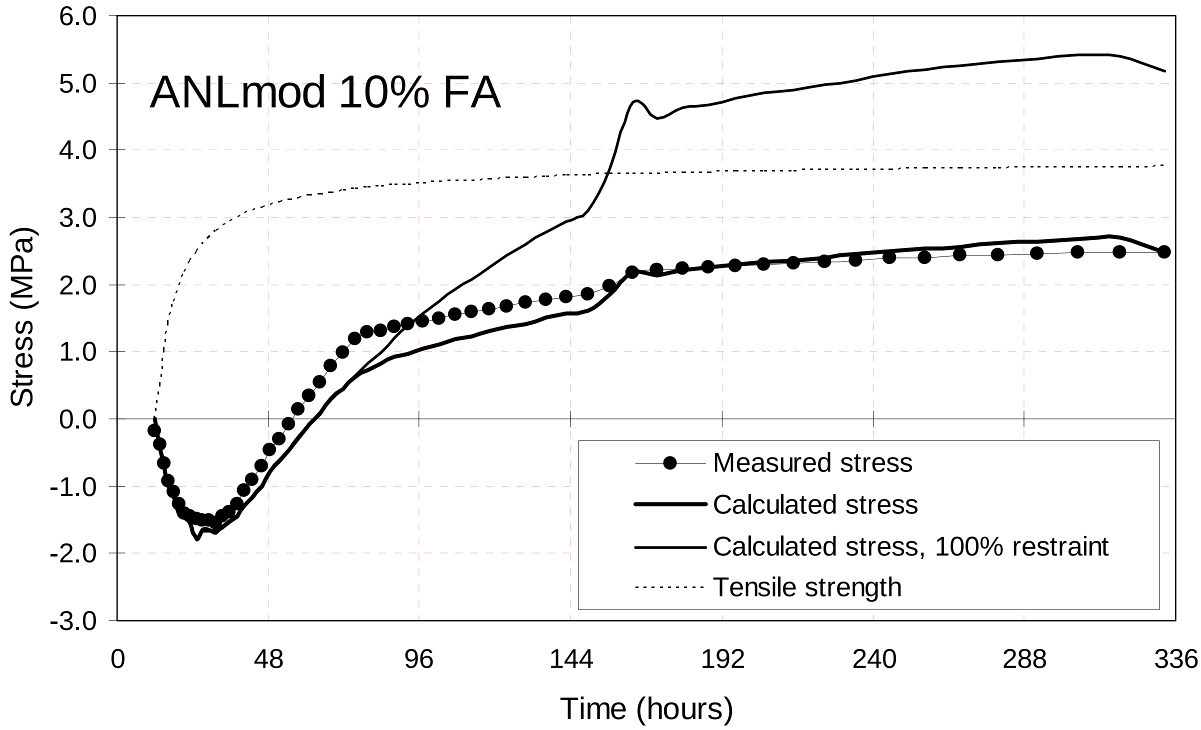

Fig. 9.7 *ANL*$_{mod}$ *10%FA:* Measured and calculated stress, semi-adiabatic conditions. The step in the curves after around 7 days is due to an unintentional drop in the specimen temperature.

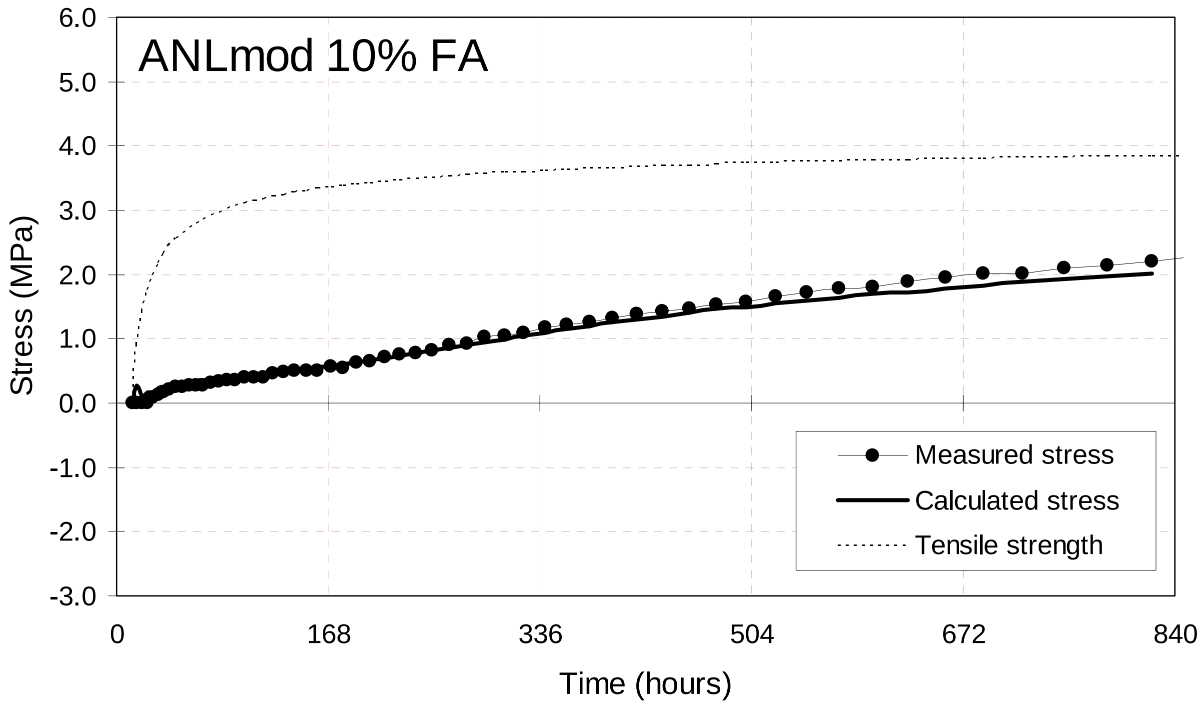

Fig. 9.8 *ANL*$_{mod}$ *10%FA:* Measured and calculated stress, 20 ^{o}C isothermal conditions.

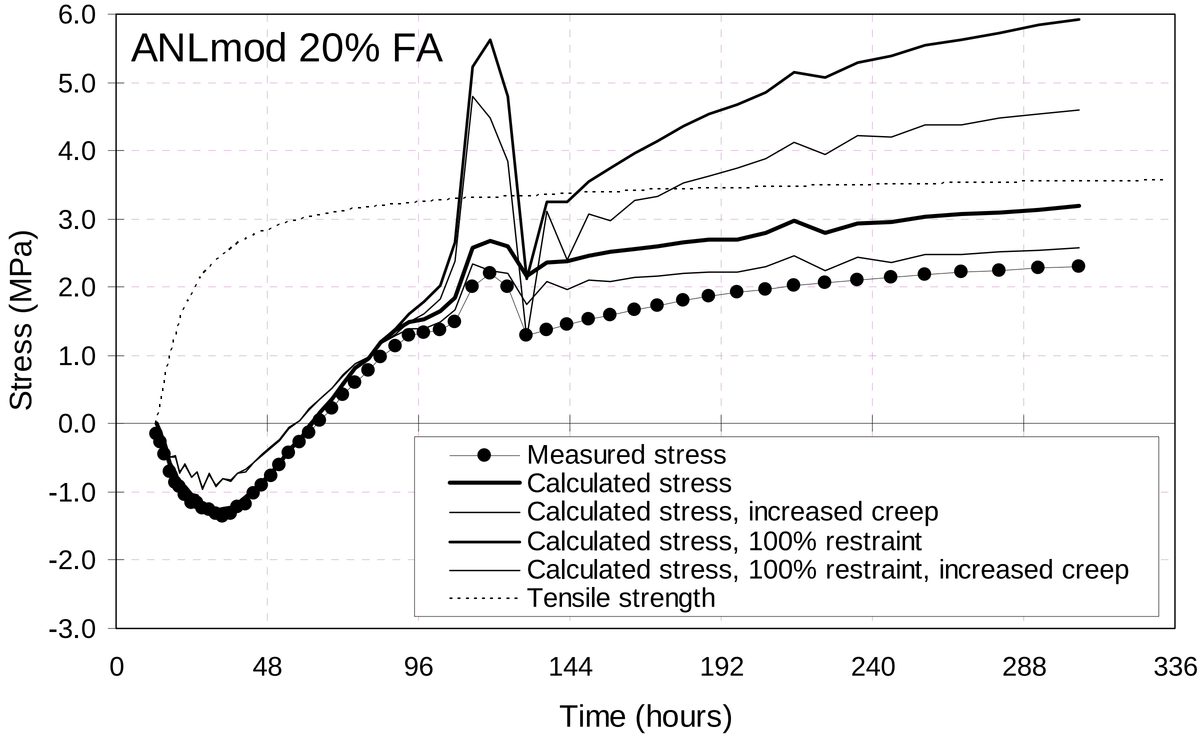

Fig. 9.9 *ANL$_{mod}$ 20%FA:* Measured and calculated stress, semi-adiabatic conditions (incl. calculation with increased creep). The peak in the curves after around 5 days is due to unintentional temperature fluctuation in the specimen.

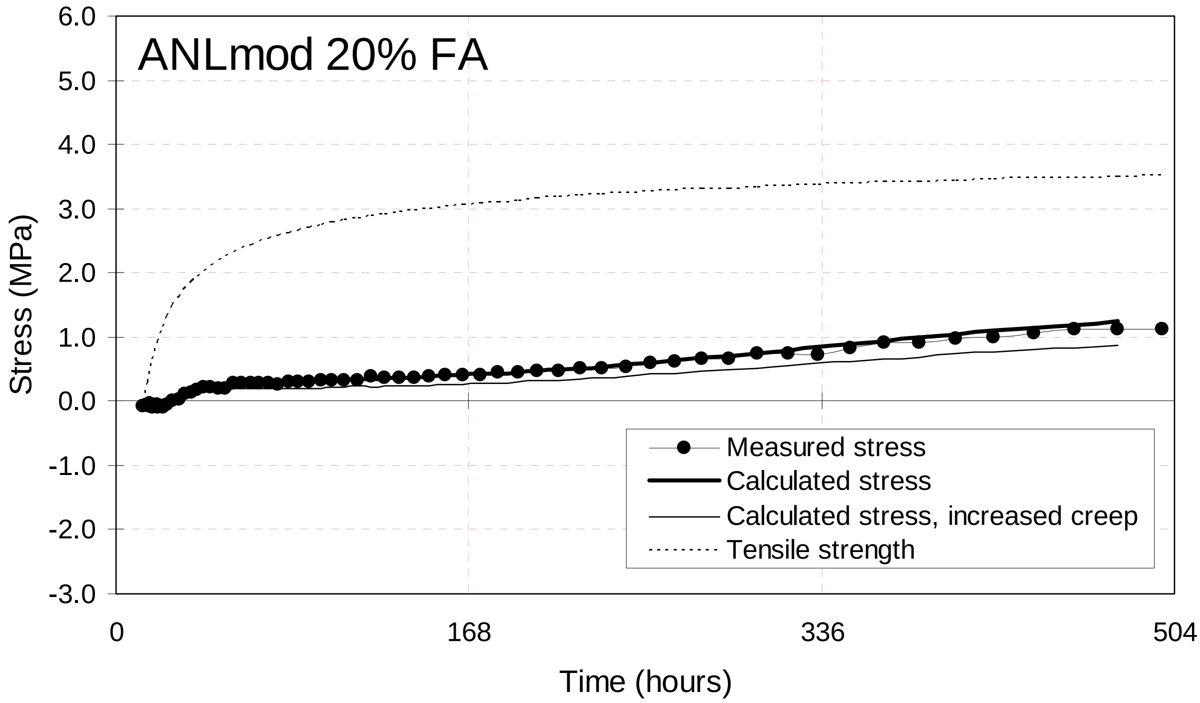

Fig. 9.10 *ANL$_{mod}$ 20%FA:* Measured and calculated stress, 20 ^{o}C isothermal conditions (incl. calculation with increased creep).

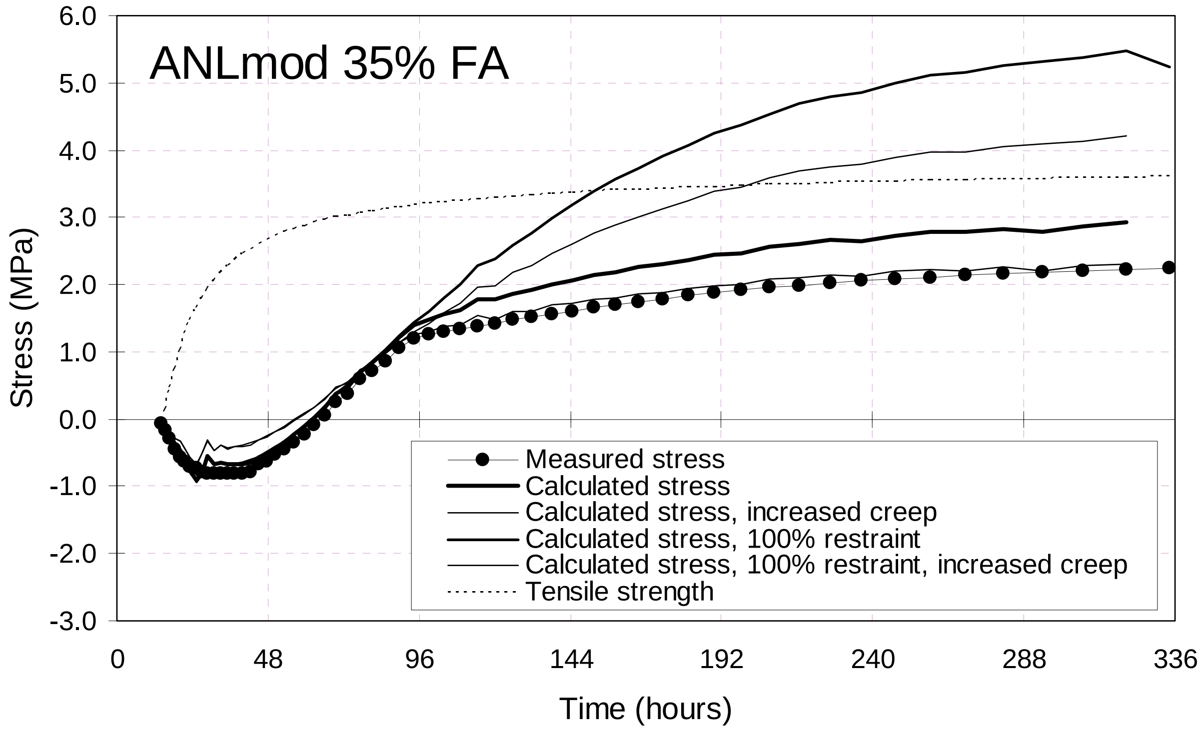

Fig. 9.11 *ANL$_{mod}$ 35%FA:* Measured and calculated stress, semi-adiabatic conditions (incl. calculation with increased creep).

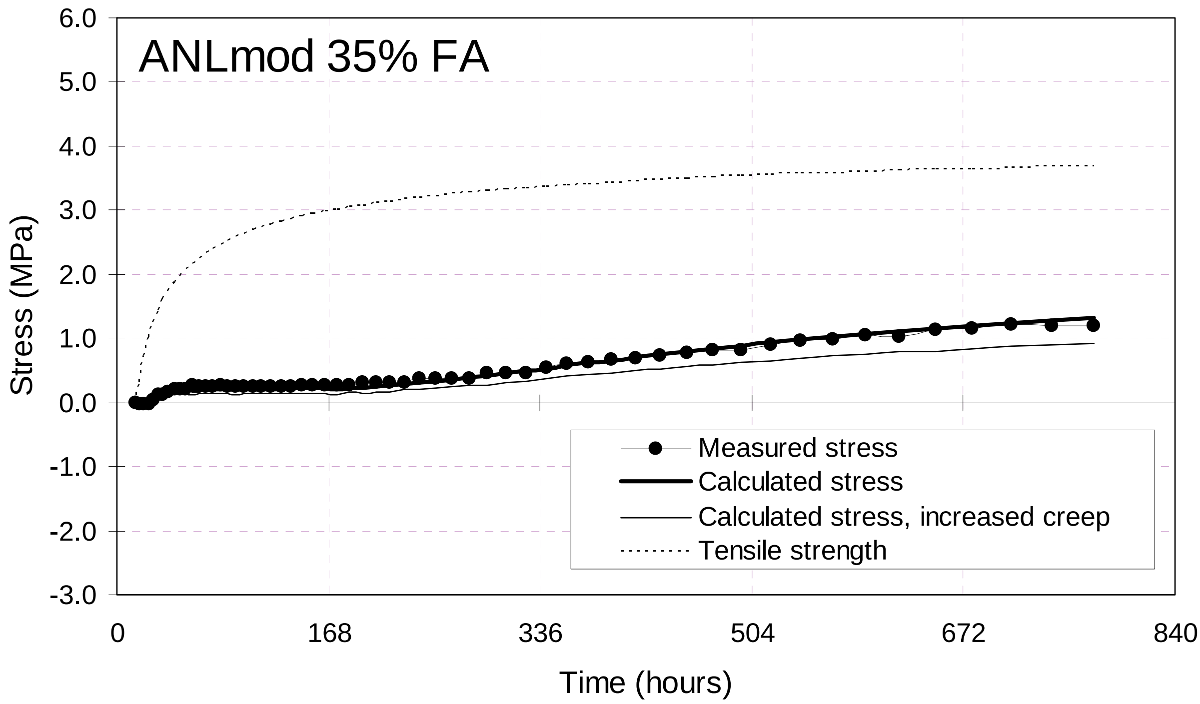

Fig. 9.12 *ANL$_{mod}$ 35%FA:* Measured and calculated stress, 20 ^{o}C isothermal conditions (incl. calculation with increased creep).

9.3 Evaluation

The calculated stresses from the previous section are plotted in Fig. 9.13 vs. measured stress in the TSTM. The comparison is made after 288 hours for the semi-adiabatic conditions and after 28 days for the 20 ^{o}C tests. The solid dots in the figure represent the results were "default creep parameters" have been used in the calculations; these results show that the calculated stress is on average 0.12 MPa higher than the measured ones, whereas the standard deviation (STD) is 0.33 MPa.

For the two concretes *ANL$_{mod}$ 20%FA* and *ANL$_{mod}$ 35%FA* and semi-adiabatic conditions, the difference between calculated and measured stress were higher than for the other concretes, indicating that creep is higher than what is reflected in the calculation by the default creep parameters. The calculation improves significantly when the creep parameter φ_o is increased from 0.75 to 1.37. This is indicated by the open dots in Fig. 9.13. Note that the two highest values are for semi-adiabatic conditions and the two lower ones (they are nearly fully overlapping) are isothermal conditions. It is also notable that, for the latter case, the increase in creep slightly increases the difference between calculated and measured stress. Nevertheless, for this case with increased creep in the calculation for *ANL$_{mod}$ 20%FA* and *ANL$_{mod}$ 35%FA* and "default creep parameters" for the rest of the concretes, the calculated stress is on average 0.04 MPa lower than the measured ones, whereas the standard deviation (STD) is 0.19 MPa. For the semi-adiabatic tests alone the corresponding values are (average deviation=) 0.03 MPa and (STD=) 0.12 MPa.

Note that the calculations with increased creep for *ANL$_{mod}$ 20%FA* and *ANL$_{mod}$ 35%FA* are used in the following evaluation.

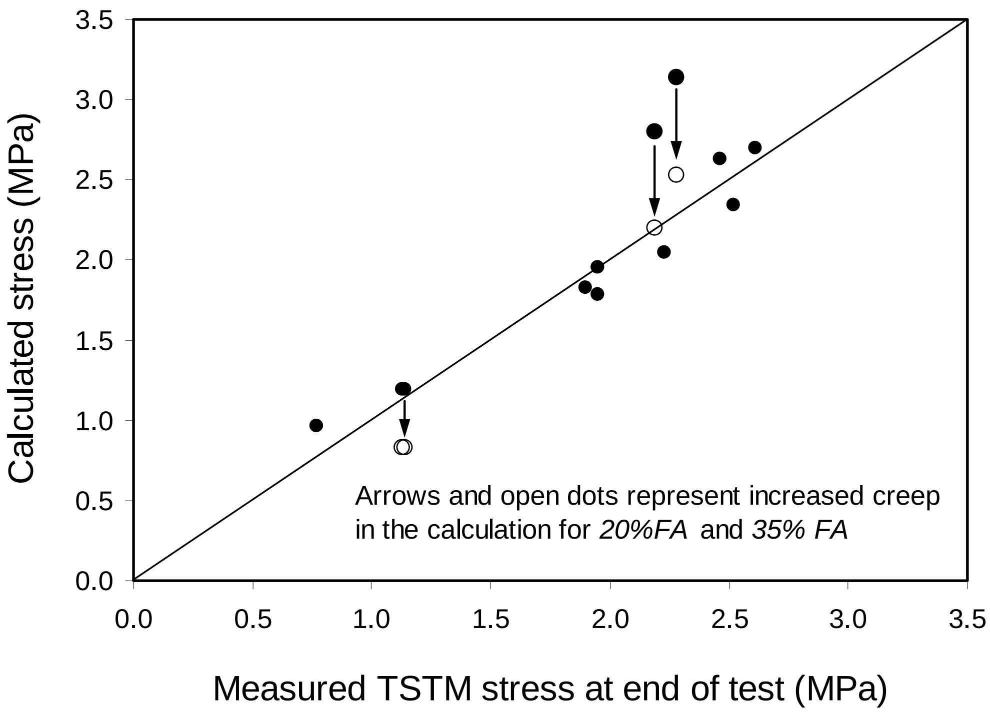

Fig. 9.13 Calculated vs. measured stress in the TSTM. A second calculation was done for both *20% FA* and *35% FA*, in which the creep was increased (marked with open dots). Note that the two lowest values are nearly overlapping.

Crack indices over time are shown in Fig. 9.14 and Fig. 9.15. Note that the curves for semi-adiabatic conditions are based on the stress calculations (100% restraint), while the isothermal ones are based on measured TSTM-stress (since the restraint is 100% in the rig during the 20°C tests); both divided by the relevant direct tensile strength in order to calculate the crack index. The stress values shown in Fig. 9.16 and Fig. 9.17 give corresponding crack indices after 288 h for semi-adiabatic conditions. Finally, Fig. 9.18 gives the same data relative to the ANL_{mod} concrete (which then gets crack index = 1.0). It is notable that the ranking between the concretes is the same for the the 20 °C and semi-adiabatic conditions.

The results for semi-adiabatic conditions show the following:
Effect of cement type: ANL_{mod} has the highest crack index, followed by *ANL* and SR_{mod}.
Effect of FA-dosage in combination with the ANL_{mod} *cement*: The crack index is systematically reduced with FA-dosage, where the 35% FA dosage gives 22% lower crack index than the one without FA. This trend is in line with previous results on the effect of FA in concretes with w/b=0.45 (0.40 here) and 5% silica fume (zero here) /9//15//16/.

Remember that the semi-adiabatic curing condition used in the tests equals to the expected average temperature development for a hardening 1 m thick and 6 m high wall structure placed on a hardened base, and with 20 °C initial concrete temperature and 20 °C ambient air temperature. Furthermore, the wall formwork is not removed from the structure during hardening which means that no major temperature gradients occur (except close to the base). The present relative ranking of the risk of through cracking after around 2 weeks, should therefore be quite representative for this structural case and ambient conditions.

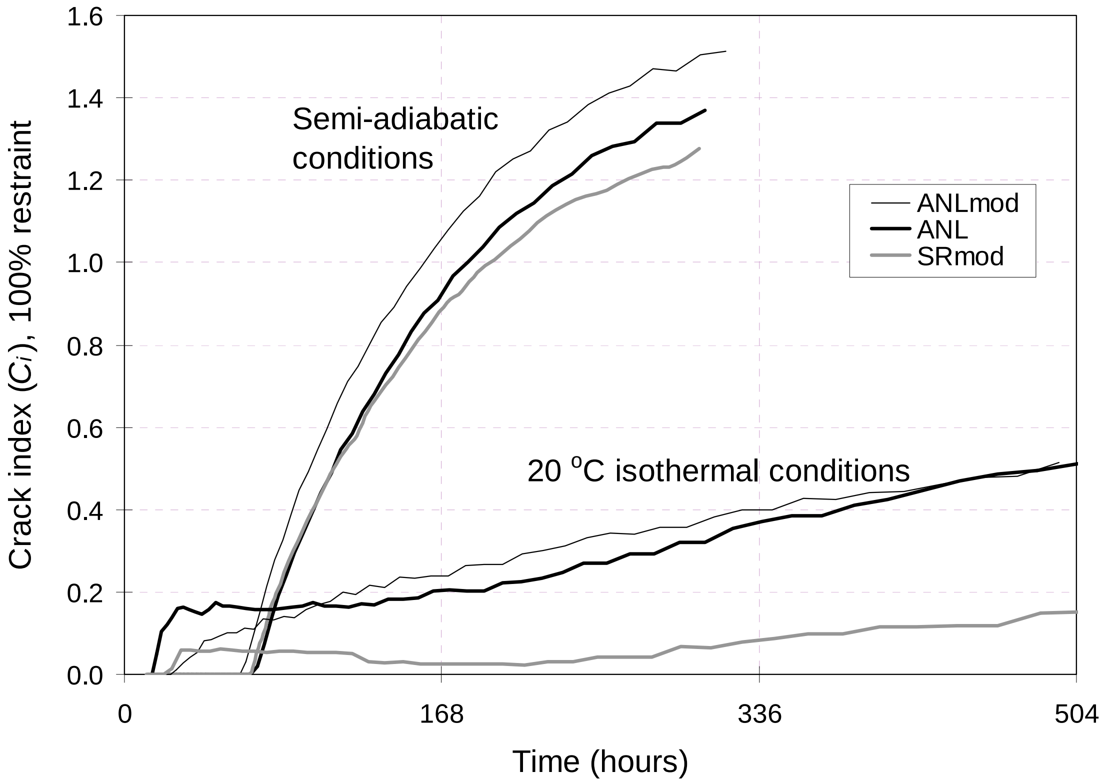

Fig. 9.14 Crack index over time. Effect of cement type.

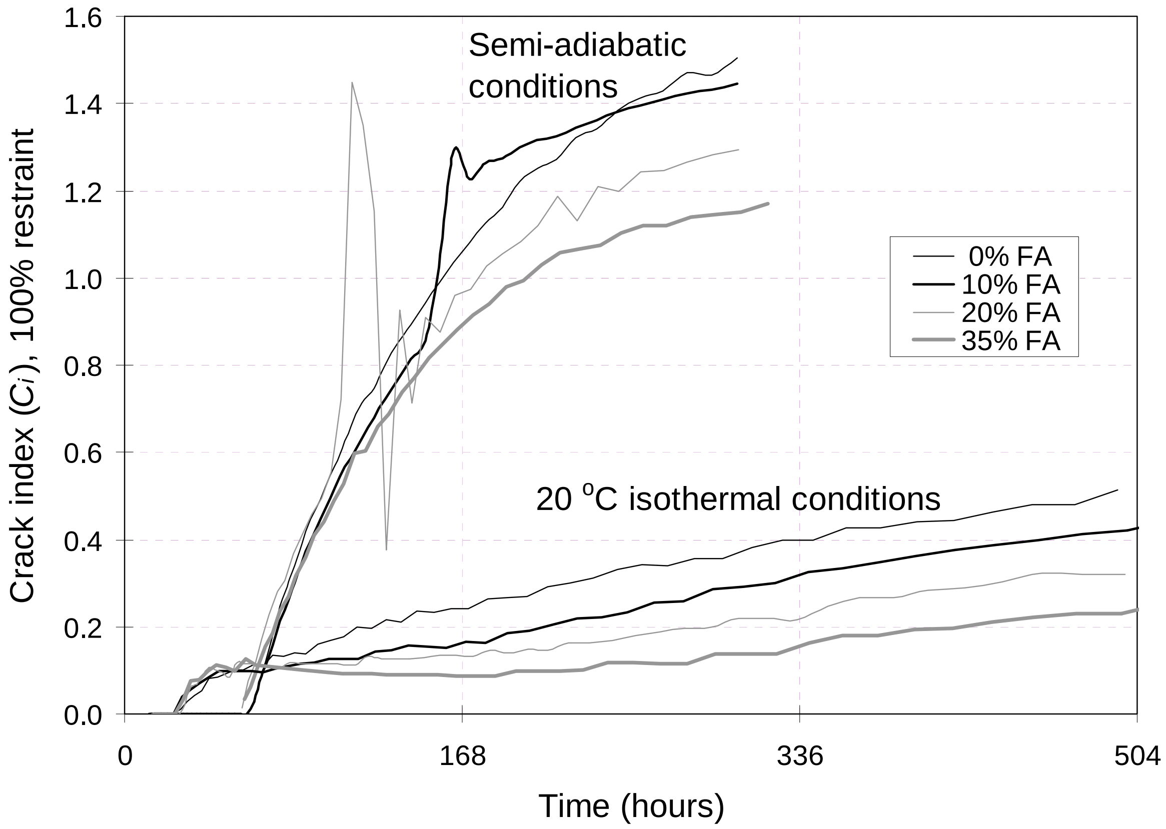

Fig. 9.15 Crack index over time. Effect of FA (in combination with ANL_{mod}).

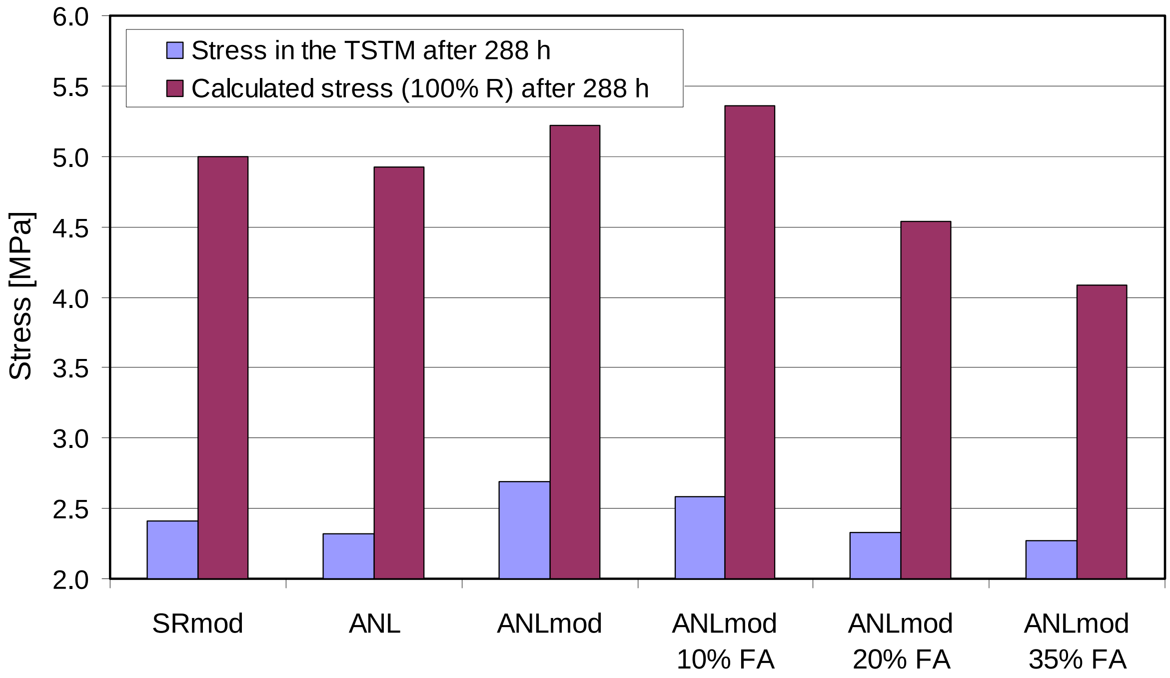

Fig. 9.16 Restraint stress after 288 hours, <u>semi-adiabatic conditions</u>. Measured stress in the TSTM (partly restraint) and calculated stress (100% restraint).

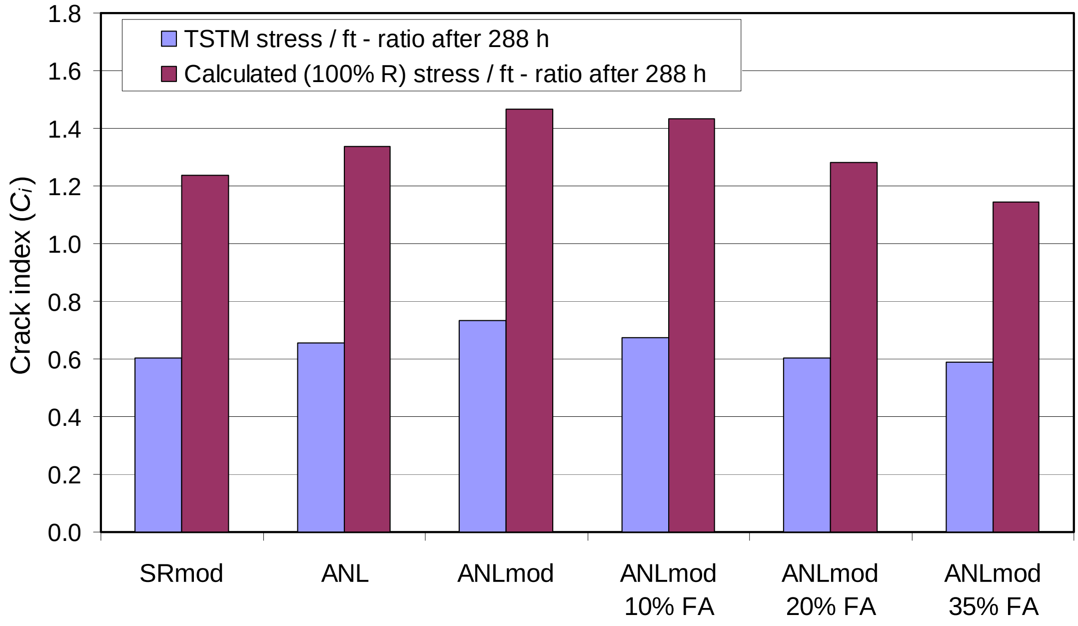

Fig. 9.17 Crack index after 288 hours based on measured stress in the TSTM (partly restraint) and calculated stress (100% restraint), semi-adiabatic conditions.

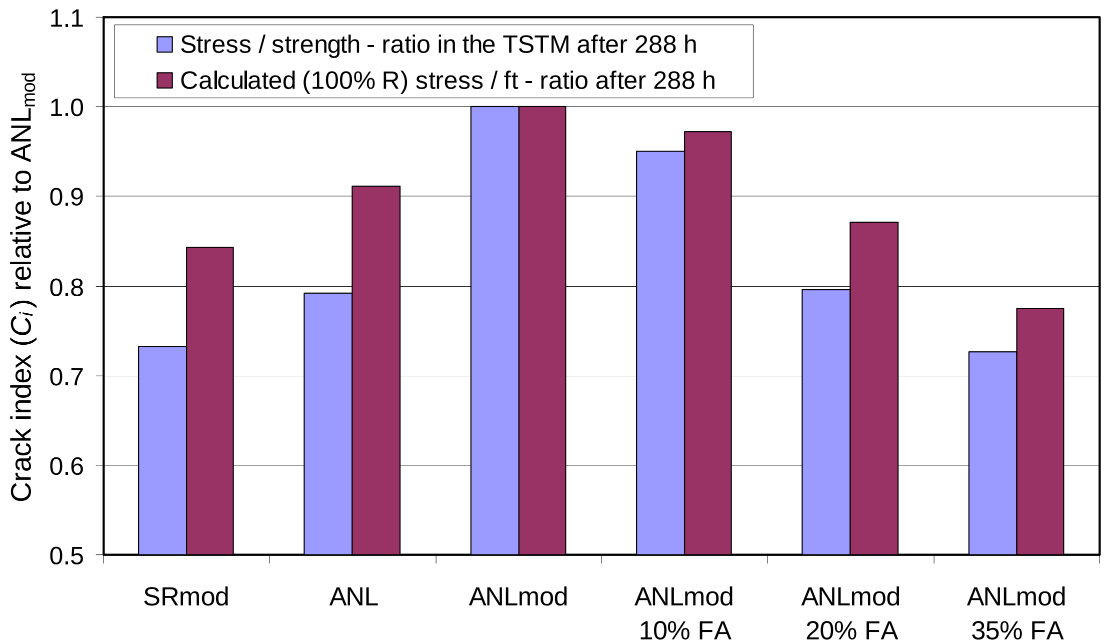

Fig. 9.18 Crack index relative to *ANL*$_{mod}$, based on Fig. 9.17, semi-adiabatic conditions.

10 Summary and conclusions

The tested concretes all have the same paste volume (28,3%), water-to-binder ratio (0.40) and k-factor = 1,0 for fly ash (silica fume is not used). The investigation of the *NL-slag* concrete was limited compared to the other concretes.

Effect of cement type:
Activation energy: The activation energy parameter A is rather unaffected by the cement type - it varies between 3750 and 3400 ^{o}K, while and the parameter B varies between 40 and 150.
Hydration heat and CTE during semi-adiabatic conditions: ANL_{mod} and SR_{mod} have about the same adiabatic temperature rise, while *ANL* is around 10% lower whereas *NL-slag* is around 25% lower. The latter concrete is made with slag cement which consists of 74% slag and 26% cement. There is no clear effect on the CTE among the tested cement types, except *NL-slag* which has a significantly higher CTE than the others.
Autogenous shrinkage during semi-adiabatic conditions: No great influence of cement type, but ANL_{mod} has somewhat more than *ANL* and SR_{mod}. (at isothermal conditions there are some differences, but this case with constant test temperature is not relevant for massive structures)
Direct tensile strength and E-modulus at semi-adiabatic conditions: No clear effect of cement type.

Effect of FA-dosage in combination with ANL_{mod}:
Activation energy: The FA-effect is not entirely systematic on the activation energy A parameter, but there is a tendency of increased A-value with FA-dosage. The parameter B decreases systematically with FA-dosage.
Hydration heat and CTE during semi-adiabatic conditions: FA systematically reduces the adiabatic temperature rise. In the NTNU-tests the 35% FA concrete gave 26% lower adiabatic temperature rise than the reference without FA. FA had little effect on the CTE in this test series.
Autogenous shrinkage during semi-adiabatic conditions: Little influence of FA, but there is a tendency of increased autogenous shrinkage with FA-dosage during the cooling period due to lower temperature maximum and, thus, less thermally induced autogenous swelling.
Direct tensile strength and E-modulus at semi-adiabatic conditions: No clear effect of FA-content.

Calculations and relative crack risk, semi-adiabatic conditions (relevant for a 1 m thick wall):
The stress calculations show good agreement with the TSTM-tests when using “default” creep parameters based on previous test results. An exception is for the two concretes with highest FA-content where an increased creep coefficient in the creep formulation had to be used to achieve good agreement. This indicates higher creep for the two concretes (also confirmed by direct creep measurements in another NTNU-investigation reported in /17/).

ANL_{mod} has somewhat higher cracking tendency (10 - 15%) than *ANL* and SR_{mod}. The reason appears to be is a combination of a slightly higher autogenous shrinkage and slightly lower tensile strength in the ANL_{mod} concrete compared to the two others.

FA gives systematically lower crack index during the cooling period. The calculations show that the concrete with 35% FA has 22% lower cracking tendency than the reference without FA. The main reason for this is the reduced hydration heat in the FA-concretes, since the other properties are not significant affected by the FA-content in this investigation.

11 References

/1/ Bjøntegaard Ø., Fosså K.T., Atrushi D., Sellevold E.J., Kanstad T., Hammer T.A and Smeplass S. (2003) Stress development and cracking tendency in hardening concrete: Test methods at NTNU, NOR-CRACK report #2.1, Subtask 2 Fundamental studies, STF22 A03607, ISBN 82-14-02582-6

/2/ Bjøntegaard Ø., Hammer T.A. and Sellevold E.J. (2004) On the Measurement of Free Deformation of Early Age Cement Paste and Concrete. Cement and Concrete Composites (2004), 26, pp. 427-435.

/3/ Bjøntegaard, Ø. (1999) Thermal Dilation and Autogenous Deformation as Driving Forces to Self-Induced Stresses in High Performance Concrete. Doctoral thesis, NTNU, Dept. of Structural Eng., ISBN 82-7984-002-8

/4/ Sellevold E.J. and Bjøntegaard Ø. (2006) Coefficient of Thermal Expansion of Cement Paste and Concrete: Mechanisms of Moisture Interaction. Materials and Structures, 39, 9, pp. 809-815

/5/ Kanstad, T., Bjøntegaard, Ø. Hammer, T.A. and Sellevold, E.J. (1999) Mechanical properties of young concrete: Evaluation of test methods for tensile strength and modulus of elasticity. Determination of model parameters. NOR-IPACS report, NTNU

/6/ Kanstad T., Hammer T.A., Bjøntegaard Ø. and Sellevold E.J. (2003) Mechanical Properties of Young Concrete: Part I - Experimental Results related to Test Methods and Temperature Effects, Materials and Structures, Vol. 36, May 2003, pp 218-225

/7/ Kanstad T., Hammer T.A., Bjøntegaard Ø. and Sellevold E.J. (2003) Mechanical Properties of Young Concrete: Part II - Determination of Model Parameters and Test Programme Proposals, Materials and Structures, Vol. 36, May 2003, pp 226-230

/8/ van Breugel K. and Lura P., "Deformational Behaviour and Selfinduced Stresses in Hardening Concrete. Experimental studies on thermal and autogenous deformations, creep and relaxation of hardening concrete". IPACS-report, Luleå Univ. of Tech., ISBN 91-89580-14–1, 2001

/9/ Bjøntegaard Ø. and Sellevold E.J. (2003) Bjørvika senketunnel - Bestemmelse av betongegenskaper relevante for evaluering av risstendens i herdefasen (in Norwegian). NTNU-report R-9-03, Department of Structural Engineering, June 2003.

/10/ Hellend S. (2001) Concrete for the Maridalen culvert, Round Robin test. IPACS-report, ISBN 91-89580-75-3, Publ. by TU-Luleå, May 2001, 27 pages

/11/ Morabito P., Bjøntegaard Ø., van Breugel K., Dalmagioni P., Gram H.-E., Gutsch A., Hedlund H., Jonasson J.-E., Kanstad K., Lura P., Pellegrini R., Rostasy F., Sellevold E., Round Robin Testing Program. Equipment, testing methods, test results (2001) IPACS-report, Ed. by P.Morabito, TU Luleå, Sweden, ISBN 91-89580-42-7, 110 pages

/12/ Prevention of Thermal Cracking in Concrete at Early Ages, RILEM report 15, State-of-the-Art report prepared by RILEM Technical Commettee 119, Ed. R.Springenschmid, E&FN Spon, ISBN 0-419-22310-X

/13/ Atrushi D. (2003) Tensile and Compressive Creep of Early Age Concrete: Testing and Modelling. Doctoral thesis, NTNU, Dept. of Structural Eng., ISBN 82-471-5565-6.

/14/ Maage M. and Helland S. (1988) Praktisk herdeteknologi - materialdata for en del norske sementer, tilsetningsstoffer og silica (in Norwegian). Norsk Betongdag 1988, 28-29 okt., Norsk betongforening, 72 pages

/15/ Kanstad T. and Guomin J. (2004) Bjørvika submerged concrete tunnel, Phase 2: Evaluation of the risk of cracking in the hardening phase. NTNU-report R-6-04, Department of Structural Engineering,

/16/ Guomin J., Kanstad T. and Bjøntegaard Ø. (2004) Analyses of the SVV double wall field test related to the Bjørvika tunnel project. NTNU-report R-7-04, Department of Structural Engineering, 13 pages

/17/ Guomin Ji G. (2008) Cracking Risk of Concrete Structures in the Hardening Phase: Experiments, Material Modelling and Finite Element Analysis, Doctoral thesis, NTNU, Dept. of Structural Eng., ISBN 978-82-471-1079-9

APPENDIX 1 Hydration heat, NTNU-results

Adiabatic temperature and isothermic heat

(v 2.7 ss 2001-02-16)

Concrete parameters

Temp. trans. coeff.	0.0181
Density	2420
Heat capacity (fresh)	1.03
Heat capacity (hardened)	1.03
Cement + Silica content	391
Set time	10.4
A - set time	20785
B - set time	2500
A - hydration	20785
B - hydration	2500
Adia. start temperature	25

Temp. trans. coeff.

dQ/dm	0.05
m>	150
m<	200

Heat function

M-limit	150
Q_∞	299
τ	18.26
α	2.09
R^2	0.8139
$\Sigma\Delta_Q$	6220

Heat polygon

Reference heat [kJ/kg cem]	*Corresp. maturity [h]*
1	0.9
4	4.2
8	8.8
12	10.8
25	12.8
40	13.9
60	15.2
80	16.4
100	17.3
120	18.3
140	19.6
160	21.4
180	23.8
200	27.3
220	32.1
240	39.5
260	50.2
280	69.4
290	92.4
295	116.7
300	172.6

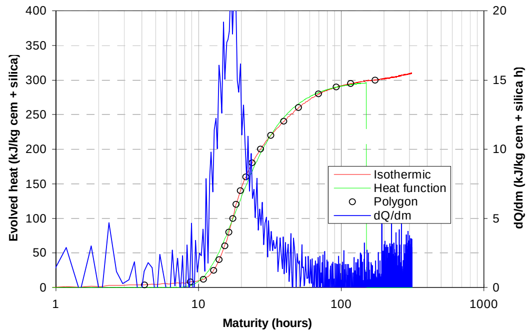

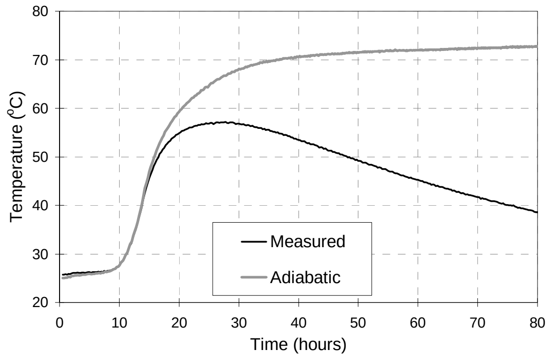

Project

Name	NOR-CRACK
Test id	T123, REF-Betong med ANLEGG (EZ2-01)
Perf. by	Betong: Ove Loraas , Forsøk: Øyvind Bjøntegaard
Date	07.06.2002

Adiabatic temperature and isothermic heat

(v 2.7 ss 2001-02-16)

Concrete parameters

Temp. trans. coeff.	0.0182
Density	2420
Heat capacity (fresh)	1.03
Heat capacity (hardened)	1.03
Cement + Silica content	391
Set time	10.4
A - set time	20785
B - set time	2500
A - hydration	20785
B - hydration	2500
Adia. start temperature	25

Temp. trans. coeff.

dQ/dm	0.05
m>	150
m<	200

Heat function

M-limit	150
Q_∞	297
τ	16.73
α	2.03
R^2	0.8162
$\Sigma\Delta_Q$	3935

Heat polygon

Reference heat [kJ/kg cem]	*Corresp. maturity [h]*
1	0.0
4	3.7
8	8.1
12	9.6
25	11.3
40	12.6
60	13.9
80	15.0
100	16.0
120	16.9
140	18.3
160	20.1
180	22.4
200	25.7
220	30.5
240	37.7
260	48.5
280	70.1
290	102.8
295	147.9
300	241.5

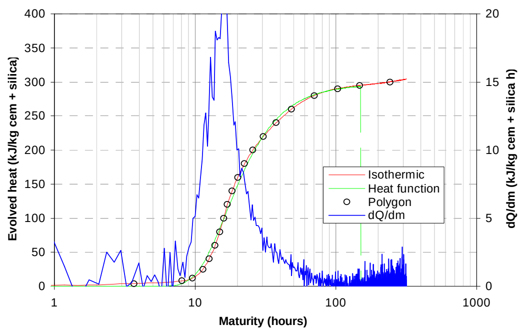

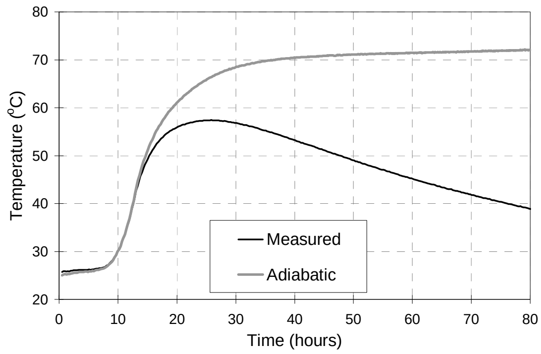

Project

Name	NOR-CRACK
Test id	T125, REF-Betong med ANLEGG (EZ2-01)
Perf. by	Betong: Ove Loraas , Forsøk: Øyvind Bjøntegaard
Date	13.08.2002

Adiabatic temperature and isothermic heat

(v 2.7 ss 2001-02-16)

Concrete parameters

Temp. trans. coeff.	0,0178
Density	2450
Heat capacity (fresh)	1,03
Heat capacity (hardened	1,03
Cement + Silica content	391
Set time	10
A - set time	28251
B - set time	1255
A - hydration	28251
B - hydration	1255
Adia. start temperature	20

Temp. trans. coeff.

dQ/dm	0,05
m>	150
m<	200

Heat function

M-limit	150
Q_∞	313
τ	17,40
α	1,73
R^2	0,9287
$\Sigma\Delta_Q$	1823

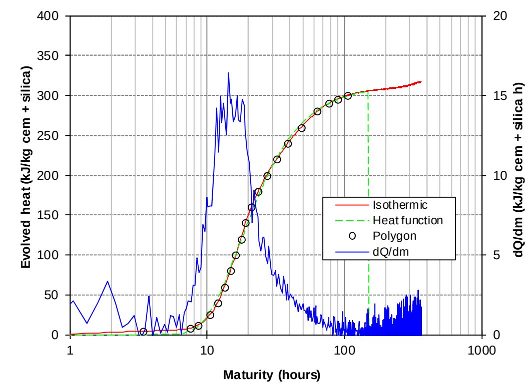

Heat polygon

Reference heat kJ/kg cem]	Corresp. maturity [h]
1	0,7
4	3,4
8	7,5
12	8,6
25	10,5
40	11,9
60	13,3
80	14,7
100	16,2
120	17,6
140	19,1
160	21,0
180	23,6
200	27,3
220	32,2
240	38,7
260	48,6
280	63,7
290	77,1
295	88,9
300	104,7

Adapt the temperature transmission coefficient: **<Ctrl> t**
Adapt the heat function **<Ctrl> h**

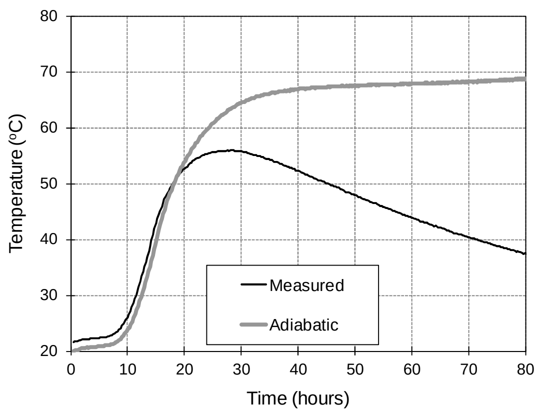

Project

Name	NOR-CRACK
Test id	T145, REF-Betong med MOD ANL (EZ33-02)
Perf. by	Betong: Ove Loraas , Forsøk: Øyvind Bjøntegaard
Date	19.03.2003

Adiabatic temperature and isothermic heat

(v 2.7 ss 2001-02-16)

Concrete parameters

Temp. trans. coeff.	0.0181
Density	2420
Heat capacity (fresh)	1.03
Heat capacity (hardened)	1.03
Cement + Silica content	391
Set time	10.4
A - set time	20785
B - set time	2500
A - hydration	20785
B - hydration	2500
Adia. start temperature	25

Temp. trans. coeff.

dQ/dm	0.05
m>	150
m<	200

Heat function

M-limit	150
Q_∞	323
τ	17.18
α	1.56
R^2	0.9313
$\Sigma\Delta_Q$	4382

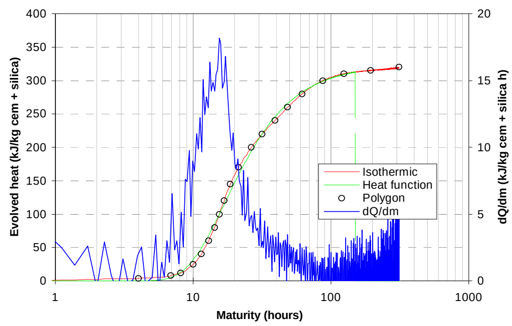

Heat polygon

Reference heat [kJ/kg cem]	Corresp. maturity [h]
1	0.4
4	4.0
8	6.9
12	8.1
25	10.0
40	11.5
60	12.9
80	14.3
100	15.5
120	16.8
145	18.6
170	21.3
200	26.5
220	31.7
240	39.3
260	48.4
280	61.6
300	87.2
310	124.1
315	194.3
320	312.8

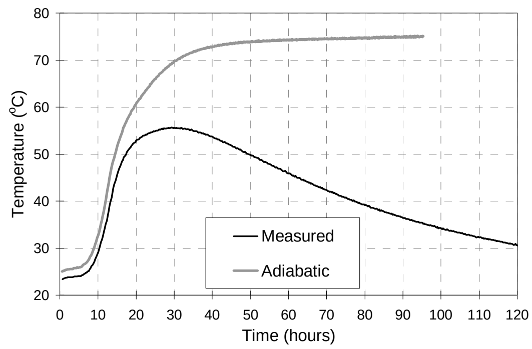

Project

Name	NOR-CRACK
Test id	T124, REF-Betong med SR (DZ9-01)
Perf. by	Betong: Ove Loraas , Forsøk: Øyvind Bjøntegaard
Date	03.07.2002

Adiabatic temperature and isothermic heat

(v 2.7 ss 2001-02-16)

Concrete parameters

Temp. trans. coeff.	0,0179
Density	2420
Heat capacity (fresh)	1,03
Heat capacity (hardened	1,03
Cement + Silica content	391
Set time	20,5
A - set time	33500
B - set time	2500
A - hydration	33500
B - hydration	2500
Adia. start temperature	20

Temp. trans. coeff.

dQ/dm	0,07
m>	150
m<	200

Heat function

M-limit	150
Q_∞	297
τ	16,73
α	2,03
R^2	0,9912
$\Sigma\Delta Q$	555374

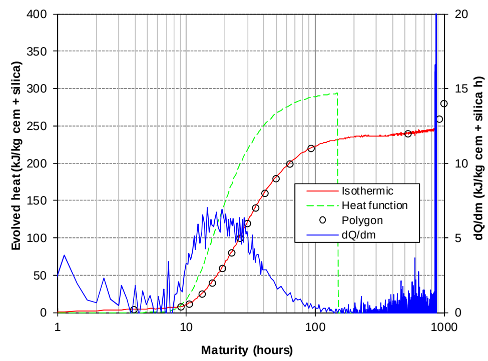

Heat polygon

Reference heat kJ/kg cem]	*Corresp. maturity [h]*
1	0,0
4	3,9
8	9,0
12	10,5
25	13,2
40	15,7
60	19,0
80	22,3
100	25,9
120	29,5
140	34,2
160	40,3
180	49,1
200	62,9
220	92,2
240	525,3
260	916,3
280	986,7
290	1022,0
295	1039,6
300	1057,2

Adapt the temperature transmission coefficient: **<Ctrl> t**
Adapt the heat function **<Ctrl> h**

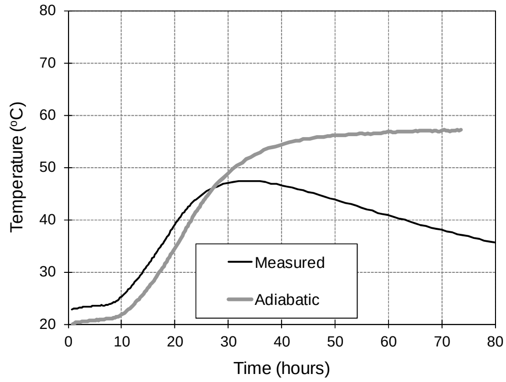

Project

Name	NOR-CRACK
Test id	T180, REF-Betong med NL-slaggsement, No P-type plasticiser
Perf. by	Betong: Ove Loraas , Forsøk: Øyvind Bjøntegaard
Date	16.03.2005

Adiabatic temperature and isothermic heat

(v 2.7 ss 2001-02-16)

Concrete parameters

Temp. trans. coeff.	0,0186
Density	2420
Heat capacity (fresh)	1,03
Heat capacity (hardened	1,03
Cement + Silica content	377
Set time	10,6
A - set time	27553
B - set time	507
A - hydration	27553
B - hydration	507
Adia. start temperature	20

Temp. trans. coeff.

dQ/dm	0,08
m>	200
m<	250

Heat function

M-limit	150
Q_∞	297
τ	16,73
α	2,03
R^2	0,9008
$\Sigma\Delta Q$	27337

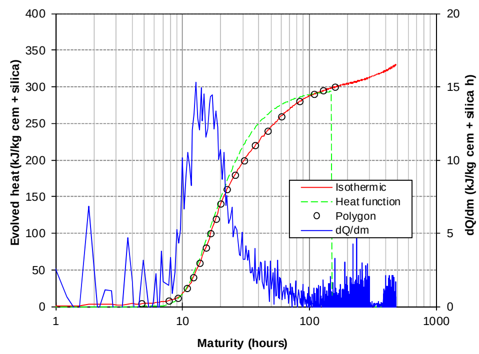

Heat polygon

Reference heat kJ/kg cem]	*Corresp. maturity [h]*
1	0,6
4	4,8
8	7,8
12	9,1
25	10,8
40	12,2
60	13,7
80	15,2
100	16,7
120	18,2
140	20,1
160	22,4
180	25,9
200	30,8
220	37,5
240	46,7
260	59,9
280	83,5
290	108,3
295	128,7
300	159,2

Adapt the temperature transmission coefficient: **<Ctrl> t**
Adapt the heat function **<Ctrl> h**

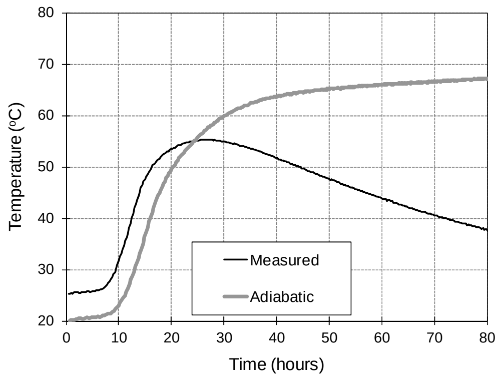

Project

Name	NOR-CRACK
Test id	T154, REF-Betong med MOD ANL (EZ33-02) og 10% FA
Perf. by	Betong: Ove Loraas , Forsøk: Øyvind Bjøntegaard
Date	26.06.2003

Adiabatic temperature and isothermic heat

(v 2.7 ss 2001-02-16)

Concrete parameters

Temp. trans. coeff.	0,0180
Density	2420
Heat capacity (fresh)	1,03
Heat capacity (hardened	1,03
Cement + Silica content	377
Set time	10,8
A - set time	31884
B - set time	166
A - hydration	31884
B - hydration	166
Adia. start temperature	20

Temp. trans. coeff.

dQ/dm	0,14
m>	150
m<	200

Heat function

M-limit	150
Q_∞	280
τ	16,73
α	2,03
R^2	0,9340
ΣΔQ	94291

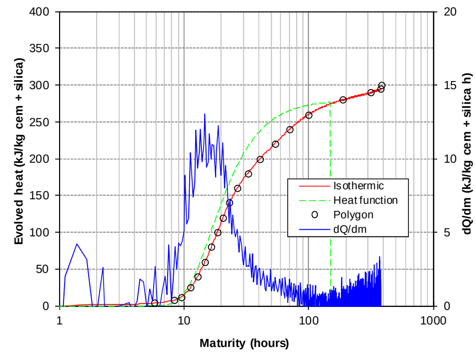

Heat polygon

Reference heat kJ/kg cem]	Corresp. maturity [h]
1	0,8
4	5,8
8	8,4
12	9,5
25	11,3
40	12,9
60	14,7
80	16,6
100	18,6
120	20,5
140	23,1
160	26,8
180	32,5
200	40,8
220	53,6
240	70,5
260	99,5
280	188,3
290	314,9
295	378,9
300	386,7

Adapt the temperature transmission coefficient: **<Ctrl> t**
Adapt the heat function **<Ctrl> h**

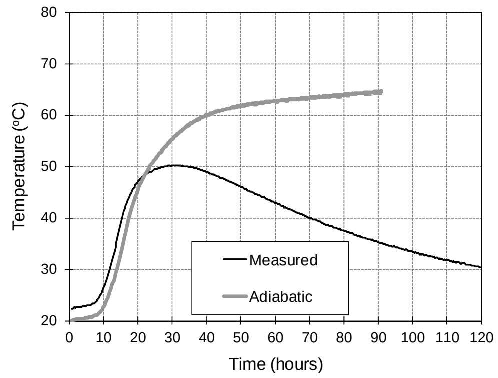

Project

Name	NOR-CRACK
Test id	T157, REF-Betong med MOD ANL (EZ33-02) og 20% FA
Perf. by	Betong: Ove Loraas , Forsøk: Øyvind Bjøntegaard
Date	30.09.2003

Adiabatic temperature and isothermic heat

(v 2.7 ss 2001-02-16)

Concrete parameters

Temp. trans. coeff.	0,0182
Density	2420
Heat capacity (fresh)	1,03
Heat capacity (hardened	1,03
Cement + Silica content	368
Set time	11,7
A - set time	35750
B - set time	0
A - hydration	35750
B - hydration	0
Adia. start temperature	20

Temp. trans. coeff.

dQ/dm	0,2
m>	150
m<	200

Heat function

M-limit	150
Q_∞	249
τ	21,19
α	1,37
R^2	0,9887
ΣΔQ	4969

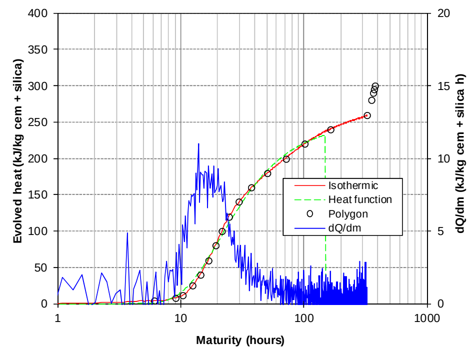

Heat polygon

Reference heat kJ/kg cem]	Corresp. maturity [h]
1	0,9
4	6,1
8	9,1
12	10,4
25	12,5
40	14,4
60	16,7
80	19,1
100	21,6
120	24,7
140	29,8
160	37,4
180	50,5
200	70,9
220	101,2
240	163,2
260	327,4
280	352,5
290	365,1
295	371,4
300	377,7

Adapt the temperature transmission coefficient: **<Ctrl> t**
Adapt the heat function **<Ctrl> h**

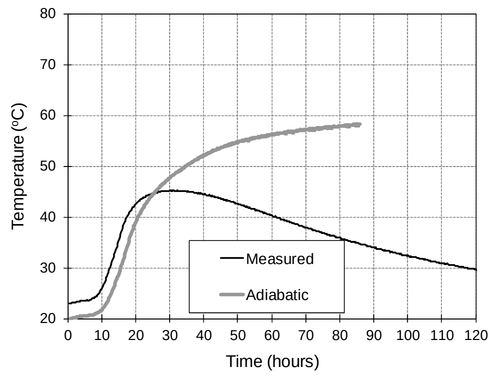

Project

Name	NOR-CRACK
Test id	T159, REF-Betong med MOD ANL (EZ33-02) og 35% FA
Perf. by	Betong: Ove Loraas , Forsøk: Øyvind Bjøntegaard
Date	05.11.2003

APPENDIX 2 Hydration heat, Norcem-results

ANL

Identification	Optional
Temp. trans. coeff.	0,0194
Density	2420
Heat capacity (fresh)	1,03
Heat capacity (hardened	1,03
Cement content	391
Set time	**9,5**
A - set time	31153
B - set time	316
A - hydration	31153
B - hydration	316
Adia. start temperature	20,5

Heat function	
M-limit	150
Q_∞	**256**
τ	**17,2**
α	**1,43**
R^2	0,9968

Heat transfer coeff.	
dQ/dt	0,08
M<	150
M>	200

Temp. trans. coeff. | Heat function | Set time

Description: DB204.03,Anl.v/c==.40, tils 0.26% P+1.0% M-150

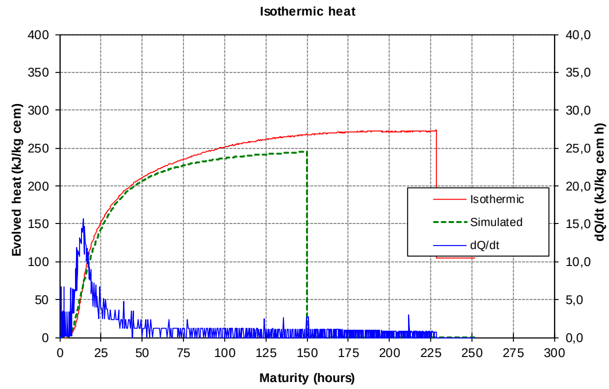

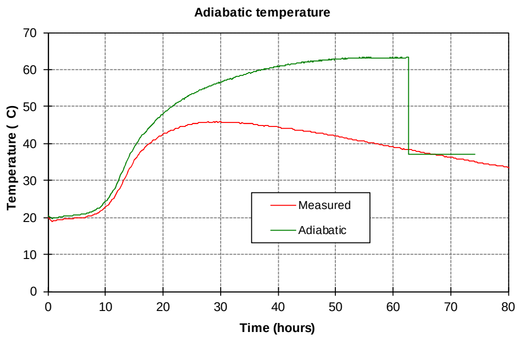

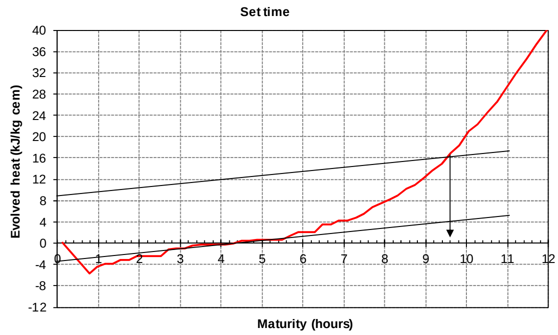

SRmod

Identification	Optional
Temp. trans. coeff.	0,0203
Density	2420
Heat capacity (fresh)	1,03
Heat capacity (hardened	1,03
Cement content	391
Set time	**8,0**
A - set time	27561
B - set time	507
A - hydration	27561
B - hydration	507
Adia. start temperature	19

Heat function	
M-limit	150
Q_∞	**316**
τ	**15,9**
α	**1,24**
R^2	0,9979

Heat transfer coeff.	
dQ/dt	0,08
M<	150
M>	200

Temp. trans. coeff. | Heat function | Set time

Description: DB119.03 SR,v/c+k=.40"Bindemidler"

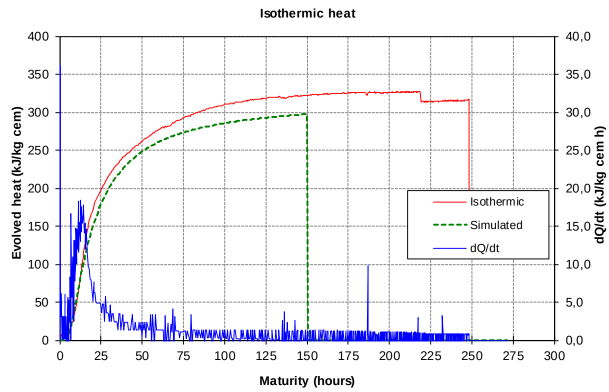

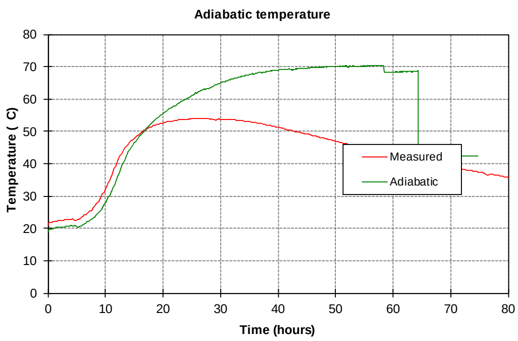

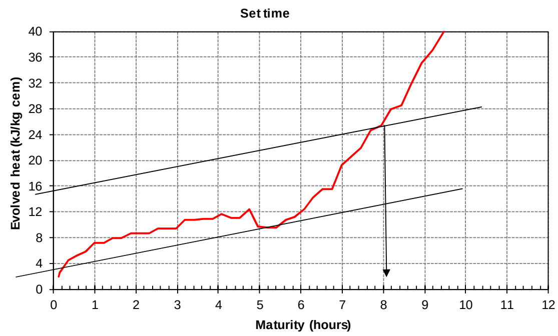

ANLmod

Identification	Optional
Temp. trans. coeff.	0,0225
Density	2420
Heat capacity (fresh)	1,03
Heat capacity (hardened	1,03
Cement content	391
Set time	**8,6**
A - set time	28251
B - set time	1255
A - hydration	28251
B - hydration	1255
Adia. start temperature	19,5

Heat function	
M-limit	150
Q_∞	**316**
τ	**16,1**
α	**1,45**
R^2	0,9991

Heat transfer coeff.	
dQ/dt	0,08
M<	150
M>	200

Temp. trans. coeff. | Heat function | Set time

Description: DB207.03,Anl.v/c=0.40, tils 0.26% P+1.0% M-150

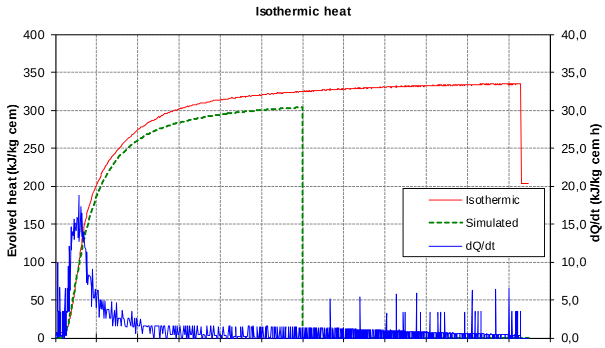

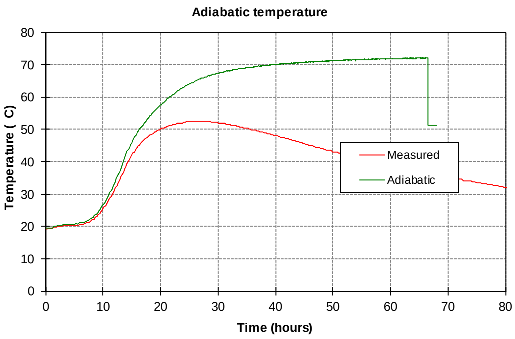

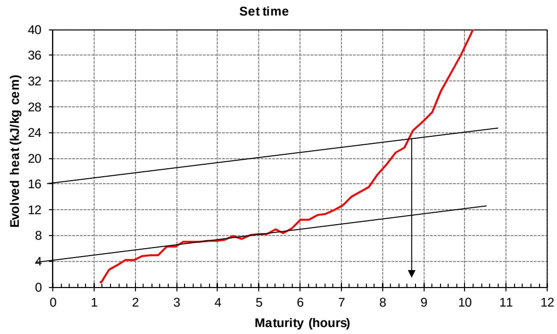

ANLmod 10% FA

Identification	Optional
Temp. trans. coeff.	0,0205
Density	2420
Heat capacity (fresh)	1,03
Heat capacity (hardened	1,03
Cement content	384
Set time	**8,8**
A - set time	27553
B - set time	507
A - hydration	27553
B - hydration	507
Adia. start temperature	19,5

Heat function	
M-limit	150
Q_∞	**305**
τ	**16,3**
α	**1,44**
R^2	0,9990

Heat transfer coeff.	
dQ/dt	0,08
M<	150
M>	200

Temp. trans. coeff. | Heat function | Set time

Description: DB107.033 Anlegg + 11.1% FA, bindemidler v/c+s=0.40 t

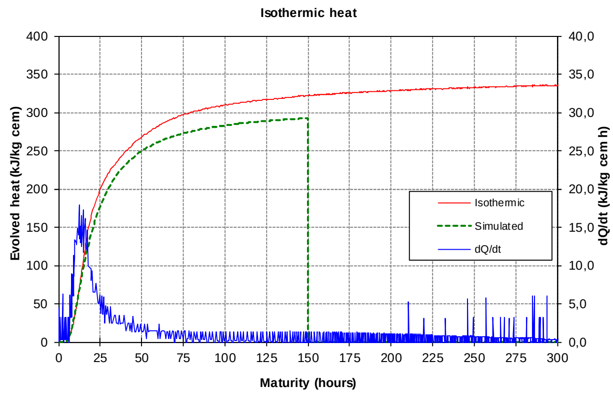

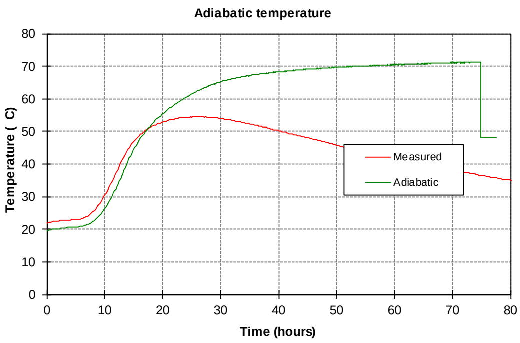

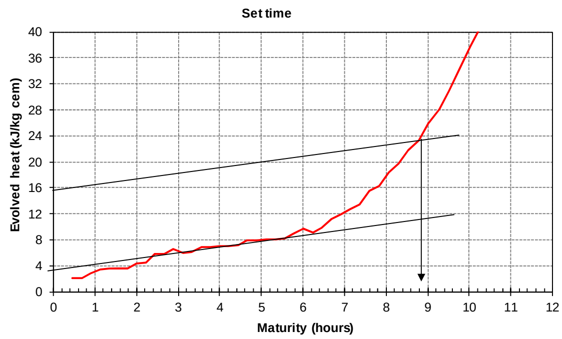

ANLmod 20% FA

Identification	*Optional*
Temp. trans. coeff.	0,0220
Density	2420
Heat capacity (fresh)	1,03
Heat capacity (hardened	1,03
Cement content	377
Set time	**8,6**
A - set time	31884
B - set time	166
A - hydration	31884
B - hydration	166
Adia. start temperature	19,2

Heat function	
M-limit	150
Q_∞	**272**
τ	**16,2**
α	**1,36**
R^2	0,9958

Heat transfer coeff.	
dQ/dt	0,14
M<	150
M>	200

Temp. trans. coeff. | Heat function | Set time

Description: DB151.03,anl."Bindemidler"v/c+ks=0.40 tils.0.27%P+1.2

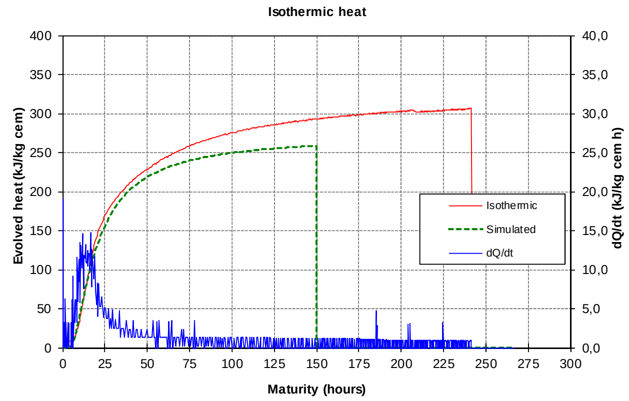

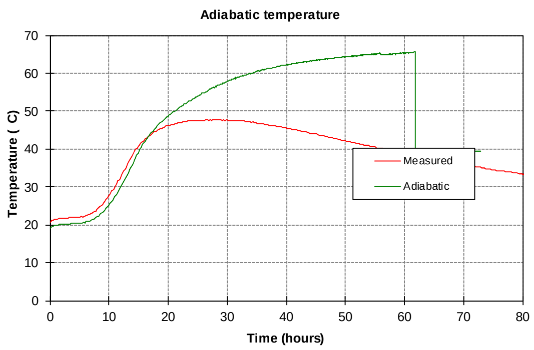

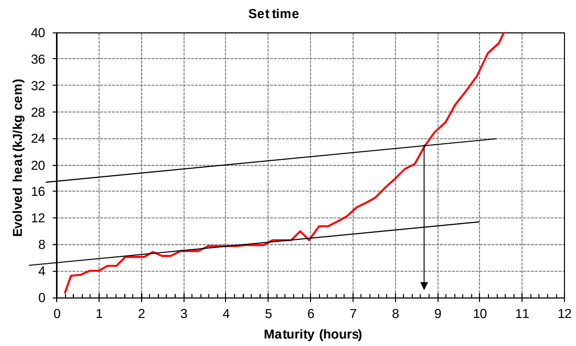

ANLmod 35% FA

Identification	*Optional*
Temp. trans. coeff.	0,0210
Density	2420
Heat capacity (fresh)	1,03
Heat capacity (hardened	1,03
Cement content	367
Set time	**11,0**
A - set time	35750
B - set time	0
A - hydration	35750
B - hydration	0
Adia. start temperature	19,7

Heat function	
M-limit	150
Q_∞	**189**
τ	**16,3**
α	**1,84**
R^2	0,9733

Heat transfer coeff.	
dQ/dt	0,2
M<	150
M>	200

Temp. trans. coeff. | Heat function | Set time

Description: DB180.03,Anlegg,v/b=0.40 erst.m.35% flyveaske tils.

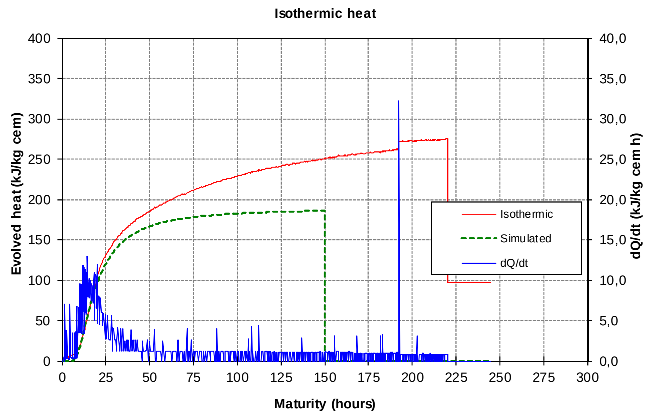

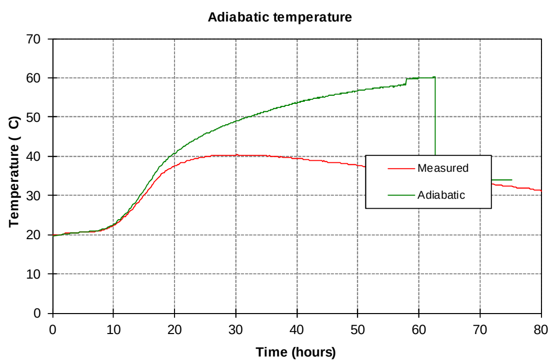

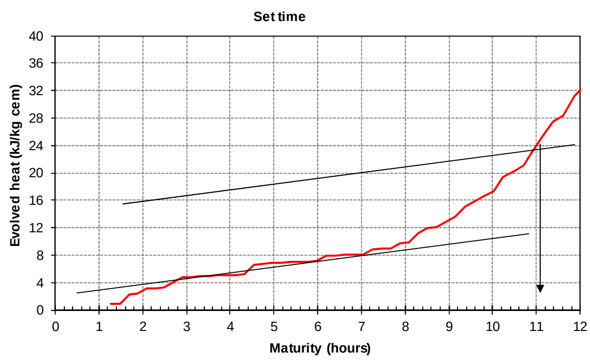

APPENDIX 3 Compressive strength, Norcem-results

FASTHETSUTVIKLING VED 5, 20, OG 35C

Time	BI 1			BL 2			BL 3		
	ANL			SRmod			ANLmod		
	DB 204 / DB 205			DB 119 / DB 115			DB 207 / DB 208		
	5C	20C	35C	5C	20C	35C	5C	20C	35C
3h			0,24						
3h 30m			0,52						
4h			1			0,19			0,2
4h 30m			2,1			0,4			0,43
5h		0,23	3,6			0,68			0,8
5h 30m			5,6			1,27		0,17	1,57
6h		0,57	7,6		0,21	2,12		0,23	2,4
6h 30m						2,84		0,27	
7h		1,26	12,2		0,34	3,78		0,42	5,2
8h	0,16	1,86			0,55	8,1		0,61	8,7
9h	0,26	3			0,92			1,3	12,9
9h 30m									
10h		4,7					0,17	2,4	
10h 30m	0,33			0,18	2,1				
11h							0,18		
12h	0,37	8,1	30,8	0,21	3,6	21,5	0,2	4,6	23
14h	0,54			0,33			0,32		
16h	0,86			0,54			0,42		
18h	1,2	20,5		0,74	13,2		0,75	15,4	
22h	2,53						1,73		
24h	3,5	30,8	47,2	1,4	22,8	38,1	2,3	25,1	42,3
26h									
29h									
48h	21	52,5	54,8	17,2	43,9	51,5	15,2	46,8	53,4
168h	61,8	67,7	63,3	53,7	66,2	69,9	53	66,2	63,4
672h	77,4	78,8	74,6	79,4	82,8	80	73,2	78,6	73,4
6480h	84,9	92,6	86,2	99,1	94,2	90,8	85,6	89,2	85,6

Time	BI 4			BL 5			BL 6		
	ANLmod + 10%FA			ANLmod + 20%FA			ANLmod + 35%FA		
	DB 107 / DB 111			DB 151 / DB 152			DB 180 / DB 181		
	5C	20C	35C	5C	20C	35C	5C	20C	35C
3h									
3h 30m									
4h			0,21			0,19			
4h 30m			0,33			0,23			
5h			0,46			0,47			0,18
5h 30m		0,17	1			0,78			0,35
6h		0,17	1,6		0,17	1,6			0,52
6h 30m		0,28			0,23				0,85
7h		0,33	4		0,28	3			1,27
8h		0,57	6,9		0,4	5,3		0,24	2,91
9h					0,78			0,33	4,6
9h 30m		1,28							
10h					1,17			0,56	
10h 30m									
11h	0,2				1,87			0,78	
12h	0,23	3,9	20,3	0,21	2,3	16,3		1,37	10,7
14h	0,33			0,27			0,21	2,25	
16h	0,43			0,41			0,29		
18h	0,62	12,6		0,62	9,4		0,4	5,4	
22h							0,6		
24h	1,8	21,2	35,8	1,6	16,4	30,2	1,05	11	22,7
26h							1,4		
29h							2,21		
48h	14,6	41,6	48,9	12	33,5	42,3	8	24,4	32,9
168h	51,8	60,6	60,6	42	52,6	56,4	32,6	41,8	52
672h	74,3	74	69,6	63,5	66,4	78,8	52,7	60,8	77,8
6480h	90,9	84,9	81	86,8	96,7	90,4	82	93,2	93,2

	TEMPERATURUTVIKLING I TERNINGER FOR FASTHETSMÅLING											
	Fersk btg temp, til logger startet etter ca 18 min		Fersk btg temp, til logger startet etter ca 18 min		Fersk btg temp, til logger startet etter ca 24 min		Fersk btg temp, til logger startet etter ca 18 min		Fersk btg temp, til logger startet etter ca 30 min		Fersk btg temp, til logger startet etter ca 30 min	
		Antatt	Antatt									
	BI 1		BL 2		BL 3		BL 4		BL 5		BL 6	
	ANL		SRmod		ANLmod		ANLm+10FA		ANLm+20FA		ANLm+35FA	
Tid (min,	DB 204		DB 119		DB 207		DB 107		DB 151		DB 180	
etter vanntils	5C	35C	5C	35C	5C	35C	5C	35C	5C	35C	5C	35C
0	19,8	19,8	21,1	21,1	19,3	19,3	21,9	21,9	20,9	20,9	19,9	19,9
6	19,8	19,8	21,1	21,1	19,3	19,3	21,9	21,9	20,9	20,9	19,9	19,9
12	19,8	19,8	21,1	21,1	19,3	19,3	21,9	21,9	20,9	20,9	19,9	19,9
18	16,9	19,7	16,3	21,7	19,3	19,3	21,8	21,9	20,9	20,9	19,9	19,9
24	10,2	27,7	10,5	28,2	17,4	19,7	13,7	28	20,9	20,9	19,9	19,9
30	6,9	32,4	7,2	32,4	10,5	27,7	8,6	32,3	16,2	21,5	15,6	19,7
36	5,6	33,7	5,8	34	7,2	32,4	6,4	33,7	10,6	28,7	10,1	27,8
48	4,8	34,2	5,3	34,3	5,8	33,7	5,6	34,2	8,2	32,5	7,4	32,3
60	4,6	34,3	5,1	34,5	5,3	34,2	5,2	34,3	7,1	33,7	6,2	33,6
72	4,3	34,3	4,9	34,6	5,1	34,3	4,9	34,5	6,7	34,2	5,6	34,1
84	4,2	34,5	4,9	34,7	4,9	34,5	4,8	34,3	6,3	34,3	5,3	34,2
96	4	34,6	4,9	34,6	4,9	34,5	4,6	34,3	6,2	34,5	5,1	34,2
108	3,9	34,6	4,9	34,6	4,9	34,6	4,6	34,3	6,1	34,6	4,9	34,1
120	3,8	34,7	4,9	34,7	4,9	34,6	4,4	34,3	5,9	34,6	4,7	34,1
132	3,7	34,7	5,1	34,7	4,9	34,7	4,4	34,3	5,8	34,6	4,7	34,2
144	3,7	34,8	4,9	34,7	5,1	34,5	4,4	34,5	5,7	34,6	4,7	34,2
156	3,5	34,6	4,9	34,7	4,9	34,3	4,6	34,5	5,6	34,6	4,6	34,2
168	3,5	34,7	4,8	34,7	4,9	34,3	4,6	34,2	5,4	34,5	4,6	34,2
180	3,5	35	4,8	34,8	4,8	34,3	4,6	34,3	5,3	34,3	4,7	34,2
192	3,5	35	4,8	34,8	4,8	34,2	4,6	34	5,2	34,2	4,7	34,2
204	3,5	35,2	4,7	34,8	4,8	34,1	4,7	34,1	5,1	34,5	4,8	34,2
216	3,7	35,3	4,7	34,7	4,7	34,2	4,8	34,2	5,1	34,6	4,8	34,2
228	3,7	35,4	4,6	34,7	4,7	34,3	4,9	34,3	4,8	34,5	4,9	34,3
240	3,8	35,7	4,4	35	4,6	34,5	4,9	34,5	4,8	34,5	4,9	34
252	3,8	35,7	4,3	35	4,4	34,6	5,1	34,5	4,8	34,5	5,1	34,2
264	3,9	35,8	4,2	35,1	4,3	34,7	5,2	34,5	4,7	34,5	5,1	34,3
276	4	35,8	4	35,2	4,2	34,8	5,2	34,7	4,7	34,6	5,2	34,3
288	4,2	35,8	4	35,1	4	35	5,3	34,6	4,7	34,7	5,2	34,5
300	4,2	35,9	3,9	35,3	4	35,1	5,4	34,7	4,7	34,7	5,3	34,5
312	4,3	35,9	3,8	35,4	3,9	35,3	5,6	34,6	4,8	34,8	5,3	34,3
324	4,4	35,9	3,7	35,3	3,8	35,3	5,6	34,8	4,8	35	5,4	34,3
336	4,4	35,8	3,7	35,6	3,7	35,4	5,7	35,1	4,8	35,1	5,4	34,5
348	4,4	35,7	3,5	35,4	3,7	35,6	5,7	35,2	4,9	35,1	5,6	34,6
360	4,7	35,8	3,5	35,7	3,5	35,6	5,8	35,4	5,1	35,1	5,7	34,7
372	4,7	35,9	3,7	35,7	3,5	35,7	5,9	35,7	5,1	35,2	5,8	34,8
384	4,7	35,9	3,7	35,7	3,7	35,8	5,9	35,8	5,2	35,3	5,8	34,6
396	4,8	35,9	3,5	35,8	3,7	35,8	5,9	35,6	5,3	35,4	5,9	34,8
408	4,9	35,9	3,7	35,7	3,5	35,8	5,9	35,6	5,3	35,4	5,9	35,1
420	4,9	36,1	3,7	35,7	3,7	35,6	5,8	35,8	5,4	35,4	6,1	35,1
432	5,1	35,9	3,8	35,8	3,7	35,7	5,8	35,7	5,4	35,4	6,1	35,2
444	4,9	35,9	3,9	35,9	3,8	35,7	5,7	35,7	5,6	35,4	6,1	35
456	5,1	35,7	3,9	36,1	3,9	35,8	5,6	35,7	5,7	35,4	5,9	35,1
468	4,9	35,7	3,9	35,9	3,9	35,7	5,6	35,7	5,8	35,4	5,9	35,1
480	4,8	35,7	4	35,9	3,9	35,7	5,4	35,7	5,7	35,4	5,9	35,2
492	4,8	35,7	4	35,9	4	35,7	5,4	35,8	5,9	35,4	5,8	35,2
504	4,7	35,7	4,3	35,9	4	35,7	5,3	35,8	6,1	35,4	5,7	35,3
516	4,7	35,7	4,3	35,9	4,3	35,8	5,2	35,8	6,1	35,4	5,7	35,3
528	4,6	35,6	4,3	35,9	4,3	35,4	5,1	35,8	6,1	35,4	5,4	35,3
540	4,4	35,6	4,4	35,9	4,3	35,3	4,9	35,8	6,1	35,4	5,3	35,3
552	4,4	35,6	4,6	35,8	4,4	35,4	4,9	35,7	6,1	35,4	5,3	35,3
564	4,3	35,6	4,7	35,8	4,6	35,6	4,9	35,7	6,1	35,4	5,2	35,3
576	4,2	35,6	4,8	35,7	4,7	35,7	4,8	35,6	5,9	35,4	5,1	35,3
588	3,9	35,4	4,8	35,7	4,8	35,8	4,6	35,4	5,8	35,4	4,9	35,3
600	3,9	35,4	4,9	35,6	4,8	35,8	4,6	35,4	5,8	35,4	4,9	35,3
612	3,8	35,4	4,9	35,6	4,9	35,8	4,6	35,3	5,7	35,4	4,8	35,3
624	3,8	35,3	4,9	35,6	4,9	35,7	4,6	35,3	5,7	35,4	4,7	35,3
636	3,7	35,3	4,9	35,4	4,9	35,8	4,6	35,2	5,6	35,4	4,7	35,3
648	3,5	35,3	4,9	35,4	4,9	35,8	4,7	35,2	5,4	35,4	4,7	35,3
660	3,7	35,3	4,9	35,4	4,9	35,8	4,7	35,2	5,4	35,4	4,7	35,3
672	3,7	35,3	4,9	35,4	4,9	35,7	4,7	35,2	5,3	35,4	4,7	35,3
684	3,5	35,3	4,8	35,3	4,9	35,7	4,8	35,2	5,2	35,4	4,7	35,3

SINTEF Building and Infrastructure is the third largest building research institute in Europe. Our objective is to promote environmentally friendly, cost-effective products and solutions within the built environment. SINTEF Building and Infrastructure is Norway's leading provider of research-based knowledge to the construction sector. Through our activity in research and development, we have established a unique platform for disseminating knowledge throughout a large part of the construction industry.

COIN – Concrete Innovation Center is a Center for Research based Innovation (CRI) initiated by the Research Council of Norway. The vision of COIN is creation of more attractive concrete buildings and constructions. The primary goal is to fulfill this vision by bringing the development a major leap forward by long-term research in close alliances with the industry regarding advanced materials, efficient construction techniques and new design concepts combined with more environmentally friendly material production.

Technology for a better society

www.sintef.no